Testing and Modeling of Shock Mitigating Seats for High Speed Craft

Christopher Liam

Thesis submitted to the Faculty of the

Virginia Polytechnic Institute and State University

in partial fulfillment of the requirements for the degree of

Master of Science

in

Mechanical Engineering

Mehdi Ahmadian, Chairman
Daniel J. Inman
Saied Taheri

May 6, 2011
Blacksburg, Virginia

keywords: shock mitigating seats, high speed craft

Testing and Modeling of Shock Mitigating Seats for High Speed Craft

Christopher Liam

ABSTRACT

This study conducted a series of tests on a shock mitigating seat designed for high speed craft using various input excitations to better understand the relationship between various seat and operational conditions, and the response of the seat. A seat model of the test seat is used for a parametric study of various spring, damping and operational configurations.

A seat shake rig is implemented to simulate motions of multiple high-speed craft as well as various defined inputs. At each test input the occupant weight and suspension preload is varied and the response is analyzed to find changes in acceleration, which is representative of the changes in force and displacement. By representing the seat as a based-excitation two-degree-of-freedom system, we develop the equations of motion and model them in Simulink to analyze the effects of various spring rates and damping coefficients.

Based on the results it is found that an increase in occupant mass results in a decrease in observed acceleration. Increasing suspension preload is found to be detrimental to the mitigating abilities of the seat, changing the dynamics to those similar of a rigid-mounted seat. An analysis of the defined inputs resulted in confirming various seat characteristics. The analysis of the Simulink model revealed that increasing the spring rate results in an increase in acceleration. An increase in damping coefficient resulted in an increase in acceleration and ride harshness.

ACKNOWLEDGEMENTS

I would like to thank my advisor, Dr. Mehdi Ahmadian, for his guidance, advice and encouragement throughout my research and graduate studies in Mechanical Engineering with the Center for Vehicle Systems and Safety. I would also like to thank Dr. Daniel Inman and Dr. Saied Taheri for serving on my graduate committee.

Thanks are also in order to NAVSEA Carderock CCD in Norfolk, VA and Mr. Charlie Weil for their technical support and various shock mitigation seats which were graciously loaned for this study. I also would like to extend my gratitude to Julie Stark who provided much appreciated knowledge relating to human factors of shock mitigating seats.

Special thanks are also in order to the members of CVeSS for their support and knowledge that helped me overcome many obstacles during this research.

I would like to especially thank my parents for all their support throughout my entire college career. Their support during rough moments in my life is much appreciated.

Contents

LIST OF FIGURES

LIST OF TABLES

Chapter 1. Introduction

This chapter presents the introductory material that aids in the understanding of the research described in this thesis. The first section describes the motivation for performing this study. Then the objectives are presented along with the approach used to solve the objectives. The chapter ends with an overall outline of the contents of this thesis which is followed by the potential contributions to the field of high speed boat seat testing.

1.1 Motivation

Operators of high speed craft are required to traverse seas in conditions that are, at times, less than favorable. The Mark V Special Operations Craft (SOC) is one of the popular choices for Special Operation Forces. The twin 2285 hp diesel engines of the Mark V are able to propel its 5 crew members and up to 16 passengers at speeds exceeding 50 knots over the sea [1]. The 82-foot aluminum hull of the Mark V has been known to deliver a rough ride; personnel have reported everything from bruises to foot and back injuries when traveling in excess of 50 knots [2]. The aluminum hull transmits a majority of the wave impact to the occupant. There are two solutions to mitigate the shock experienced by the occupants of high speed craft; one is to redesign the hull to absorb more of the impact and the other solution is to isolate the occupant from the hull to mitigate the shock forces. The later of the two choices is chosen for a quick and relatively efficient solution.

Although it may seem that implementation of shock mitigating seats has solved the issue of shock transmission, the seats themselves have introduced problems into the situation. The first problem is with the development process of shock mitigating seats. Currently a majority of testing is done while underway in a high-speed craft at sea. At-sea testing is very costly due to the requirement of a qualified crew and cost of fuel. The unpredictable nature of the sea makes testing difficult and even impossible at times. When specific testing conditions are desired there could be a long waiting period for the desired conditions. Also, some sea states only occur during certain seasons and sometimes only occur at certain geographic locations requiring costly travel. When testing at sea the test conditions could also change during the test depending on the environment and distance

traveled. For example, when traveling at a constant heading the conditions at the beginning of a test could differ from that at the end if a large distance was traveled. Although at sea testing is the best way of testing shock mitigating seats, at the moment these complications make testing difficult.

Most of the shock mitigating seats currently in use implement a passive suspension system to absorb the shock transmitted through the hull. A passive suspension system can only be tuned for a specific condition because of its non-adjustable nature. Some passive systems have the ability to be manually adjusted before use but are difficult to adjust while underway during extreme motion. A high speed craft may encounter different environmental conditions on the same voyage, varying from calm seas at harbor to violent rough waves away from shore. Also, the occupant of the seat is not always constant, meaning that occupants of different size and weight may operate the seat at different times. The variability in operating conditions makes it difficult to design an ideal suspension system to be implemented on shock mitigating seats. As a result naval personnel often prefer standing to sitting while operating their vessels, believing that they could use their legs from a standing position to absorb impacts [3].

Most tests of shock mitigating seats are conducted with a human occupant. These tests can be very difficult to interpret due to the subjective nature of the results. The response of the occupant varies greatly depending on the background of the test subject and the subject's tolerance to harsh sea conditions. Even when using the same test subject the tests remain highly subjective, which degrades the significance of the results.

There have been studies done in the field of shock mitigating seats but there remains areas for improvement. Most of the studies on shock mitigating seats have been conducted by the seat manufacturers themselves. This creates a level of bias which is inherent in all the studies conducted. There isn't much public information on third party testing of shock mitigating seats which is not endorsed by a manufacturer.

An independent study has been done to create a seat testing rig to accurately test the dynamics of seats with high repeatability in a lab environment. The study resulted in a drop test rig which is able to accurately simulate a singular wave impact event. Although

the study has provided substantial contributions to the field of seat testing, measuring the performance of a shock mitigating seat that will be operated on a high speed craft should not be done on the basis of a singular impact event.

There are still many areas of improvement with the design and testing of shock mitigating seats. Shock mitigating seat design is relatively new and current seats are far from perfection. Testing of the seats is highly subjective and comparisons of test results have high levels of experimental variability. Lab tests mainly consist of drop testing, which can only simulate a single wave impact. The research presented in this study focuses on improving these areas in the field of shock mitigating seats.

1.2 Objectives

The primary objectives of this research are:

1. Create a seat testing system that is capable of simulating high speed craft motions with high repeatability.
2. Test and evaluate the performance of a shock mitigating seat under various test conditions.
3. Create a computer model of a shock mitigating seat which closely matches the response of the seat during experimental testing.
4. Use the model to test non-adjustable seat parameters to see the effects on the system.

The overall objective of this research is to create a seat testing system and computer model of a shock mitigating seat to improve on the design and testing of these seats. Current research in the field has revealed much variability in at sea testing and the only effective seat test systems in a laboratory environment can only replicate a singular drop impact event. A repeatable seat testing system can provide accurate results which will allow accurate comparisons of shock mitigating seats while eliminating the need for costly and time consuming at sea testing.

1.3 Approach

The approach used to address the issues presented in this study is the following:

- Perform a comprehensive survey of past studies in the areas of ship motion, shock mitigating seats and the physiology of a seated person.
- Create a seat shake rig using 80/20 pieces and implement a hydraulic actuation system to excite the system with user defined inputs which will include simulations of ship motion.
- Create a computer model that simulates the response of a shock mitigating seat to user defined inputs and also allows modification of suspension parameters.

A preliminary literature review revealed that there were a number of studies conducted on the topic of shock mitigating seats. A majority of the research on shock mitigating seats are focused around testing and comparison of various seats in comparison to non-shock mitigating seats. There are also some studies on wave impacts and the effects on the ship structure; this topic is relatively new due to the recent demand for high speed craft. There were not any studies on replicating ship motion with a focus on measuring the response of shock mitigating seats. The only study found on laboratory seat testing was of replicating a singular wave impact event.

To create a seat testing rig multiple pieces of 80/20 aluminum were used to construct a rigid frame for single axis actuation. The design of the seat shake rig consisted of an outer rigid frame to restrict motion in the vertical direction while an inner carriage would act as a moveable base for a solid mounting point to place the seat. An MTS hydraulic actuation system is implemented to simulate the desired input excitation into the system for testing. A Stidd 800v5 shock mitigating seat is placed on the inner carriage for experimental testing. The seat was then instrumented with multiple accelerometers and a string potentiometer to measure acceleration and relative displacement at multiple points of the seat. The combination of a rigid seat shake rig, a hydraulic actuator able to replicate motions accurately, and multiple sensors enables the system to conduct tests with high levels of accuracy and repeatability.

The computer model is created by use of Simulink modeling software. The seat system is modeled as a 2-degree-of-freedom system with base excitation, with the first degree of freedom representing the coil-over suspension system and the second representing the seat cushion itself. The equations of motion from each degree of freedom are modeled using Simulink blocks. The model is then verified to the experimental data collected using the seat shake rig test system to ensure that the model accurately represents the seat.

Once the model is verified against the response of the seat collected using the seat shake rig the parameters of the model can be varied to examine their effects on the dynamics of the system. The same input excitations used for the seat shake rig are used for the model excitation. Using these excitation inputs the spring rate and damping coefficients are varied from the original values to examine the impacts on the dynamics of the seat.

1.4 Contributions

The potential direct impacts of the proposed research presented in this study to the field of high speed craft shock mitigation are:

- Establishing a seat shake rig system that is able to simulate high speed craft motion with great repeatability in a laboratory environment.
- A better understanding of the Stidd 800v5 shock mitigating seat dynamics and the response of the system to changes in operating conditions.
- An analysis on possible changes to the spring rate and damping coefficients of the suspension system of a shock mitigating seat, and the effects of these changes on the seat occupant.

In addition to these direct impacts to the field of shock mitigating seats for high speed craft there are some indirect impacts. The seat testing system created in this study can be used to create a testing standard to quickly compare various seat designs by exposing the seats to repeated tests and establish the performance of the seat objectively.

The analysis of the current seat design widely in use can lead to improvements in suspension geometry of seats and an improvement in overall system efficiency. An improved seat design could have many possible benefits in the field such as:

- Increased situational awareness of the high speed craft operators in all sea conditions.
- A decrease in likelihood of injury to the seat occupants while underway which could lead to increase in mission effectiveness.
- A greater reduction of shock to the boat operator will permit longer and faster transit in rough sea conditions.
- Reduce the need to test shock mitigating seats in an at sea test. Thus reducing the development time and cost of designing shock mitigating seats.

1.5 Outline

The contents of this thesis are organized into nine chapters. Chapter 2 explains the basics of ship motion, effects of the seated position on the human body and then ends with a literature review on past shock mitigating seat studies. Chapter 3 describes the experimental setup that was used for testing. In this chapter the seat shake rig, hydraulic system, instrumentation and test inputs are described in detail. Chapter 4 presents the repeatability tests and results that were conducted on the seat shake rig. Chapter 5 presents the results on the comparison analysis of the shock mitigating seat with and without the shock mitigation system. Chapters 6 and 7 present the analysis of the response of the shock mitigating seat under various input excitation files. Chapter 8 describes how equations of motion were implemented to create a Simulink model of the seat. Then later in the chapter the results from testing of the model are explained. Chapter 9 provides an overall summary of the entire study and important conclusions along with suggestions on future work.

Chapter 2. Background

This section presents background information necessary towards understanding the issues of shock mitigating seat design in relation to high speed craft comfort and fatigue. The accumulation of this background information was acquired through a literature review of both past and present research in the field of suspension seat design. The section begins with a discussion of wave slamming and ship motion. Then an overview of how vibration affects the human body in a seated position is presented. The chapter then concludes with a literature review of past work done in the field of shock mitigating seat research with a focus on high speed craft.

2.1 Ship Motion

To analyze shock mitigating seats it is required to first understand the environment in which it operates in. The stochastic nature of waves and the ocean environment make it difficult to characterize simply. The scale used for classification of sea conditions is the World Meteorological Organization Sea State Code or Douglas Scale with the sea state classification system, which goes from 0 to 9 [4]. Each individual state is characterized by multiple variables; these include significant wave height, wind speed and significant wave period. Sea state conditions are typically determined by wave buoy measurements. This scale is used to asses testing conditions for in-sea trials for many tests. The flaw with this method of environment classification is that each sea state classification corresponds to a wide range of conditions.

In general, high speed craft motion can be placed in one of two types of motion [5]. The first type is predominantly characterized by repeated shocks or transient vibrations which are created by multiple wave impacts. This is sometimes called repeated shock and can cause extreme injury to human occupants. This type of motion usually occurs in higher sea states while operating at a high speed. An example of this motion is shown in Figure 2-1, multiple shock events are shown as sharp peaks in the acceleration plot. The second type is characterized as a sinusoidal nature, where occasional shocks and transients are present but do not dominate the state. This motion usually occurs in mild sea states at

moderate to low speeds. While this motion can cause motion sickness, serious injury is unlikely.

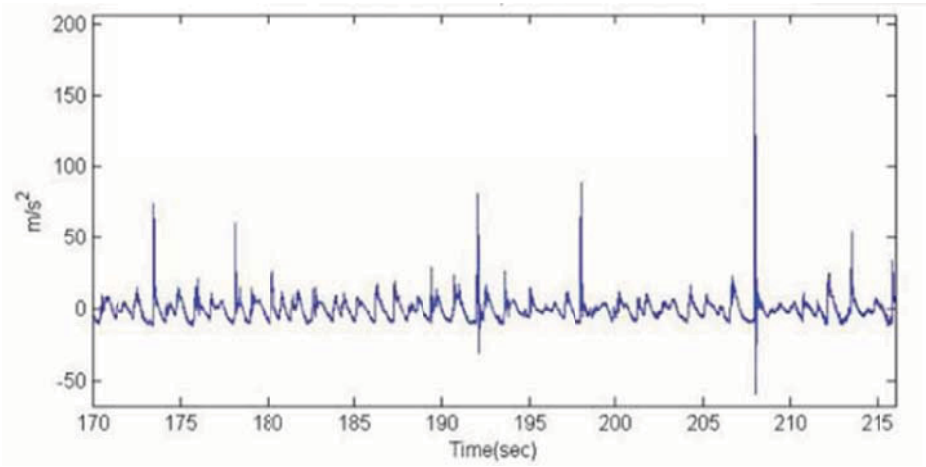

Figure 2-1. An example of repeated shock events from a 28 foot RIB in sea state 1-2 [5].

Repeated shock is the most severe type of motion. Repeated shock is essentially a combination of multiple distinct impulsive forces or loads. Impulsive forces are typically defined as large magnitude forces that act over a short period of time [6]. A shock event is typically observed when a planing craft is jumping from a wave crest and then proceeds to fall back down to the wave surface after the wave crest in a violent manner [7]. This is also called hull water entry and focus is emphasized on when the hull returns to the water surface. The orientation of the hull with relation to the water surface upon contact determines the severity and nature of the shock event experienced which can vary significantly. Acceleration levels can reach as high as 10 g's for such events, where 1 g represents either 9.8 m/s^2 or 32.3 $ft./s^2$ of acceleration. The duration of most shock events are within the time limits of 30 to 75 milliseconds. Figure 2-2 describes the acceleration observed for a single wave impact event on an MkV Special Operations Craft.

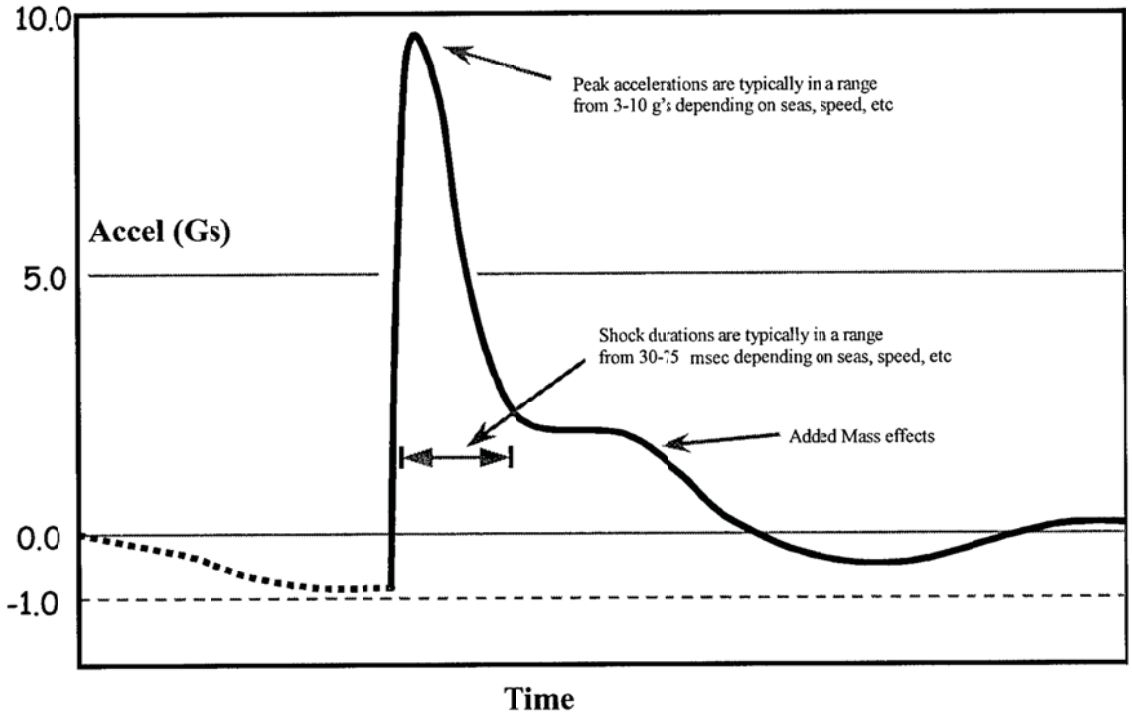

Figure 2-2. Typical characteristic acceleration curve observed for a single wave impact on a SpecOP boat [8]**.**

The impact event shown in Figure 2-2 can be characterized as an extreme jerk observed as a sharp initial increase in acceleration, this is followed by a slightly less extreme decrease in acceleration, then constant acceleration is observed which is caused by added mass effects due to the hull-water interaction, and finally ending with a slow return back to a level of equilibrium. The acceleration shown in Figure 2-2 also matches that of model drop tests conducted at the Costal Systems Station [9], verifying its results. Many factors can affect the general curve shown above. These factors include the speed of the craft and the height of the wave that caused the initial impact. The direction in which the craft is traveling with respect to the waves also impacts the severity of the exposed acceleration, the highest accelerations are usually observed while traveling in a head sea direction [10]. At faster craft speeds and larger wave heights the initial jerk event will have a greater magnitude and shorter duration than at slower craft speeds and smaller

wave heights. When multiple shock impulse events are linked together the result can be extremely damaging to the craft structure and crew.

2.2 Wave Slamming

A ship motion that is of particular interest with current development of high speed crafts is wave slamming. A wave slam is similar in nature to what was previously described as a shock impulse event. A wave slam event is described as an impact that imparts a high localized pressure in the region of the impact and a large global load onto the vessel's structure, mainly the hull girder [11]. The dynamic response of the global structure is observed as shudder after a slam event has occurred, also known as whipping [12]. The first study on wave slamming was conducted on the landing impact of seaplane floats, this research mainly used expanding plate theory to approximate the forces and motions observed. The research gained from seaplane landing impacts was later adapted to ship motion.

Whipping is of concern to modern high-speed craft due to its damaging effects on the hull structure. The combination of high speed and flexible light-weight aluminum materials has increased the vulnerability of high-speed vessels in terms of strength and fatigue life [13]. The effects of whipping on larger and heavier vessels are much smaller since the vibratory motions are less prevalent when a large amount of mass is present. A single slam event applied at the bow of a ship usually excites the first longitudinal mode in the vertical plane. This causes a singular bending motion across the entire global structure. The whipping response due to a slam event is examined using a 2.5 meter long model of a high-speed catamaran, the result is shown in Figure 2-3. The response can be described as a decaying sinusoidal wave.

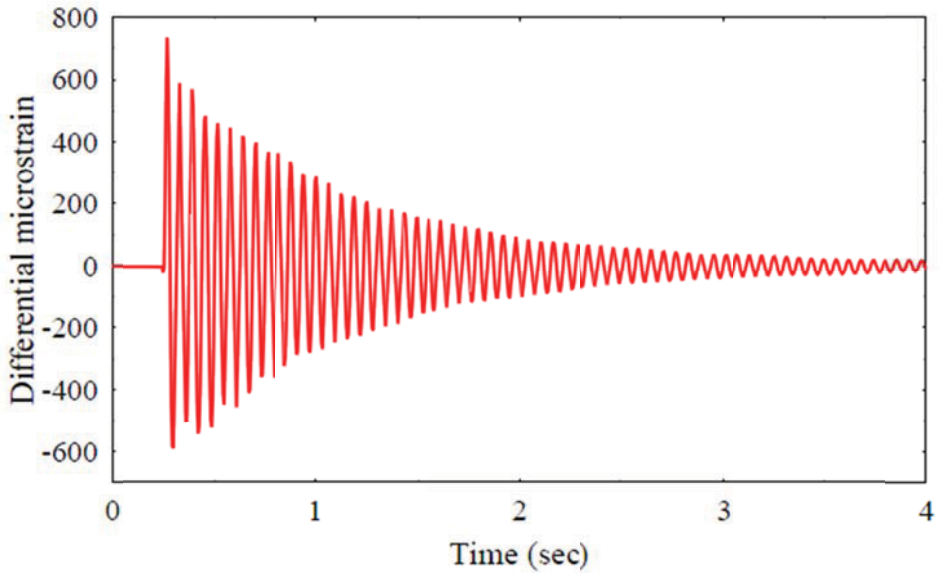

Figure 2-3. Whipping vibratory response from a catamaran model measured using strain gauges mounted on the hull structure [12].

High Speed Catamaran Study

Most recent research on wave slamming and whipping has been conducted on high speed vessels with a catamaran hull shape used as ferries. For these hull structures a wave slam is typically defined as a wet deck slam event. A wet deck slam event is an event in which the cross-deck structure or center bow archway of a catamaran impacts with the water surface when operating in rough seas. High speed catamaran ships are chosen for research testing due to their long at-sea voyages in rough water. For example, one test was of an 86 meter Incat high-speed catamaran in Australia during a regular delivery trip from Sydney, New South Wales to Fermantle, Western Australia had a 4 day trip duration. During its 4 day nonstop voyage the vessel encountered rough sea conditions. The ship in which the test was conducted on is pictured in Figure 2-4.

Figure 2-4. High-speed 86 meter Incat ferry used to take wave slamming data while on voyage off the coast of Australia [12].

For the voyage multiple sensors were placed on the hull of the ship to detect, measure and record slam events when occurred. These sensors included a radar based wave meter, vertical accelerometers and pressure sensors. The rough sea conditions experienced from the voyage off the coast of Australia provided many examples of wave slam events. There currently is no standard for distinguishing a wave slam event from recorded data sets so specific criteria pertaining to this test is established. The criterion that was established was that a slam event would be an instance where a high-rate of stress was subjected to the hull. The threshold established was a change of hull stress of 5 MPa/sec, since it is higher than the global loads experienced by the structure, and the event had to correspond to a wave height of 0.9 meters or greater. Once the data was filtered for slam events based on the established specifications to identify slam events, 565 slam events were identified. The peak stress for each event was then normalized based on the mean of the slam peaks of all the events. An interesting discovery from the normalized data was that 70% of the slam events had a peak stress that was less than or equal to the mean stress. When wave heights of each slam event were analyzed it was discovered that the number of slams per hour increased when the wave heights increased. It was also found

that wave slams often occurred sequentially in groups. This can be explained by the phenomenon that ocean waves travel in groups.

Examination of Sea Fighter

Another past study that revealed vital information in the field of wave slamming analysis is the characterization of Sea Fighter, FSF-1. Sea Fighter is a high speed experimental vessel developed by the Office of Naval Research. The vessel is an 80 meter aluminum catamaran powered by two diesel engines and two gas turbines that drive four water jets which are capable of propelling the vessel at speeds greater than 50 knots [14]. The vessel is pictured in Figure 2-5, notice the novel hull design required to achieve high speed for a vessel of this size. This hull shape is similar to that of a high speed catamaran.

Figure 2-5. Sea Fighter FSF-1 experimental high-speed catamaran used in testing wave slam motion [14].

During a trip from British Columbia, Canada to San Diego, CA in the spring of 2006 rough water trials were conducted to evaluate the vessel's performance in high sea states. Sea states of 4 and 5 were observed, corresponding to wave heights of approximately 6 to

12 feet. Data was recorded using GPS sensors to determine ship location and speed, accelerometers were used to determine ship motion and ultrasonic sensors to record the wave field in front of the ship.

The data revealed that four distinct slam events occurred while underway. A wave slam was characterized as a shock event that was outside of the usual motion observed during a specific time period. All four slam events that were recorded were similar. A wave slam event began with wave heights of about 2 meters, then the vessel typically encounters a series of waves that are of amplitudes much greater than the average 2 meter amplitude which cause the bow of the ship to lift out of the water surface and then collide with the last wave, which usually is the largest in height, causing the shock impulse characteristic of a wave slam event. The slam event is indicated by a large amount of white water or water spray when the bow comes into contact with the water surface. Each slam event occurred when the ship's bow pitched down below the normal pitch boundary and then pitched up towards the upper boundary of the envelope. This general motion was observed in all slam events that were recorded and identified.

The slam events that were recorded during the rough water testing of the Sea Fighter vessel are characteristic of typical slam events. Wave slam events usually don't occur when only one singular shock event is observed but rather a series of wave impacts. Another key characteristic is that the slam event itself usually occurs when the bow of the ship lifts out of the water surface and then returns violently. This would be predicted from the previously mentioned research on water entry and the harsh after effects. Also, the most extreme events are observed when successive wave crest of increasing amplitudes.

2.3 Effects of the High-Speed Craft Environment on the Human Body

Tremendous recent development in the design and construction of high speed craft has created faster and larger vessels that travel at much higher speeds than traditional ships. The harsh environment in which high speed craft are exposed to is transmitted to the occupants and operators that are on the craft [15]. Quantitative evidence demonstrates

that high-speed boat crew have a high incidence of hospitalization [16]. Surveys of self-reported injuries among special operation boat operators revealed the extreme nature of the environment. Of the population that was surveyed 64.9% reported at least one injury, some operators reported up to three injuries [17]. These injuries range from sprains/strain to chronic pain and more severe stress fractures. These injuries result in a high hospitalization rate that compares to those of construction-men, firemen and airmen.

Most of the injuries that occur while underway can be placed in the category of fatigue induced. Many that are not familiar to the environment and definition of fatigue will associate the term with comfort. The definition of comfort is vague and typically depends on the application at hand. It is generally defined as a lack of comfort [18]. For seat design purposes it typically refers to the short-term effect of a seat on the human body; that is, the sensation that commonly occurs from sitting on a seat for a short period of time. The short-term comfort offered by a seat is relatively easy to determine, the best method is to survey potential users and measure the "feel" that each user reported for the short period of time in which they are using the seat. Comfort is in most cases a subjective measure and can be hard to quantify at times.

While in contrast to comfort, fatigue is more clearly defined as the physical impairment that results from the exposure to the seat dynamics for a long period of time. These impairments are cognitive in nature and include deficiencies in attention, perception, decision-making, vigilance, and reaction time. For the automotive field driving fatigue is thought of as falling asleep while driving, a decline in driving performance often precedes sleep. This is proven by the U.S. Department of Transportation which found that the most influential factor of driver fatigue was the time of day [19]. For reference, some of the recognized causes of automotive driver fatigue are: driving with sleep debt, night-time driving, extended driving time, physical work that is in addition to driving and monotonous driving conditions. For the environment of high-speed craft fatigue is caused by the human body's reaction to the motion of the high-speed craft which is usually referred to as motion induced fatigue (MIF). The cause of MIF is due to the physical work associated with mitigating the shocks during transit [5]. The purpose of shock mitigating seats is to reduce the effects of MIF in all conditions.

The research presented here focuses mainly on fatigue, more specifically the MIF that high speed craft operators experience. Many studies have shown that there is little correlation between comfort (the short-term sensation) and fatigue (the long-term physical effect) of a seat. In other terms, what may be comfortable at first contact may not be less fatiguing during a long duration of time. An inverse relationship between comfort and fatigue has been supported by research that found that comfort evaluations for short-term and long-term driving do not agree [20].

The Effects of Vibration on the Human Body

When studying methods of reducing fatigue it is important to analyze the causes of fatigue itself. A cause of fatigue in the high speed craft environment is vibration. Vibration exposure can cause a broad spectrum of sensations to the human body depending on the type of vibration, the physical characteristics of the person and the duration of exposure. The high-speed craft environment is dynamic in nature; the seated occupant is exposed to vibrations from the sea environment and the engine. The ability of the ship to minimize the transmission of these vibrations is of major concern.

Vibration can cause a lack of comfort and fatigue but in different ways. Discomfort is caused by the dynamic properties of the human body and how it reactions to vibration. For an example, the human body experiences discomfort when the head and neck are shaken at their resonant frequencies. Fatigue due to vibration is caused by prolonged muscle activity-both voluntary and involuntary-resulting from the body's attempt to counter act the vibration. The muscle tissue and organs act as shock absorbers that dampen vibration and can become fatigued over a long duration of time. Fatigue can be more apparent when the vibration exposed is at the resonant frequencies of the human body. For example, research has shown that humans reach a level of fatigue much quicker when subject to 4 to 8 Hz vibration in the vertical direction and 1 to 2 Hz in the transverse direction [21]. Other resonant frequencies include 20 to 30 Hz for the head, neck and shoulders and approximately 60 to 90 Hz for the eyes [22]. In general, the human body's reaction to vertical vibration can be considered linear below the frequency of 100 Hz.

Pressure Distribution while in the Seated Position

The distribution of weight among the different parts of the human body varies depending on the position and orientation of the body. Of main concern is the distribution of weight while in the seated position. This is noticeable when examining the amount and type of the injuries of high speed craft operators, 34% of the injuries are of the lumbar spine [23]. While in the seated position a majority of weight is placed on the ischialtuberocities of the pelvis and the surrounding soft tissues [22]. The pie chart shown in Figure 2-6 below shows the distribution of weight while a person is in the seated position. The chart below shows that about 45 percent of the weight is placed on the ischialtuberocities.

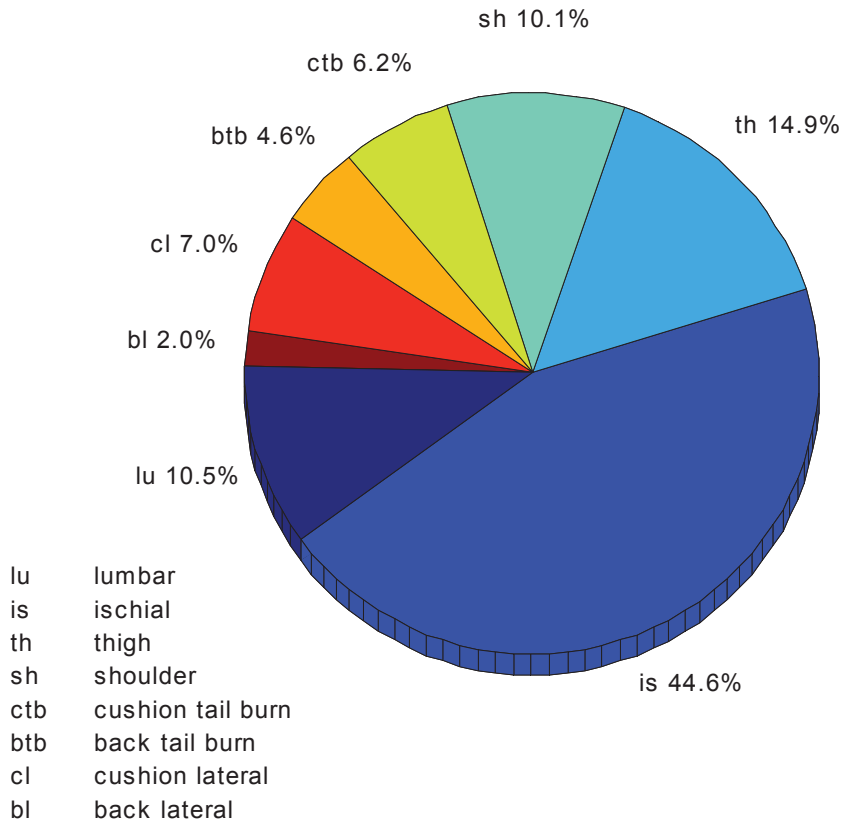

Figure 2-6. Typical weight distribution of a person in the seated position [24].

Weight bearing on soft tissue is unavoidable. Thus for the seated position, posture is of importance. Figure 2-7 shows the pelvis at various positions which include sitting and standing. As a person moves into a seated position the pelvis rotates backward and the

lumbar spine tends to flatten. In an upright position the peak pressure on the soft tissue would be from the ischialtuberocities or bony prominence of the pelvis. However, when seated in a slumped position the peak pressure is shifted away from the ischialtuberocities to the coccyx or the lower sacrum. When a person tilts sideways, the trochanters will bear the greatest peak pressure. The shifts in pressure distribution between the different areas of the pelvis prove that maintaining an ideal posture, usually the upright position, is of great importance. Maintaining posture can be difficult while in the extreme environment of a high speed craft but is extremely important to avoid injury.

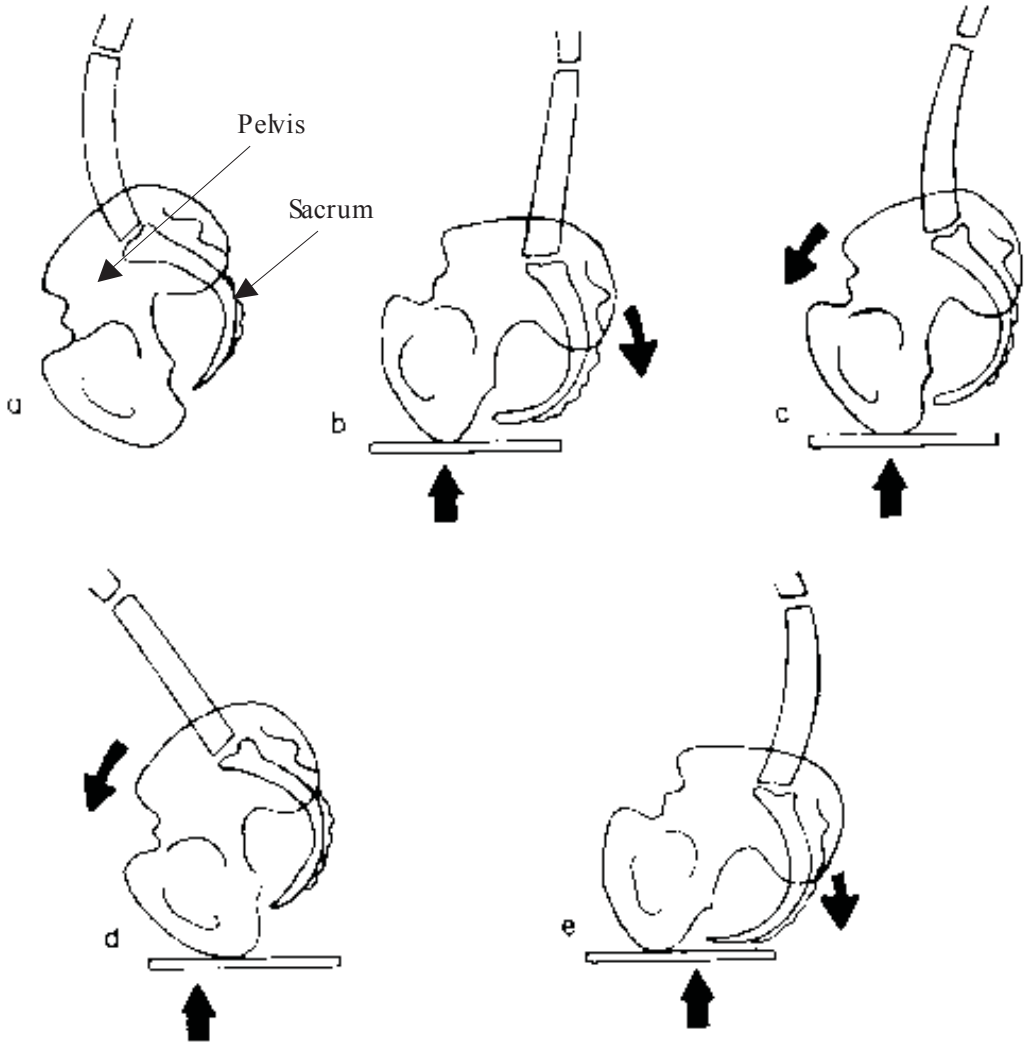

Figure 2-7. Pelvis orientation when (a) standing; (b) sitting relaxed; (c) sitting upright; (d) sitting forward; (e) sitting back. [22]

In most environments the interface between seat and human are of the utmost importance. The ideal situation is to maintain seat cushion pressure between approximately 60 mmHg and 120 mmHg, these pressure represent the average blood diastolic and systolic pressures. The reason for keeping the pressure within this range is to prevent blood starvation which could deprive cells of an adequate supply of nutrients, and especially oxygen. In most cases where a person assumes a seated position for a long period of time blood starvation occurs when exposed to unfavorable cushion pressure. Figure 2-8 shows the general relationship between cushion pressure and seated duration. A higher pressure can be tolerated for a short period of time while providing comfort and not causing adverse effects to the occupant. Although, for the environment of the high-speed craft this seat cushion pressure is not as critical. The large amplitude of the vibration and shock events cause the occupant to accelerate upwards slightly allowing excess pressure with the seat cushion to be relieved. This is in contrast to the more static environment of most seats, such as an automotive seat.

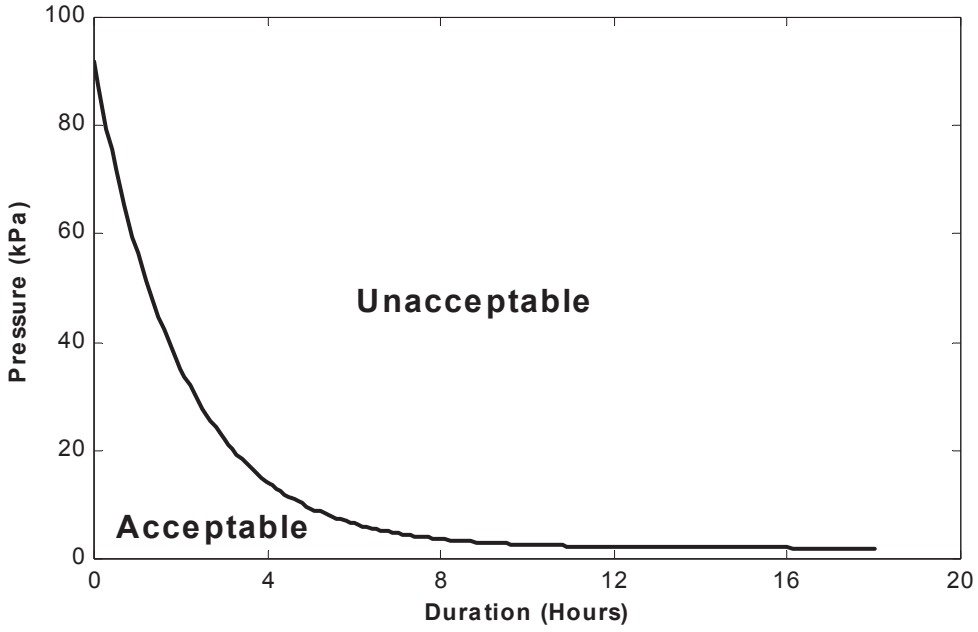

Figure 2-8. General relationship between seat cushion pressure and seated duration [25].

There are many models and standards that are currently in use by the International Organization for Standardization and military for evaluating vibration and shock exposure on a human occupant. Since the occurrence of severe injury due to the extreme environment of high speed craft is fairly new there are no established standards for the naval environment. Many standards are adopted from other fields to characterize the effects of high speed craft motion exposure on the human body. Two popularly used models are the Dynamic Response Index (DRI) from the air force and Vibration Dose Value (VDV) from the automotive environment.

Based on researching past work on high speed craft motion the best model that can be used to characterize the environment is the Dynamic Response Index (DRI). The DRI was originally created to characterize the effects of aircraft ejection seats on the human body. To place in perspective the severity of an aircraft ejection event, typical acceleration levels experienced during an emergency ejection event is usually just less than 15 g and the onset rate is approximately 250 gs^{-1} [26]. When ejection seat technology was first implemented there was a large likelihood of spinal injury due to the extreme acceleration in the same direction as the spinal column. A majority of the damage done to the spinal column happens when the ejection sequence is first initiated and there is a sudden acceleration onset in the vertical direction. The injury experienced is usually not permanent and most pilots are able to continue flying after a three month convalescence [26]. This type of injury is typical of high speed craft operators.

DRI is a representation of the maximum dynamic compression of the vertebral column of the human body. The DRI equation is derived by representing the human spinal column as a spring mass damper system modeled by equation 1-1. Equation 1-2 represents the calculation used to quantify the DRI value based on the parameters from equation 1-1. By substituting these suggested values into equations 1-1 and 1-2, equation 1-3 is formed. Thus the equation to calculate the DRI value for a specific instance is simply a function of the maximum compression observed. Seen in the final equation the DRI value is largely a function of the maximum compression of the spinal column which usually happens at the point of maximum acceleration. DRI is a good representation of high

speed craft motion since most of the damaging impacts occur at the maximum acceleration points.

$$\frac{d^2\delta}{dt^2} + 2\zeta\omega_n\frac{d\delta}{dt} + \omega_n^2\delta = \frac{d^2z}{dt^2} \tag{1-1}$$

$$DRI = \frac{\omega_n^2\delta_{\max}}{g} \tag{1-2}$$

$$DRI = 173.6\delta_{max} \tag{1-3}$$

The other commonly used model is Vibration Dose Value (VDV). The VDV number is representative of the cumulative effect of complex vibration which includes high crest factors, intermittent events or shock events [27]. VDV is used mostly in the automotive field since most vibration is experienced as a constant frequency low amplitude nature with occasional large impacts which are typically not severe in nature. VDV measurements are typically used to evaluate the effects of Whole Body Vibration (WBV) on the human body [28] which is usually measured and stated for a specific duration, mostly 8 hours which is representative of a typical work day. Equation 1-4 shows the calculation used to evaluate the VDV of the exposed motion [27]. As seen by the nature of the equation, VDV places a heavy emphasis on the average acceleration observed and less on the maximum impact value. This is to be expected in the automotive environment which mostly consists of paved roads that are fairly smooth. In a high sea state ocean environment the large impacts are mainly the source of human injury. Based on these facts the Vibration Dose Value (VDV) is not the optimal method of characterizing the high speed craft environment but can still be used as a comparison to other environments where VDV is calculated.

$$VDV = \left[\int_{t=0}^{t=T} a^4(t)dt\right]^{\frac{1}{4}} \tag{1-4}$$

2.4 Past Studies on Seat testing

This section presents past work that was accomplished specifically on shock mitigating seats on high speed craft. First presented is a study on implementing a drop table to simulate a single impact event. Then a review of a study on multiple suspension configurations of the Stidd 800v5 shock mitigating seat and its performance during at sea trials is presented.

Implementation of Drop Table Testing

Research in high-speed craft motion has been conducted multiple times in past work with the focus of reducing impact harshness on occupants. Sean D. Kearns at the Massachusetts Institute of Technology conducted a study on the Analysis and Mitigation of Mechanical Shock on High Speed Planing Boats [8]. The object of the research was to conduct a comprehensive analysis of the problem, to research methods by which the problem can be mitigated, and to develop and validate a method for laboratory design, test and evaluation. An analysis of the mechanical motion of high speed craft identified hull water entry and wave slamming as key contributors to shock impulses. Rough water test data was recorded using the SnapShock-PLUS self-contained acceleration recorder from Instrumented Sensor Technologies (IST). Data was recorded on a NSW RHIB and Mark V SOC in Sea State 2 and Sea State 3 conditions. The SnapShock-PLUS only records magnitude acceleration from each shock event. Figure 2-9 shows an example of the data taken using the SnapShock-PLUS on the Mark V SOC. Although this represents the nature of the motion exhibited on these craft, only limited deductions can be made without the waveform time data.

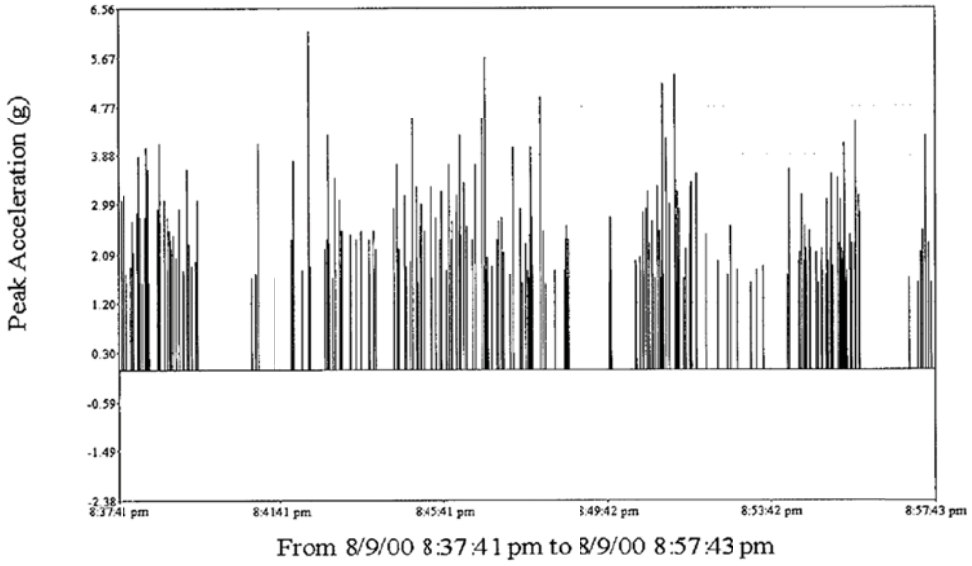

Figure 2-9. Data taken using a SnapShock-PLUS recorder onboard an MkV SOC vessel. Only shock magnitude and time of occurrence is recorded [8].

To gain a better understanding of the typical motion of high speed planing crafts waveform data needed to be acquired. An EDR-3 recorder from IST was implemented on at-sea trials of Mark V SOC at Combatant Craft Department (CCD) of the Carderock Division in Suffolk, VA. The raw data was filtered to reveal a trend in the shock impact events. The filter level was set to eliminate all frequencies above those that would have an adverse effect on the human body. From analyzing the filtered data it was found that a half-sine wave with a period of about 40 to 60 milliseconds and amplitude in the range of 5 to 12 g's can be used to simulate a wave impact shock event.

Conducting at-sea trials is a common occurrence in designing and testing shock mitigation methods due to the abundance of readily available high speed craft, even though in sea testing is time consuming and costly. One of the goals, however, was to create a reliable and repeatable way to test shock mitigating solutions in a laboratory environment. The solution is to utilize a drop table to simulate singular shock events. A drop table test setup contains a stiffened platform "table", guide rails, means of raising and releasing the table and a hard solid surface to impact against on base of the assembly. A detailed drawing of a drop table similar to that used during testing is shown in Figure

2-10. The table, which is mostly accelerated by gravity, can be pushed or pulled downwards in the vertical direction to create the desired impact force. The wave shape of the impact can be further altered by changing the shape and material of the impact surface to create the desired impact. The drop table used in the experiment was tested using simple masses and proved sufficient at simulating a shock impact event characteristic of those experienced on high speed craft.

After the drop table was verified to be sufficient for testing; a Stidd 800v5 shock mitigating seat was attached to the drop table. The seat cushions were removed to isolate the suspension system for analysis by removing the additional suspension characteristics of the cushion. A lumped mass attached to the seat was varied from 180 lbs. to 205 lbs. to simulate a human occupant. Drop heights were from 6 to 18 inches to simulate the 5 to 12 g acceleration range experienced on high speed craft.

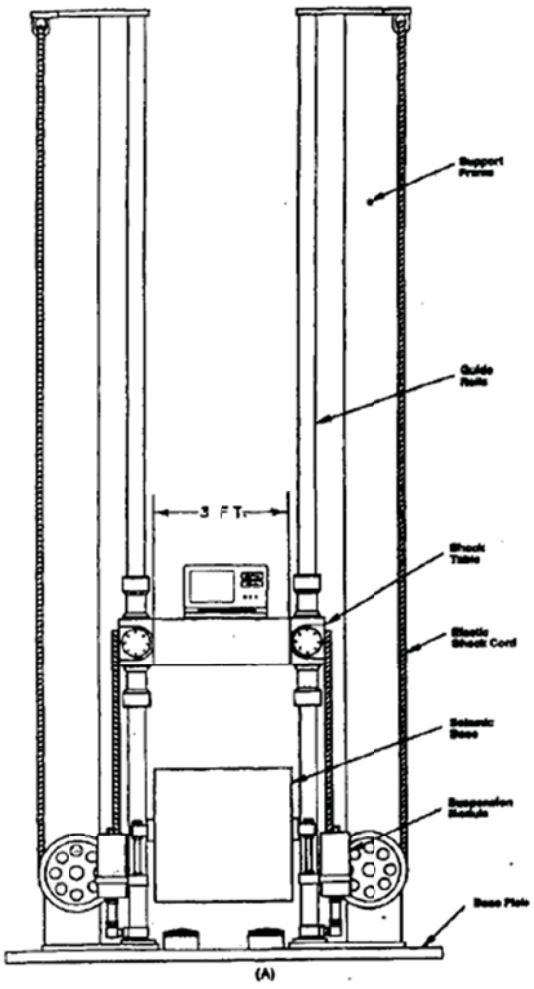

Figure 2-10. Drop table test setup used to simulate singular shock impact events.

Test data revealed that impact characteristics were repeatable and accurately simulated real world in sea events. The seat performance was assessed based on the percent reduction in shock, DRI numbers between different shock events, and transmissibility calculated. Even though exact values of percent reduction varied for the various test parameters, a clearly visible reduction in shock impulse harshness was evident for all the tests. The DRI values revealed that low to moderate impacts were attenuated well due to resulting DRI values below 5. A DRI value of 5.9 for the highest drop height used to simulate the most violent impact event revealed poor performance in extreme conditions. For comparison, a DRI value above 5 usually indicates a high likelihood of potential personal injury if enough impacts of this magnitude are experienced. Transmissibility

was then calculated to determine the frequency range in which the seat operates optimally. The transmissibility curve calculated is shown in Figure 2-11. Plotting of the transmissibility curve revealed that at excitations of 5 Hz or greater had a transmissibility of 1.0 or less. At excitation frequencies of 8 to 10 Hz the transmissibility dropped dramatically.

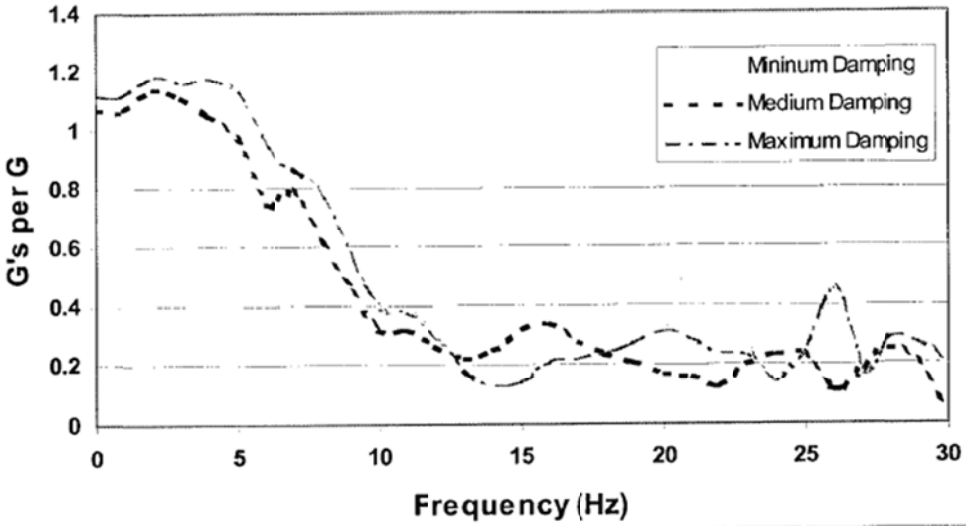

Figure 2-11. Transmissibility curves resulting from drop tests at varying heights and occupant masses [8].

Conclusions were made based on the acquired data. Based on the percent reduction of shock experienced between the base and seat the Stidd 800v5 is effective at reducing impact harshness. The DRI values indicated that the seat is most effective at reducing impact events with low to moderate magnitudes. The seat is not effective at reducing high magnitude impact events indicated by high DRI values resulting from the highest drop height. The transmissibility curve indicated that the suspension is tuned for reducing excitations of 5 Hz or greater with an extreme reduction in transmissibility in the range of 8 to 10 Hz. Seat performance should be optimal in the environment of high speed crafts due to the result that a majority of ship motion has a period in the range of 40 to 60 milliseconds. When comparing the seat performance results to the in sea testing data the seat is determined to be effective in mitigating shock impact.

Development of a Passive Shock Isolation System

Research on the shock isolation system for high speed craft has been previously conducted by Alan Klembczyk from Taylor Devices. A parametric study was conducted on the suspension system of a Stidd 800v5 shock mitigation seat with a focus on the spring rate, damping coefficient and suspension travel to find the optimum solution. This study focuses on the typical motion of the Mark V Special Operations Craft since the Special Operation Forces (SOF) utilize this boat for most of their missions and the best shock mitigation system to isolate the occupants from the harsh environment exposed.

A passive shock isolation system was chosen for its simplicity and high level of effectiveness. SOF desired a low risk, highly robust, reliable, and cost-effective solution for the Mark V SOC that would minimize any impositions on the mobility of the operators and crew [17]. Even though a fully active system has been developed and proved superior in isolating occupants from vibration and shock a fully active system requires external power, regular maintenance and is a more complex system. A semi-active system, while being less complex, still requires an external power. This established a passive isolation as being the optimal choice.

To conduct an analytical parametric study on choosing the optimal suspension parameters a two-degree-of-freedom spring-mass-damper model was used ,shown in Figure 2-12. The first system is the spring (Ks) and damper (Cs) of the shock isolation system. The second system is the spring (K1) and damping effects (C1) of the operator. Since the shock isolation system only attenuates motion in the vertical direction the other two axes are ignored to reduce complexity. Models of the system were also developed using the Taylor Shock Isolation Simulation Program and used to verify analytical results.

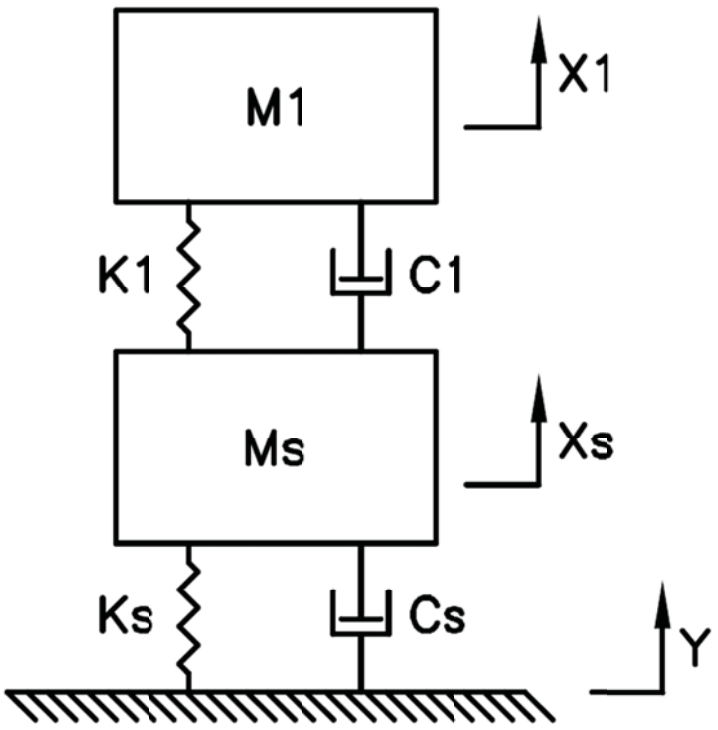

Figure 2-12. Two-degree of freedom system used to represent the shock isolation system of the seat and the human body's input to the system [17].

The first parameter to be analyzed is the spring rate of the shock isolation system. The suspension travel is first limited to the amount of available travel provided by the existing seat design; this limited the available travel to between 6.5 and 7 inches. A low spring rate would isolate the occupant better at low sea states, and reduce both Se and DRI values but would be ineffective at high sea states. A high spring rate would transmit more motion at low sea states but would be more effective at high sea states and prevent the system from being able to bottom out. A progressive spring rate is determined to be optimal. A lower spring rate is used for the initial displacement of the spring to maintain an acceptable comfort level while in low sea states and a high spring rate is used later in the suspension stroke to accommodate for more severe conditions.

After establishing an optimal spring rate a damping coefficient is then chosen to compliment. To determine the optimal coefficient a cost function was created based on DRI and Se calculated values. When testing multiple damping values the spring rate was held at a constant value. The motion from the system that is desired is to have enough

force to prevent the system from hitting the bump stops while allowing the system to follow the periodic nature of wave motion. A variable damping coefficient that was velocity dependent was chosen as the optimal solution to the varying input forces. This variable coefficient also proved to be efficient at adapting to varying occupant weights where the calculated DRI and Se values differed by a small percentage between the heaviest and lightest occupants.

The last parameter to be examined was whether an increase in suspension travel would prove beneficial. When a longer suspension stroke was implemented it was discovered that a lower spring rate had to be used to accommodate for the extended stroke, at the longer stroke the spring force dominates the suspension characteristics in an adverse manner. This resulted in having a spring rate that was uncomfortable, as was proven through in field test surveys. A longer stroke would also create visibility issues at certain areas of the suspension. For example, at the fully compressed position the occupant might have an issue seeing above the horizon line of the boat. When DRI and Se calculations were conducted it was found that suspension travel increase from 6.5 inches to 10 inches provided marginal improvements and did not warrant a change in design. A suspension travel length of 6.5 inches was proven to be optimal.

After the optimal parameters were calculated and simulated, at-sea trials were conducted to verify the system. The optimal shock isolator was built and fitted to a Stidd 800v5 seat on a Mark V SOC. Two boats were used on a test trip from Little Creek, Virginia to King's Bay, Georgia. One boat was fitted with multiple shock mitigating seats and another was fitted with standard rigid mounted seats. For the duration of the trip occupants were switched around between boats and between different shock mitigating seats. After the trip occupants were asked to complete questionnaires and provide feedback on the ride comparison. The ride quality was greatly improved by implementing shock mitigating seats. The ride was described to be completely comfortable, even after airborne events. The new shock isolators were proved to be superior to existing designs.

2.5 Summary

The research presented in this study is based on the background information given in this section and relies on objective measures for evaluating the efficiency of shock mitigating seats at isolating occupants from the high speed craft environment. Current research has provided knowledge on the response of high speed craft to wave slam events, methods for evaluating shock mitigating seats during at sea trials and a method of replicating a singular wave slam event in a laboratory environment repeatedly. There still remains very little work on replicating the harsh at sea environment of high speed craft in a laboratory environment. Also, testing a shock mitigating seat designed to be implemented on a high speed by subjecting the seat to singular drop tests impacts is not representative of high speed craft motion which usually results in personnel injury.

The major problem with current shock mitigating testing is that the only true representative way of evaluating the response of the seat towards high sea states on a high speed craft is to conduct in sea testing. There is currently no way of testing and evaluating shock mitigating seats in a laboratory environment while effectively simulating the motion of high speed craft. The ultimate goal of this work is to create a test method that is representative of a wave slam event and can be conducted repeatedly without the need of at-sea trials. This will be done by implementing a hydraulic actuator to simulate the high speed craft and measuring the response of the seat pan, then comparing the response to that of an in sea trial. The seat will also be evaluated on its response to multiple wave slam events.

Chapter 3. Shock Mitigating Seats

This chapter presents background information necessary in understanding the operation of shock mitigating seats. The information presented in this chapter is accumulated from a literature review of boat seat designs currently in use and in the design phase. The first section describes the three main types of suspension design. This is followed by a study of current shock mitigating seat designs. The section is then concluded with a comprehensive study of the Stidd 800v5 shock mitigating seat in which this research is based on.

3.1 Suspension Design

There are multiple ways to reduce the amount of shock in which the occupants of high speed craft are exposed to. Options for controlling shock on high speed craft include the design of the vessel, control of the vessel and shock isolation of the occupants [29]. The most effective solution to isolating occupants on high-speed craft that are currently in service is to implement shock mitigating seats. Shock mitigating seats can be installed in place of standard boat seats with minimal modifications to the ship structure, resulting in a relatively low cost solution that ensures occupant safety while underway. Shock mitigating seats implement a shock isolation system to absorb and reduce the forces transmitted to the occupant. The shock isolation systems implemented by various manufacturers are similar to those implemented in automotive suspension applications. The system includes use of a spring to absorb motion and damper to absorb the energy input to the system in the form of motion; together they greatly reduce motion and shock.

There are three types of shock isolation systems that can be implemented. The first and most commonly used of these systems is the passive isolation system. This includes the use of a spring and damper to absorb and dissipate motion. The damping coefficient of the damper in a passive system does not automatically adjust for varying environment conditions. A component diagram of a coil-over system is shown in Figure 3-1; this system setup is commonly used. A passive system is simple and effective at attenuating motion of specific conditions. From a ship design perspective, the shock isolation system

can be tuned for a specific sea state and occupant weight. Since the system does not require any sensors to read environment conditions no power source is required. The lack of a power source requirement and simplicity of application makes this system the most common choice.

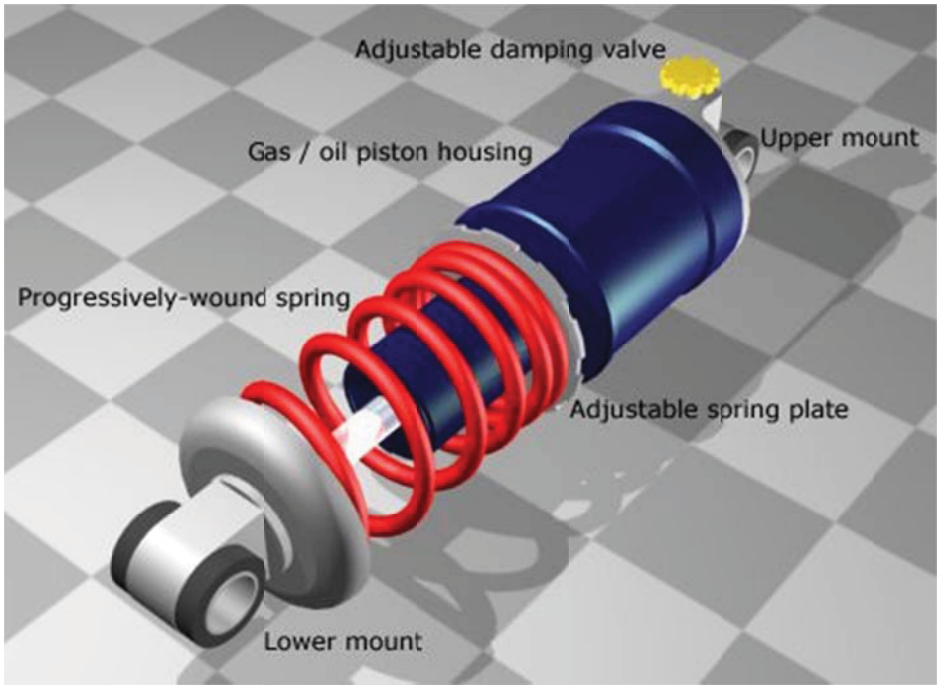

Figure 3-1. Coil-over suspension component break down. The silver and blue parts are the shock damper assembly while the red part is the spring energy [30].

The second most commonly used system implemented is the semi-active suspension system. The semi-active suspension also incorporates a spring and damper system just as the passive system. The damping coefficient of the damper changes in real time to accommodate for changes in the environment. The system incorporates a control scheme which uses sensors that read environment conditions to change the damping characteristics to best dissipate energy. The damping characteristics are changed by controlling the fluid valves within the shock assembly or by using Magneto Rheological (MR) technology to control the fluid characteristics. The MR dampers use magnetic fluid within the damper and a magnetic coil usually located on the piston assembly, damping characteristics are changed by varying an electric field generated by the coil which then

changes the fluid characteristics within the damper. The physical layout of a dual rod shock assembly is shown in Figure 3-2 to illustrate MR damper component structure. Semi-active seats require an energy source to operate. This dependency on an energy source sometimes detracts shock mitigating seat designers from using this system.

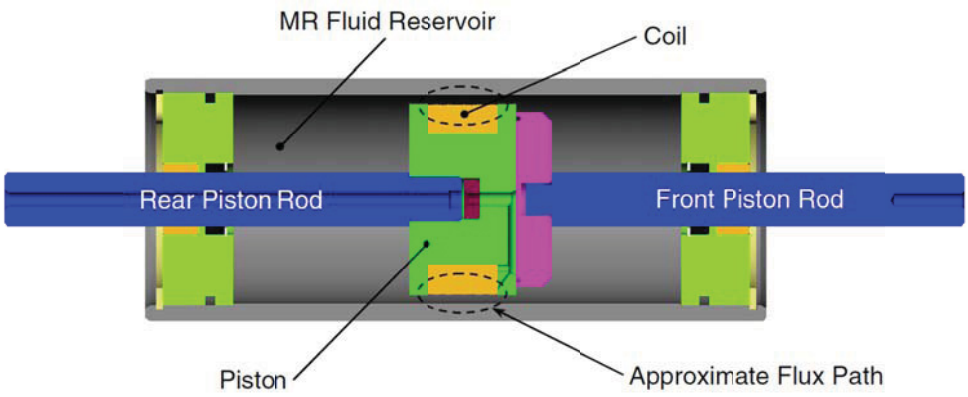

Figure 3-2. Dual rod MR damper component diagram showing MR fluid and magnetic coil location.

The third suspension system is the fully active or active system. This is most effective and complex system since an independent force can be exerted to control motion. In an active system an actuator is added to exert an independent force in the required direction to limit motion. Hydraulic, magnetic or electric actuators are used for force exertion. The addition of an actuator allows designers to completely control the dynamics of the suspension system. External sensors are used to determine environment conditions and focus is placed onto determining the environment ahead to allow the actuator to prepare the system for future outside input. An active suspension is rarely implemented due to the complex nature and high power requirements.

3.2 Shock mitigating seat design

There are multiple shock mitigating seat designs currently used by military and civilian high-speed craft today. These seats implement a variety of suspension designs and systems. One of the more popular shock mitigating seat designs for naval application is the jockey seat design manufactured by Ullman Dynamics. The Ullman jockey seat design is shown in Figure 3-3. The Ullman jockey seat utilizes swing arm suspension

geometry with one end mounted to the seat base assembly and the other end is connected to the suspended seat. The seat uses a simple spring and damper system to control motion. The seat is designed to optimize body posture to reduce personal injury during shock events [31]. The small size of the seat also makes it optimal for some of the smaller ships in service.

Figure 3-3. Ullman jockey seat design [31]

An advanced seat design was developed by VSSL to be operated in all sea conditions. The seat is able to achieve this versatility by implementing an advanced fully active shock mitigating system. A look ahead detection system is implemented to analyze on coming waves to determine the optimal parameters for the suspension system. The suspension system utilizes double swing arm geometry, much similar to a double wishbone suspension system of a racecar. The fully active system consists of an electric motor attached to a rack and pinion system to exert force on the seat, an adjustable damper and coil spring assembly. There are simple spring and damper coil-over

assemblies mounted horizontally on the base mount plate to control lateral motion. A detailed drawing of the seat is shown in Figure 3-4 to show the suspension geometry and components. The system is designed to operate as a passive system in the case of power failure. The complexity of the electronic control system and large design are the major drawbacks of this suspension design.

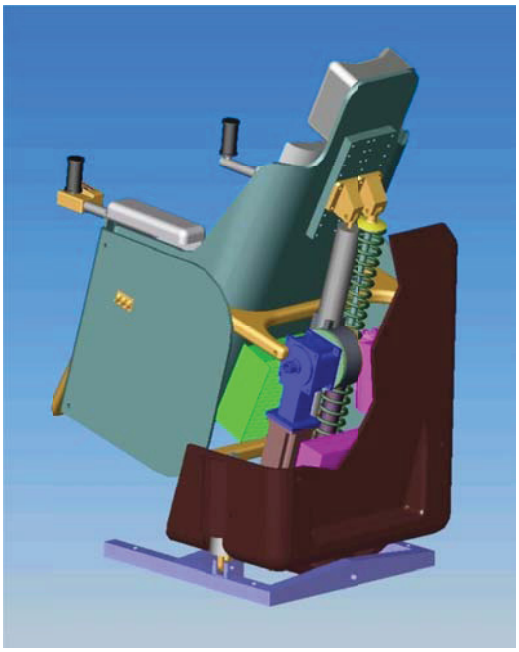

Figure 3-4. VSSL fully active shock mitigating seat diagram showing various suspension components and geometry [32].

A commonly used shock mitigating seat for the Navy and the main focus of this study is the Stidd 800v5 shock mitigating seat. The system consists of a suspended seat assembly using simple rod and linear bearings mounted vertically to only allow vertical motion. The seat frame is constructed from aluminum to reduce weight while maintaining structural integrity. The Stidd 800v5 uses a passive suspension system by implementation of a coil-over spring and damper. An example of the Stidd 800v5 is shown in Figure 3-5. The system consisted of an adjustable damper and spring preload to account for different occupant weights and ensure optimum system performance. The Stidd 800v5 replaced the Stidd V4 model which shared a similar base mount foot-print and was an easy solution in reducing shock harshness in vessels currently in service. The seat was tested in high sea

states at 50 knots on an MkV Special Operations Craft to validate that it provides superior comfort and safety for its operators [33].

Figure 3-5. Stidd 800v5 shock mitigating seat

3.3 In depth analysis of Stidd 800v5 shock mitigating seat

Quasi-static Analysis of Stidd 800v5 Suspension

A quasi-static analysis was conducted to determine the characteristics of the coil spring at various displacements and forces. A series of weights were placed on the seat and the displacement of the suspension system was then measured. The amount of weight that was placed on the seat varied from a value of zero which represented the static sprung weight of the seat assembly itself to a maximum value of 550 pounds in addition to the seat weight. The displacement was measured using a string potentiometer and the signal was recorded in dSPACE. The data was uploaded into Matlab to determine what force characteristic the spring contained. From a physical examination the spring was estimated

to have a linear characteristic since the spring diameter and coil spacing interval is constant throughout the spring. The data was plotted and a curve fit was conducted based on the data to determine the force curve of the spring. The data and line of best fit are shown in Figure 3-6 below. In Figure 3-6, the blue signal represents the data from the string potentiometer and the red signal represents the curve fit line that was given by Matlab's polyfit command for a single degree polynomial. The equation given from the polyfit command is 109.45x + 32.99, this represents a spring coefficient of 109.45 pounds per inch of spring displacement. The offset of 32.99 pounds could be caused from the fact that the spring had a slight preload set for optimum performance while at sea. The spring characteristic measured by the quasi-static test did match well with our hypothesis based on the physical geometry of the coils of the spring.

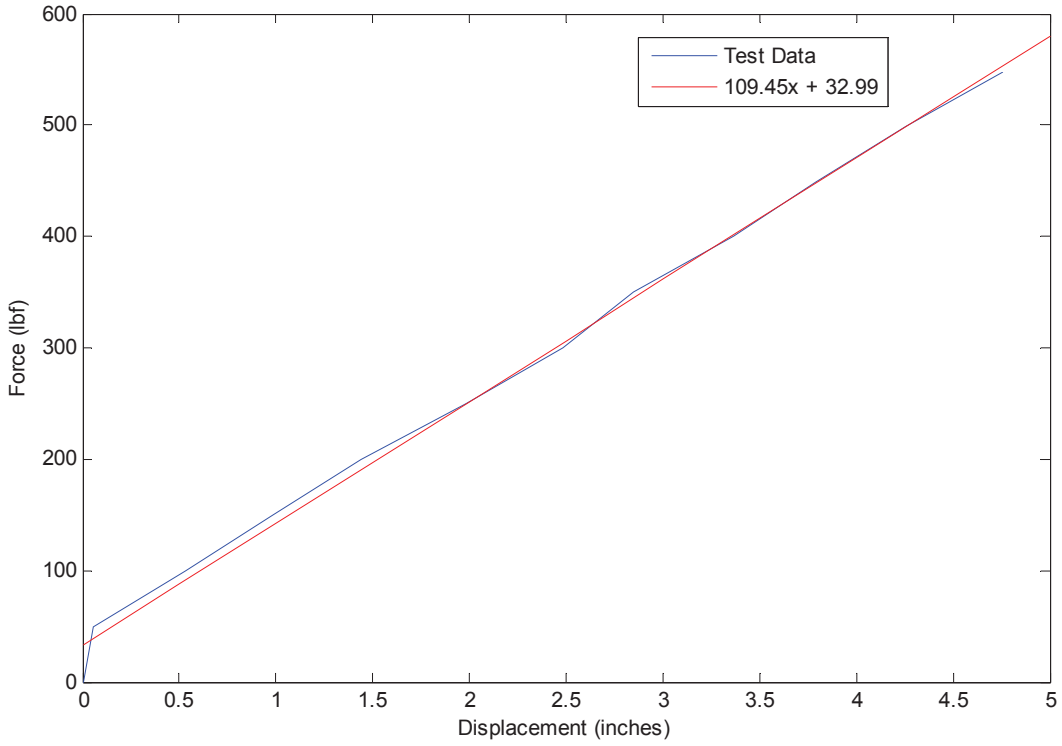

Figure 3-6. Quasi-static data used to determine the spring characteristics. Notice the linear nature of the data and curve fit line

Shock Disassembly and Testing

During initial validation tests it was observed that a slight amount of oil was leaking from the damper. To fully determine the cause of the leaking oil the shock assembly had to be taken apart. This also creates a great opportunity to better understand the dynamics of the shock by examining the internal components. The coil over spring is first removed from the damper assembly to allow for easy disassembly of the damper. The rod, rod guide, and piston were removed as a single assembly from the shock cylinder body. This single assembly is shown in Figure 3-7.The rod and piston assembly was then taken apart to allow access to the rod seal which is predicted to require replacement. Figure 3-8 shows the components that were taken apart from the rod assembly. Looking at Figure 3-8 the green component located at the left of the figure attaches the top of the rod to the seat assembly by use of a spherical bearing. The orange disc placed to the left of the green top connector is the rubber bump stop which prevents metal to metal contact in the that the shock uses its entire displacement. The green metal cap is used to hold the nylon rod guide which is the white object to the right and seal housing assembly to the bottom shock cylinder which is not pictured. The cylinder assembly pictured in the right of the figure is the brass piston/valve which controls the dissipation of energy from the system. The piston has a spring loaded cover which closes the orifices in the piston during a high acceleration event on the compression stroke to increase the damping coefficient.

Figure 3-7. Rod and piston assembly removed from shock cylinder.

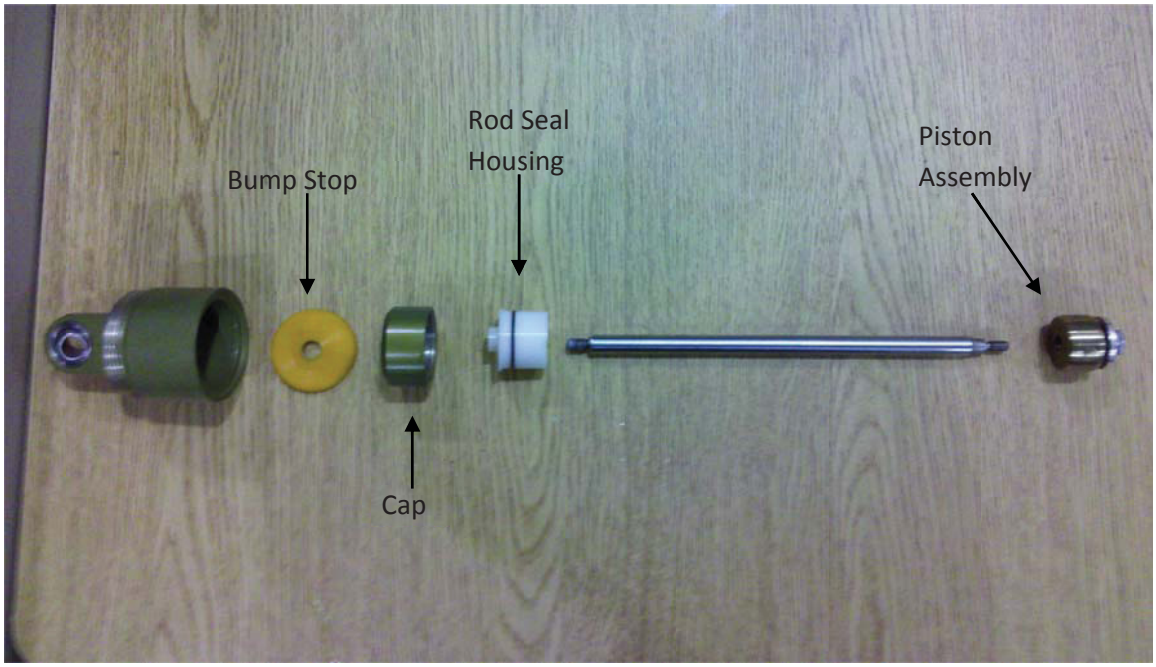

Figure 3-8. Rod assembly taken apart for a complete component break down

The nylon rod guide assembly was taken further apart to remove the rod seal for examination. Once the rod seal was removed it was clear that a replacement was required due to extreme deformation. The defective seal is a spring energized rod seal made of Teflon hard rubber material, pictured in Figure 3-9. A replacement seal was unavailable, a suitable rod seal was sourced to fit within the similar dimensions of the nylon piston top. A T-Lon Products Teflon Spring Energized Seal with an outer diameter of 0.625 inches and an inner diameter of 0.437 inches was used to replace the damaged original seal.

Figure 3-9. Original damaged rod seal removed from the shock assembly.

Once the T-Lon seal was implemented a replacement for the damper fluid was needed. Motorcycle fork oil was chosen for a replacement due to the similar operating conditions. Without much information pertaining to the dynamic properties of the originial fluid a dynamic viscosity test was conducted. Viscosity is simply the measure of a fluid's resistance to flow. A simple way of measuring the viscosity of a liquid is to measure the time it takes an object to sink a specific distance in the fluid. Equal amounts of original fluid and multiple weights of fork oil were placed into clear plastic syringes with a small air bubble of equal volume in each syringe, shown in Figure 3-10. Each syringe of fork oil was flipped right side and up side down along with the syringe of original fluid for comparison. A 40 weight heavy duty fork oil had the closest comparable viscosity to that of the original fluid and was chosen for the replacement fluid.

Figure 3-10. Viscosity test setup with equal amounts of fluid in each syringe and same air bubble volume

Once the replacement damper fluid was determined the damper was rebuilt. The damper was then charged to a pressure of 150 psi of nitrogen via the external bladder. The rebuilt damper was then placed on a Roehrig shock dynamometer to determine the force velocity characterisitcs. A peak velocity plot test was conducted at velocities of 1, 2, 5 and 10 in/s. The force and velcoity relationship derived from the peak velocity plot test is shown in Figure 3-11 where the negative velocity is the compression and the positive velocity represents the jounce. The initial charge pressure causes an initial force of 18.5 pounds at a velocity of 0 in/s with an initial displacement of 2 inches. The damper also demonstrates a bi-linear relationship in its damping characteristics. The damper provides a larger damping coefficient at lower velocities than higher velocites, the trend is more evident in compression than rebound. The change between the two damping coefficients seems to happen at about 1 in/s as indicated by the change in slope of the damping force curve in Figure 3-11.

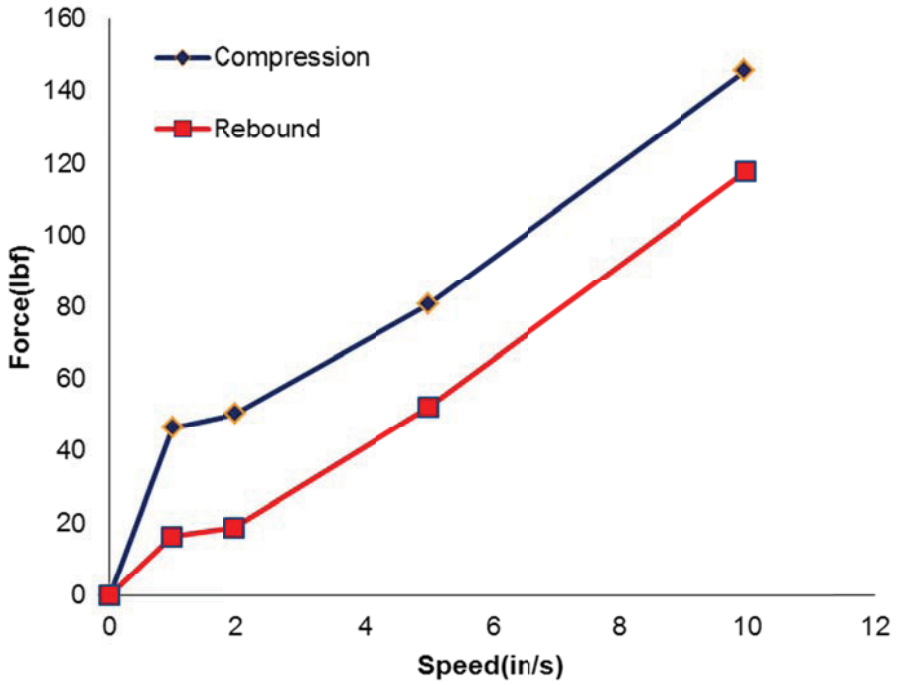

Figure 3-11. The higher compression resistance and digressive nature of the shock can be seen here.

The shock exhibits lower damping forces during rebound than in compression to prevent suspension jacking from occurring. Suspension jacking occurs when the system is compressed and does not fully extend before the following impact event, thus increases the risk of bottoming out the suspension. The lower damping force during rebound allows the system to return to its optimum position faster.

Chapter 4. Experimental Setup

The following chapter includes a detailed description of the experimental setup used for all the testing of shock mitigating seats during this study. The experimental setup section includes descriptions of testing equipment, data acquisition hardware and software, and testing procedures. The chapter is then concluded with an overview of the input excitations used for testing.

4.1 AVDL Seat-Testing Rig

The test rig was designed to provide a controlled environment for evaluating dynamics of a shock mitigating seat and the effects of extreme shock to the human occupant. The rig simulates motion in only the vertical direction. The rig is shown in Figure 4-1 below.

Figure 4-1. AVDL seat-testing rig.

The rig consists of an outer frame supporting structure with a mobile inner carriage made of 80/20 pre-formed aluminum. The outer structure is designed to be extremely rigid by implementation of diagonal and horizontal braces between the four vertical uprights. Early testing without the use of diagonal braces resulted in flexing of the outer structure and a collapse of the inner mobile structure. The outer frame is also bolted to a 3 ft square solid steel plate measuring 1 in thick that is bolted to a concrete floor. The inner carriage is also made using pre-formed aluminum to form a mobile carriage that is free to move in the vertical direction but is constrained in all other directions, as shown in Figure 4-2, ball bearing rollers permit low friction movement of the inner carriage.

Figure 4-2. Close-up shot of 80/20 rollers used to constrain motion in the horizontal plane while allowing freedom in the vertical.

The shock mitigating Stidd 800v5 seat is mounted to a 1 in thick solid steel plate that is bolted to the mobile inner carriage to ensure a solid mounting structure. A MTS hydraulic actuator is attached to the other side of the solid steel mounting plate of the carriage to

excite the seat in the vertical direction. The actuator is capable of simulating the high acceleration and shock that is experienced while underway in a high speed craft.

Hydraulic Actuation System

The test rig simulated ship motion with a hydraulic actuation system manufactured by Material Testing Systems (MTS). The hydraulic system is capable of simulating multiple types of events ranging from single frequency to multiple frequency waveforms. Force is introduced into the seat-testing rig by use of a hydraulic actuator pictured in Figure 4-3. The actuator used was a MTS model 242.09 actuator with a dynamic stroke of ±2 inches and a force capacity of ±2200 lbf. The MTS 242.09 is built with an internal load cell and Linear Variable Differential Transformer (LVDT) that allow accurate measurements of force and position. To avoid lateral loading on the actuator the attachment points at each end of the actuator are made with double revolute joints allowing complete freedom in the lateral direction.

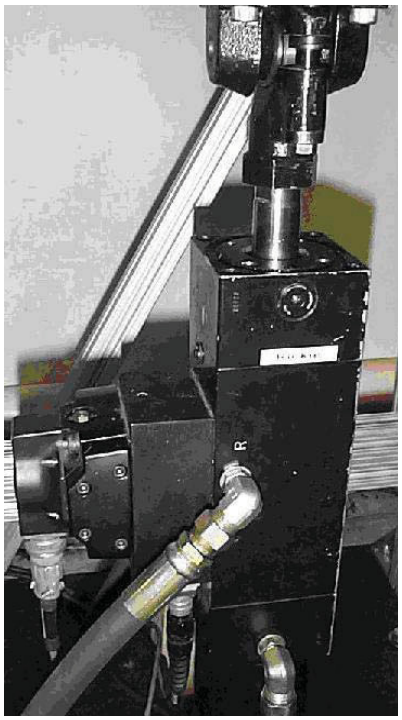

Figure 4-3. MTS 242 series hydraulic actuator used for input excitation

The actuator is controlled by the MTS 407 digitally supervised servo controller shown in Figure 4-4. The MTS 407 offers two modes of control, displacement or force, through a

single channel to the actuator. The controller is able to simulate a sine, square, triangle or external signal at various frequencies and amplitudes. All input signals to the actuator, whether it is an internal or external input, are sent through the MTS 407 controller.

Figure 4-4. MTS 407 Controller used to control the displacement of the MTS 242 actuator

The MTS 505.20 SilentFlo Hydraulic Power Unit was used to provide high pressure fluid to the actuation system. The hydraulic power unit used is shown in Figure 4-5. The power unit has a flow rate of 20 gal/min and an operating pressure of 3000 psi.

Figure 4-5. MTS 505 series hydraulic power unit used to provide pressurized hydraulic fluid

Pressure and flow of the hydraulic fluid from the MTS hydraulic power unit is regulated using the MTS model 263 hydraulic service manifold. The manifold used is pictured in Figure 4-6. A constant regulated flow is necessary to provide consistent and repeatable dynamic actuation of the actuator.

Figure 4-6. MTS hydraulic service manifold used to regulate fluid pressure and flow

3.2 Data Acquisition System

The data acquisition system is used to measure and record the signals coming from various sensors on the seat and test rig. Acceleration and displacement are measured using three accelerometers, an LVDT, a string potentiometer, a dSPACE digital signal processor, the MTS 407 hydraulic controller, and a laptop computer. The software used for the user interface was MATLAB/Simulink and dSPACE Control Desk. The following section is divided into two sections; one describes the hardware used for measurements while the second describes the software.

Data Acquisition Hardware

Multiple instruments are used to measure the response of the seat during testing. Three accelerometers are used to measure the acceleration of the seat floor, seat pan and mass of the seat. A PCB Micro-Electro-Mechanical Systems (MEMS) 3741D4HB10G accelerometer is used to measure the acceleration experienced at the seat floor or steel plate of the mobile seat testing rig inner carriage, the mounted accelerometer is shown in Figure 4-7. The accelerometer is mounted to the plate using vibration resistant superglue to ensure a strong hold while not introducing any unintended damping to the system. The MEMS accelerometer measures acceleration in only the vertical direction. A PCB 3713D1FD20G tri-axial MEMS accelerometer is used to measure the acceleration of the

seat pan. The tri-axial accelerometer measures acceleration in both the horizontal and vertical direction. This accelerometer is attached to the bottom of the seat pan, as shown in Figure 4-8, by use of superglue. A PCB 352C65 shear piezoelectric accelerometer is used to measure the response of the occupant mass on top of the seat cushion. The occupant accelerometer only measures acceleration in the vertical direction. The piezoelectric accelerometer is attached to the occupant mass by use of the provided wax. The accelerometer is shown in its test location in Figure 4-9.

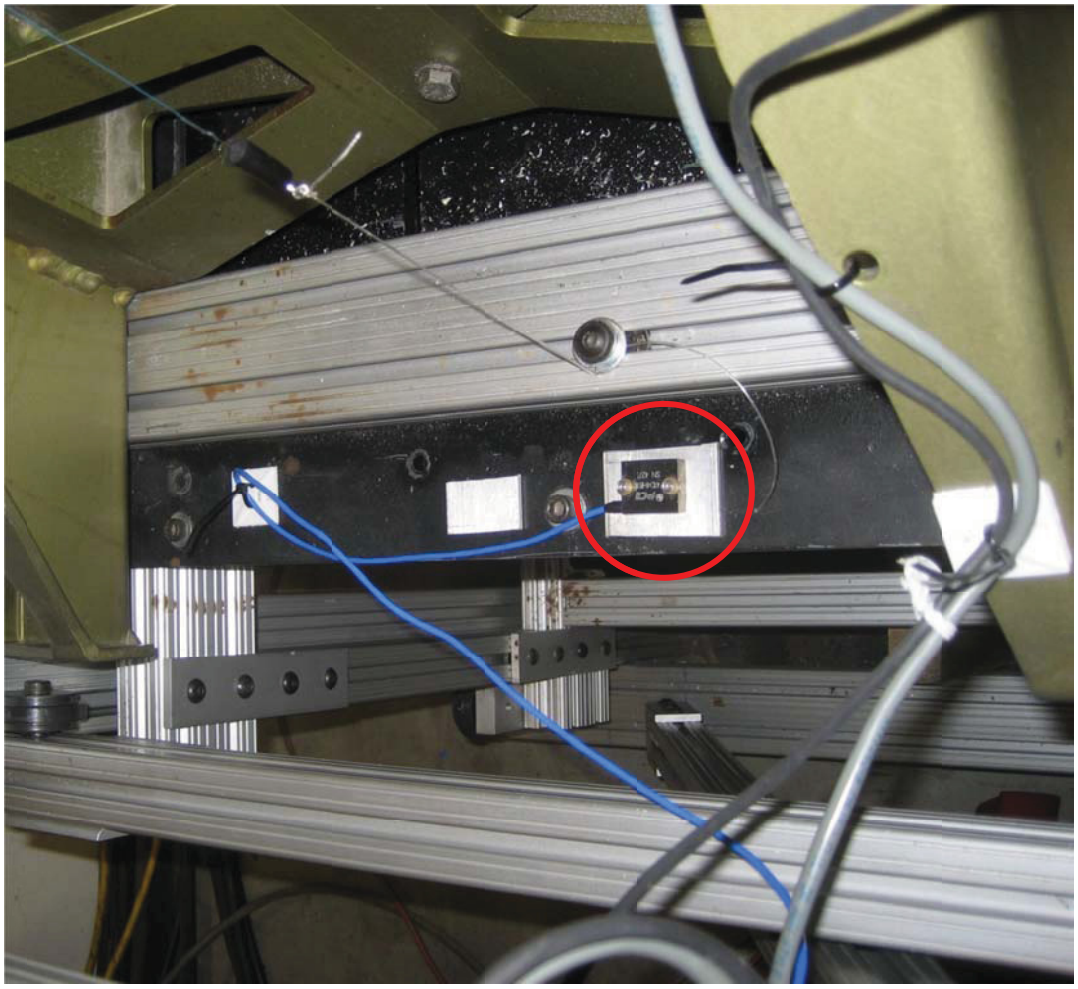

Figure 4-7. MEMS accelerometer, circled in red, mounted on the base of the seat shake rig.

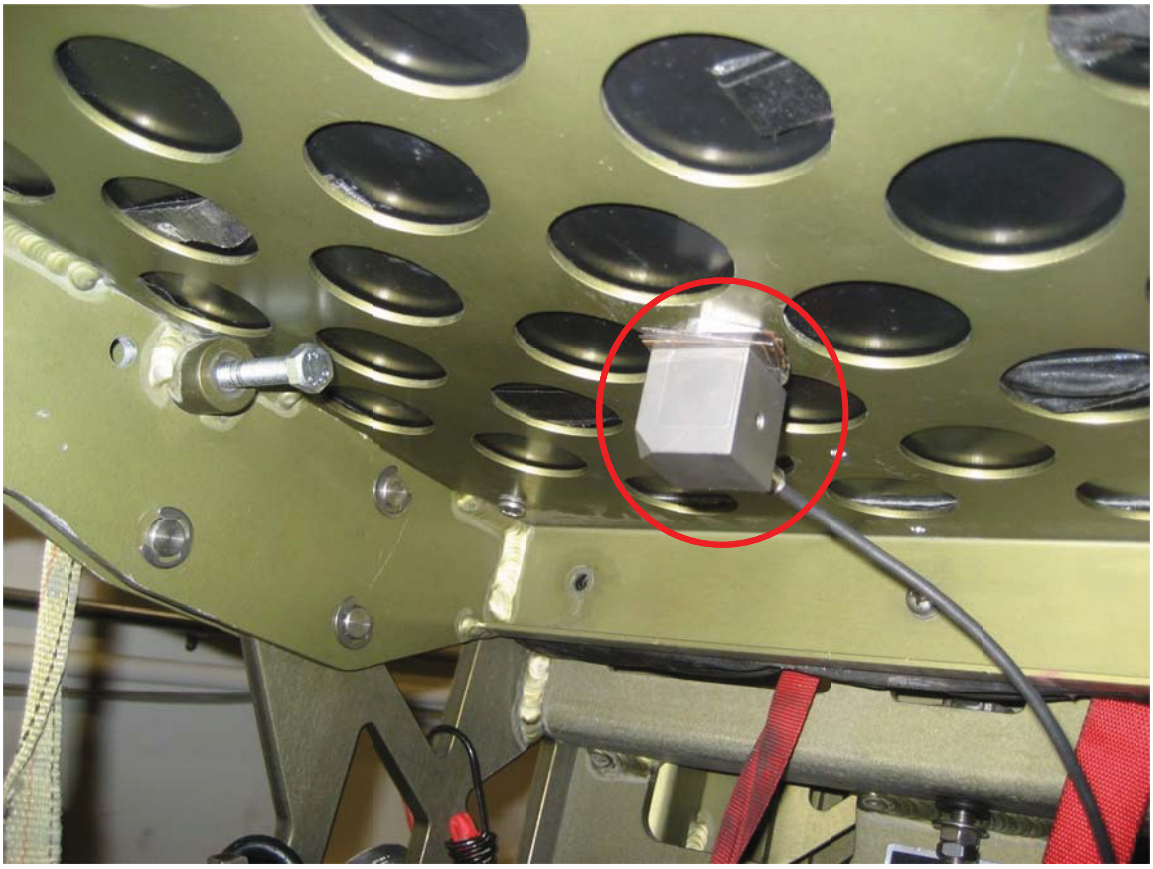

Figure 4-8. MEMS tri-axial accelerometer, circled in red, mounted under the seat pan

Figure 4-9. Shear accelerometer, circled in red, mounted on top of the occupant mass weights

A string potentiometer is used to measure the position and velocity of the shock mitigation system throughout the entire 6 in stroke of the damper. The string potentiometer is mounted on the bottom of the seat pan mounting brace shown in Figure 4-10. The string from the potentiometer is attached to the steel base plate floor of the inner carriage of the seat-testing rig. The string is positioned parallel to the suspension system to ensure that the measurements taken are consistent with the real time displacement of the suspension.

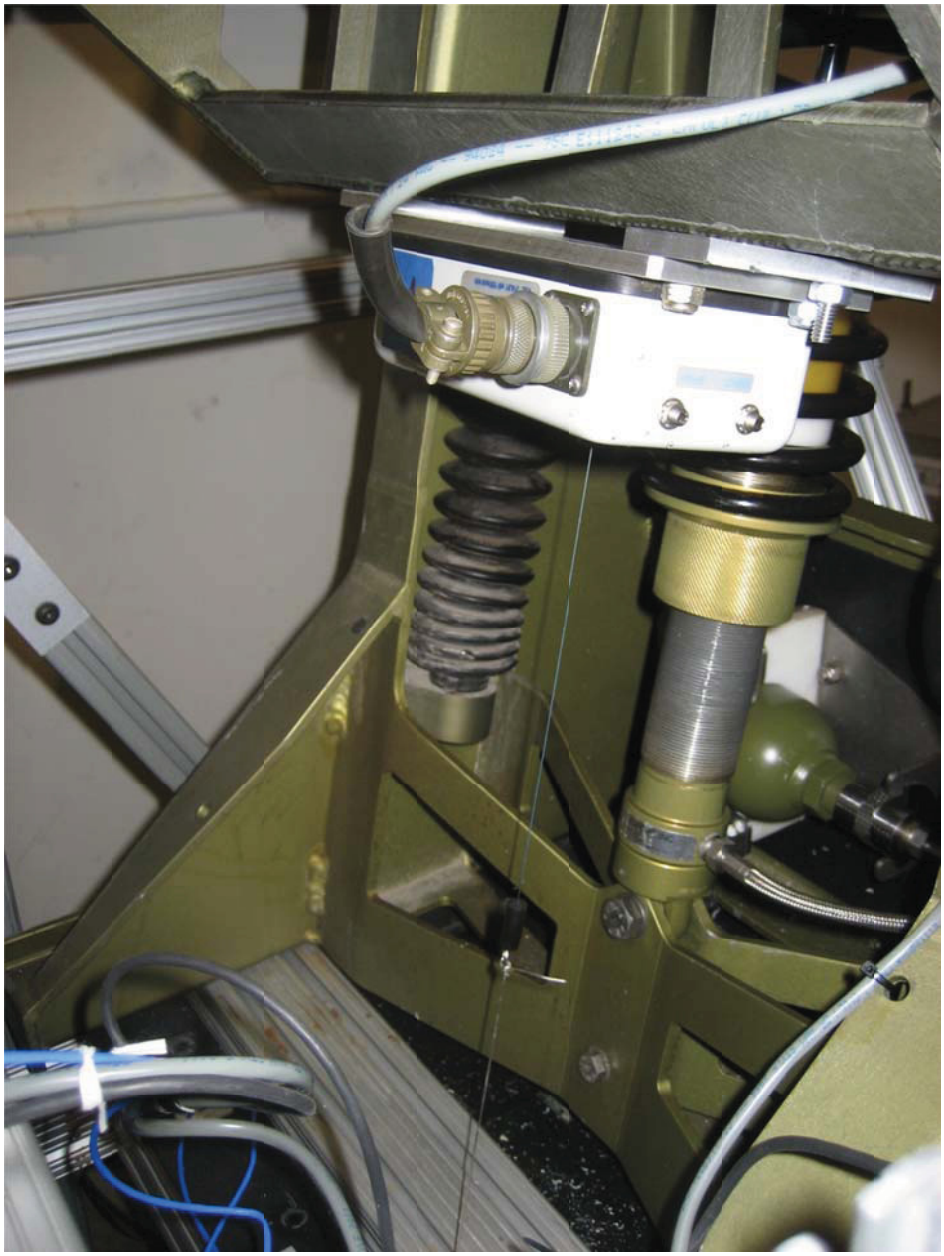

Figure 4-10. String Potentiometer mounted under the seat pan bracket parallel to the shock assembly

The position and force input into the test rig is measured using built-in sensors within the MTS 242.09 actuator described earlier. An LVDT measures the exact position of the actuator at all times, permitting the verification of system actuation. A load cell returns the force exerted by the hydraulic actuator in real time.

Signals from the accelerometers, string potentiometer, the internal load cell and LVDT of the actuator are connected to a DS2201ADC analog to digital converter then to the dSPACE AutoBox which is pictured in Figure 4-11. The AutoBox provides digital signal processing of all of the recorded signals measured rig. The AutoBox contains a DS 1003 processor board with an I/O card with 20 inputs and 8 outputs which is used to collect data and output control signals.

Figure 4-11. dSPACE AutoBox used for digital signal processing

The signal from the AutoBox is then sent to the laptop computer via Ethernet to be recorded and processed. Using Simulink a model for data acquisition and controller implementation is built for all inputs and outputs. The 20 input channels of the I/O card are multiplexed into 5 ports with 4 input channels per port; this data is then sent from the AutoBox to the PC computer. In the Simulink model the signals pass through a Demux that separates the incoming signals. Multiple block diagrams are used to specify and manipulate output controller signals and input sensor signals.

For real-time control and recording of the signals dSPACE Control Desk 3.0 software is used. The block diagrams created in Simulink are downloaded into the Control Desk software which communicates with the AutoBox. Control Desk provides a user friendly interface in which data can be viewed and model parameters can be changed in real-time. Various different displays can be used such as plots, numeric displays and indicators to create the user interface The Control Desk interface that was created to display the signals coming from the seat rig is pictured in Figure 4-12.

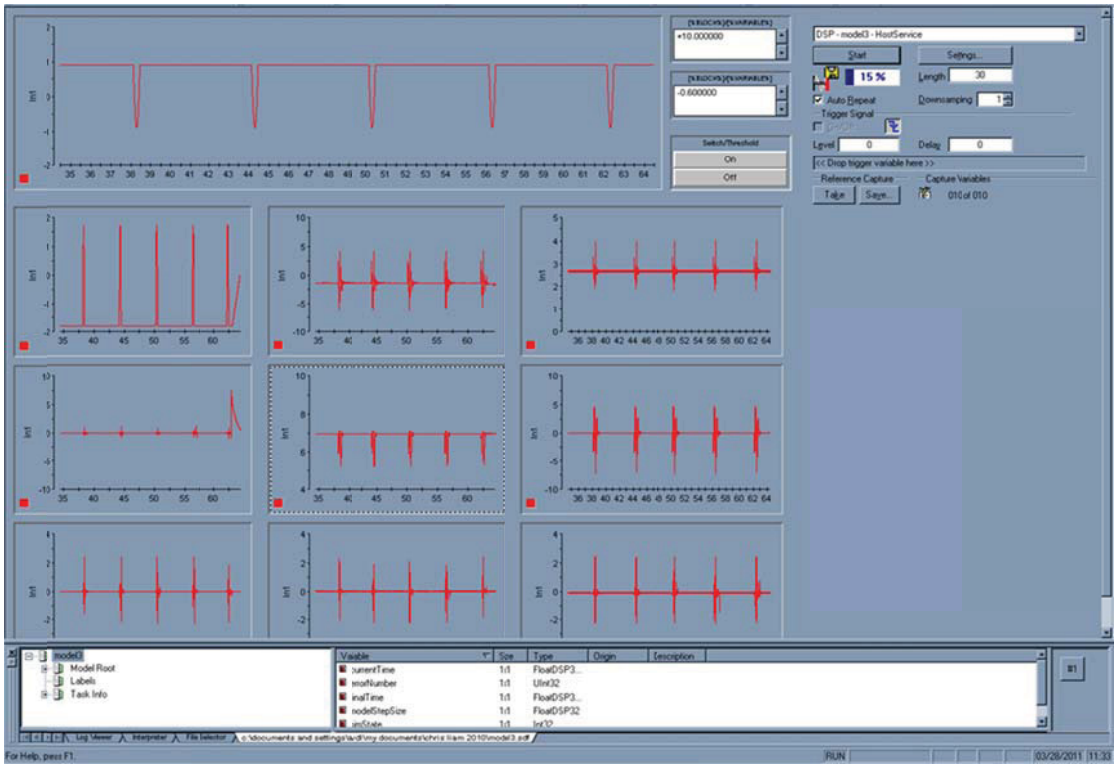

Figure 4-12. Screenshot of the Control Desk interface used to acquire data

The entire hardware structure used to acquire data and send an external signal to the hydraulic system is show in Figure 4-13. The flowchart in Figure 4-13 shows the transfer of data between the different hardware components of the data acquisition system.

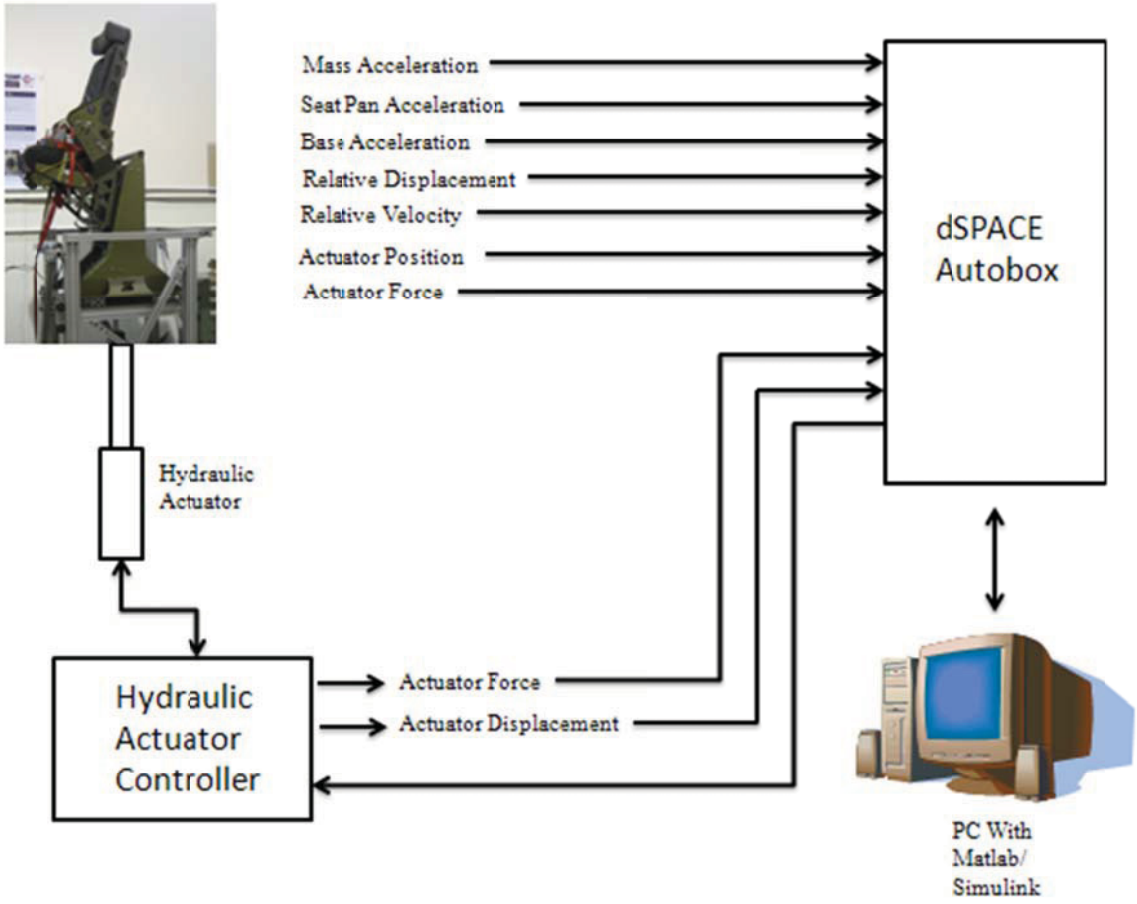

Figure 4-13. Flowchart of the data flow between the various hardware components of the data acquisition system

4.3 Terminology

Acceleration measurements are made at the seat floor, seat pan and occupant mass of the seat-testing rig. Transverse acceleration of the seat pan and relative measurements to the base are also measured.

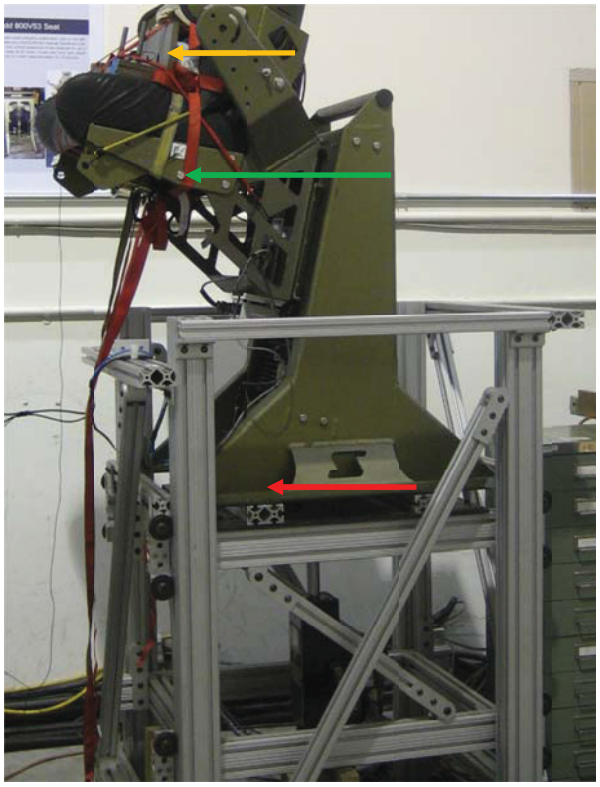

Figure 4-14. Seat Tester with indications of the positions of dynamic measurements. The red arrow represents the base(1), the green arrow represents the seat pan(2) and the yellow arrow represents the mass(3)

Referring to Figure 4-14, the terminology is as follows:

(1) Base: vertical measurements made at the interface of the seat attachment boat structure.

(2) Seat pan: tri-axial measurements made of the suspended metal seat frame under the seat cushion

(3) Mass: vertical measurements made on top of the occupant mass which is above the seat cushion

Based on these definitions, the following are defined:

- Transverse: horizontal measurements made at the seat pan
- Relative displacement: displacement of the seat pan relative to the base.

4.4 Input Signals

High Speed Craft motion can vary depending on various conditions similar to sea states. Due to the great variation in motion it is difficult to simulate all types with a singular input. For this reason multiple input signals were used to evaluate the characteristics of the Stidd 800v5 shock mitigating seat. Ship motion from a small, medium and large high speed planing craft was simulated. A half sine wave and square wave input were used to gain the free response of the system and also to measure the response of the seat to singular events. A chirp signal was created to measure the response of the seat at various frequencies. The input signals either were derived from integration of at-sea ship testing accelerometer data or created using MATLAB to get a desired response from the system.

High Speed Planing Craft

Acceleration data taken from at-sea testing of the Stidd 800v5 Shock mitigating seat was integrated to produce displacement data. The at-sea testing accelerometer was located at the base of the seat. Testing took place on an 89 foot high speed planing craft which represents fairly large ship. The displacement data is then filtered to isolate frequencies between 1.49 and 20 Hz so that the maximum displacement is ±2 inches. Figure 4-15 shows the time response data that is used while testing.

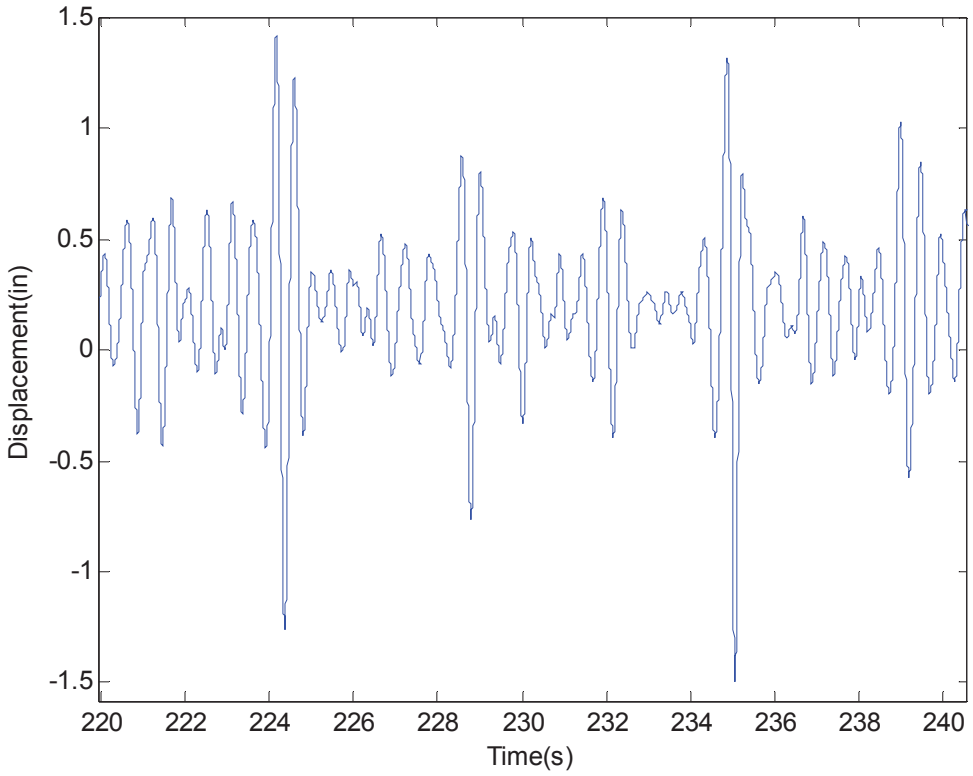

Figure 4-15. Sample of the data used to simulate an 89 foot high speed planing craft

36 foot USN Planing Craft High Sea State Test Data

Acceleration data taken from a 36 foot USN planing craft was also integrated to produce displacement data. Since the 36 foot USN is a small craft, the motion of the ship is fairly violent when compared to the larger 89 foot craft mentioned previously. There are also two different test files used, one is with the ship traveling so that the waves are impacting in a head direction and the other in the stern direction. The displacement data is then filtered to isolate frequencies between 2.1 and 70 Hz so that the maximum displacement is ±2 inches. Figure 4-16 shows the time response data of the head sea ship direction and Figure 4-17 is the time response data of the stern sea ship direction.

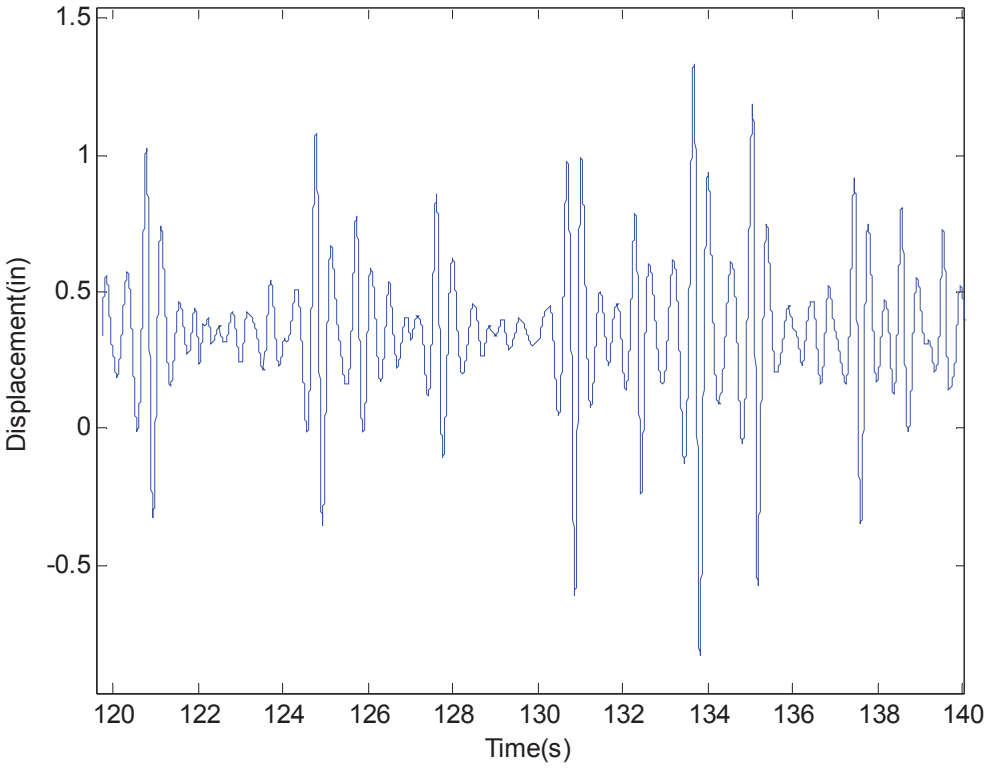

Figure 4-16. Sample of the data used to simulate a 36 foot USN craft in head seas

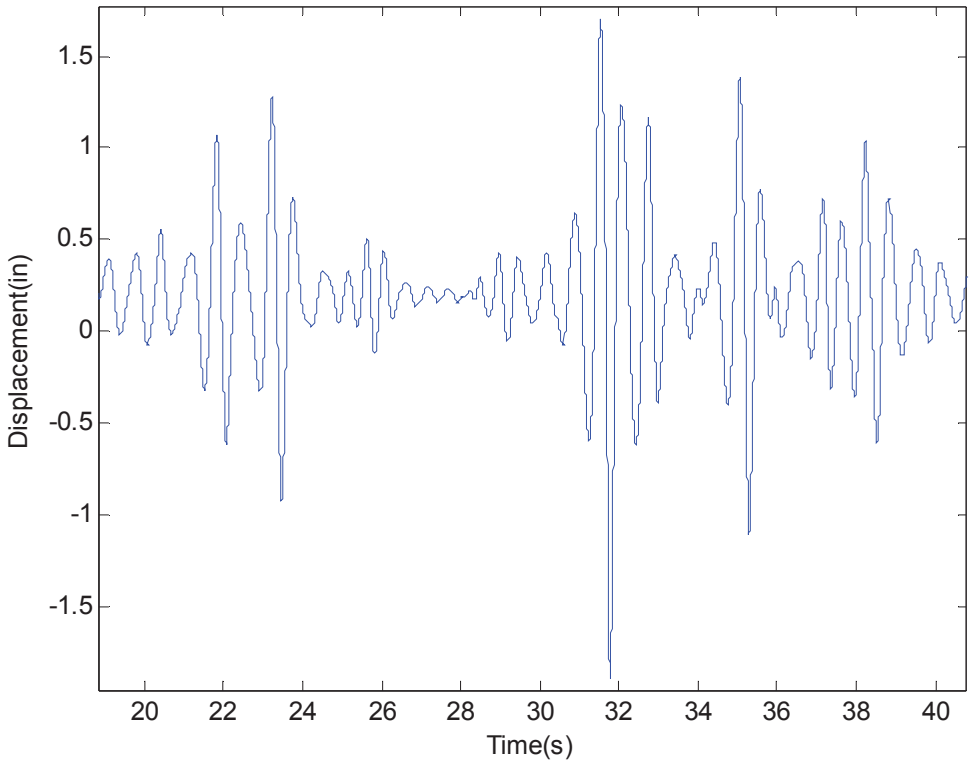

Figure 4-17. Sample of the data used to simulate a 36 foot USN in stern seas

47-foot Motor Life Boat (MLB)

Acceleration data taken from at-sea testing of a 47-foot Coast Guard Motor Life Boat (MLB) was integrated to produce displacement data. The accelerometer used for testing was located on the floor of the ship wheel house. The MLB is capable of being operated in extreme conditions due to its strong hull structure and self-righting characteristics. From the available at sea data the MLB would represent the medium size boats that the seat would be placed on. The displacement data is also filtered to isolate the data at frequencies between 1.3 and 12 Hz so that the maximum displacement is ±2 inches. Figure 4-18 shows the time response data used for testing.

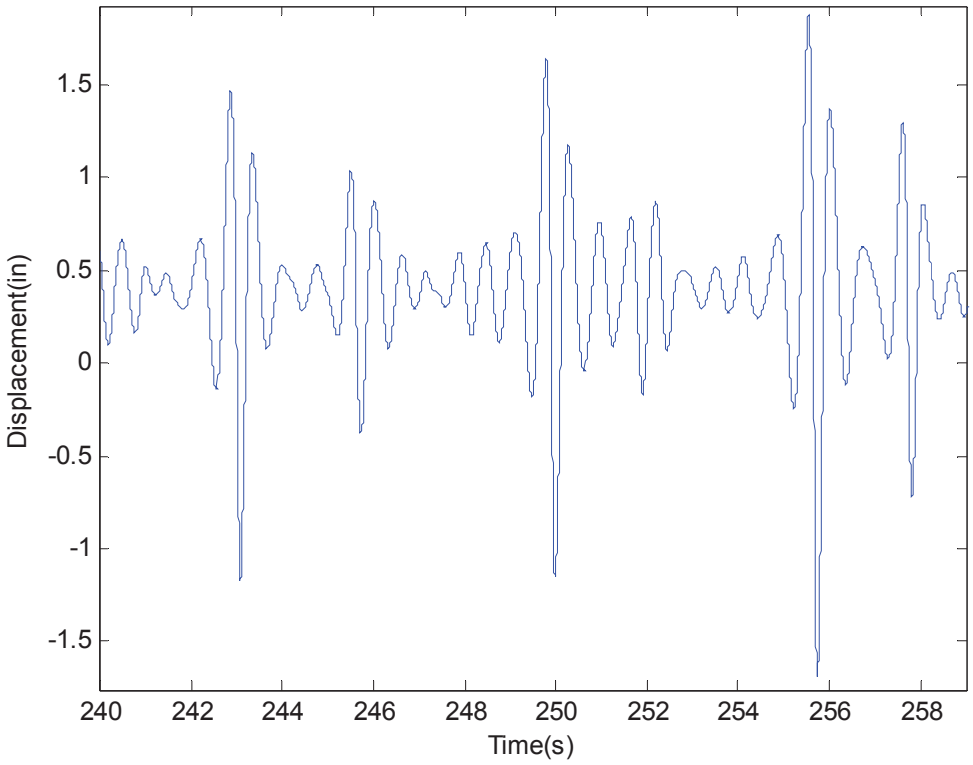

Figure 4-18. Sample data used to simulate the motion of a 47 foot motor life boat

Generated Signals

To produce the maximum shock possible from the test rig, input signals were created based on the abilities of the hydraulic system. To simulate the greatest amount of shock possible a square wave is created using the maximum amplitude of 2 inches in which the hydraulic actuator is able to produce at a frequency of 0.1 Hz. A sample square wave is shown in Figure 3-19. A half sine wave is also created at amplitude of 4 inches and a frequency of 1.5 Hz. This was tested to be the highest frequency in which the hydraulic system was able to fully complete the entire cycle. The generated half sine wave input is shown in Figure 3-20. To analyze the frequency response characteristics of the seat assembly a chirp input was created. The chirp signal started at a frequency of 0.5 Hz and amplitude of 0.9 inches, it then progressed at a constant rate over a 120 second time span to a frequency of 15 Hz and amplitude of 0.05 inches. The chirp input signal can be seen in Figure 4-21.

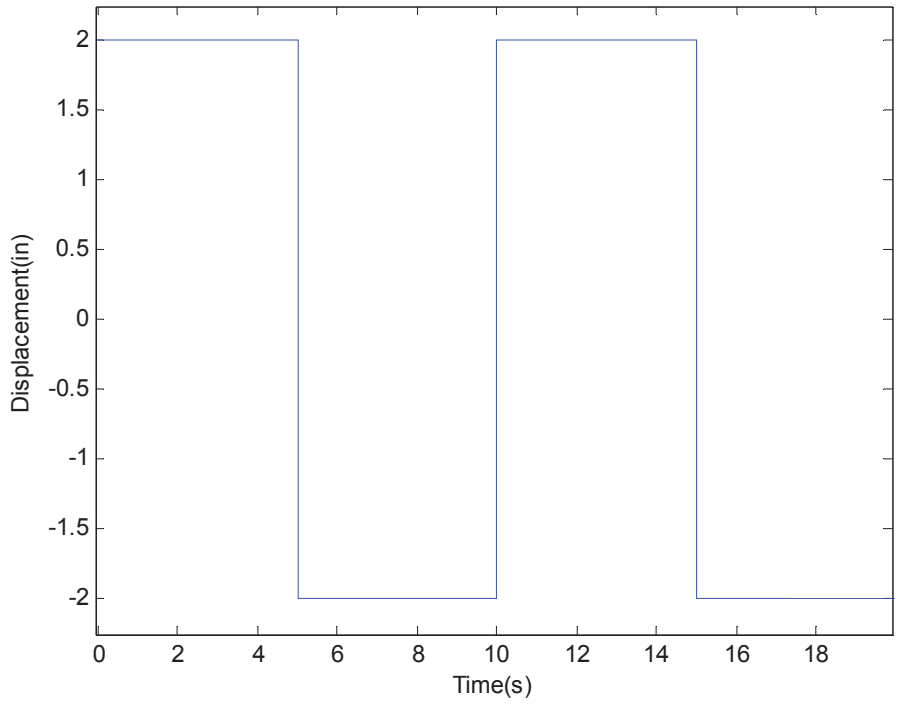

Figure 4-19. Square wave used for testing the largest and quickest drop event

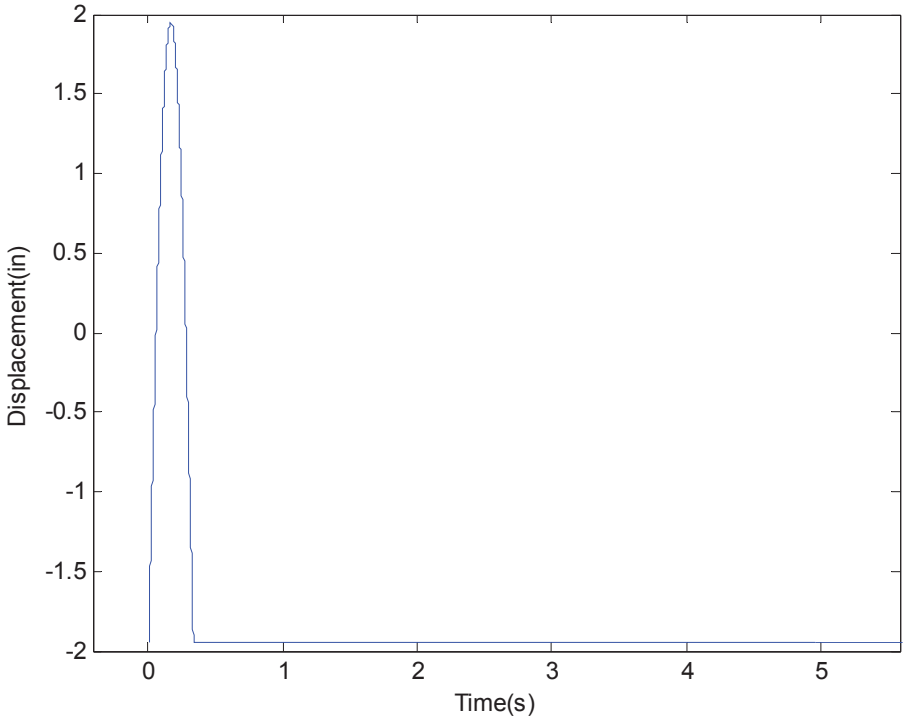

Figure 4-20. A half sine wave with amplitude of 1.5 Hz used to simulate the largest up and down event possible with the actuator

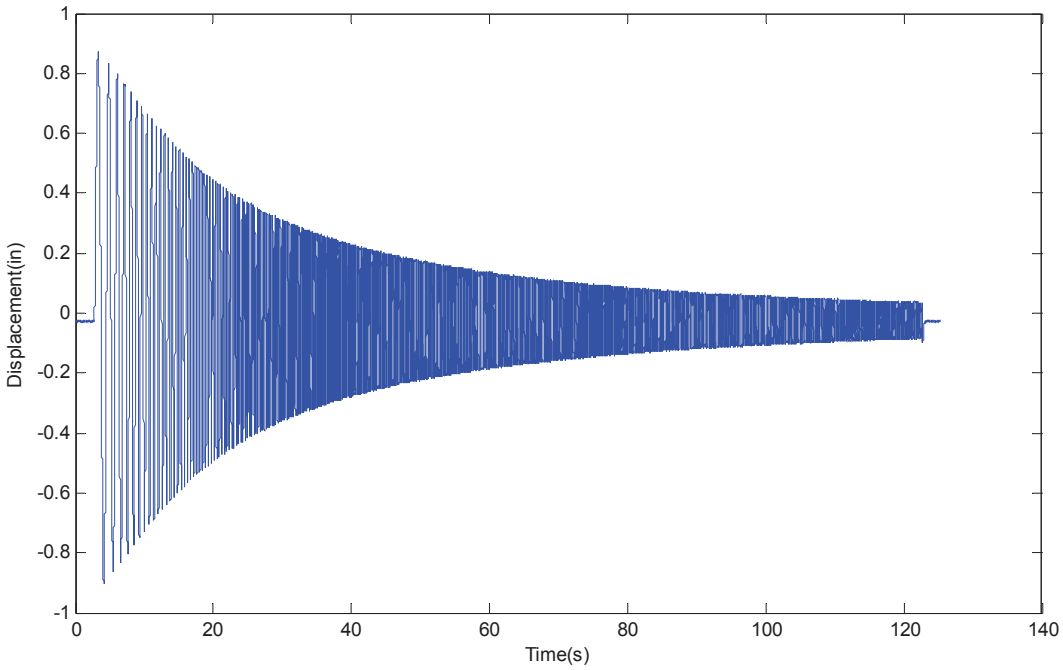

Figure 4-21. The chirps signal starting at a frequency of 0.5 hz and ending at 10 hz over a 2 minute time span

Chapter 5. Test Repeatability

The following chapter includes a detailed analysis of the repeatability of the experimental setup. The data set that was used for the analysis of repeatability was the data set derived from simulating the at-sea motion of an 89 foot high speed planing craft. To determine the extent of repeatability three different runs of the same base excitation were compared. The double integrated displacement occupant mass acceleration data was examined. This particular signal was chosen because the occupant mass data set would have the highest amount of variation when compared to the other recorded data sets. The sources of variations include the response of the coil over system, the response of the seat cushion and the variation in occupant mass location. The variation in occupant mass location is caused by the natural movement of the occupant mass due to the slack in the strap restraints. The slack in the traps is used to simulate a real at-sea situation where the human occupant would move around in the seat during large impacts.

The occupant mass acceleration data from the three separate runs were first synchronized to ensure that each test started and stopped at the same time, this is accomplished by setting the zero time to when the first excitation event occurred. Then the three data sets were overlaid on the same plot axis, a portion of the overlaid time series data is shown in Figure 5-1. Visual examination of the overlaid plot of the time series data reveals a good amount of repeatability between the runs.

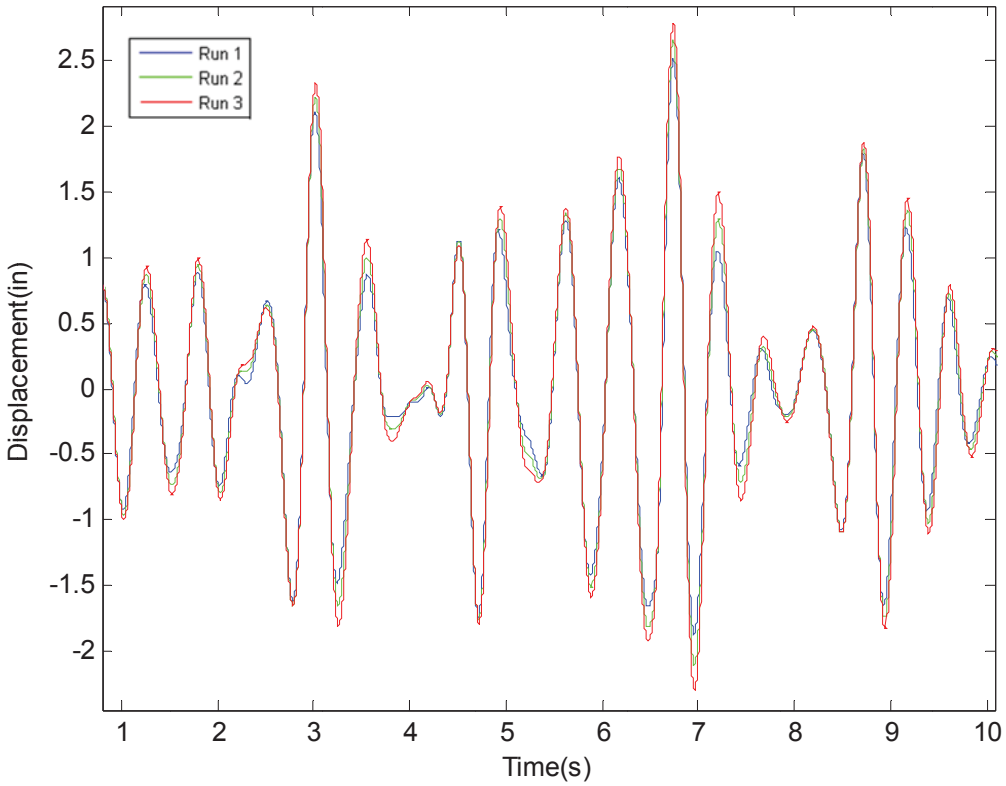

Figure 5-1. Overlaid time series data from 3 separate runs of the high speed planing craft at sea data

The repeatability of the three test runs were then quantitatively determined. The first data set, represented by the blue trace in Figure 5-1, was used as a baseline for the comparison. The difference between data sets 1 and 2 was determined, and then the differences between data sets 1 and 3 were determined. The calculated differences are plotted in Figure 5-2; the blue trace is the difference between runs 1 and 2 while the green trace is the calculated difference between runs 1 and 3. A majority of the differences are within the range of ±0.2 inches. The differences between data sets 1 and 3 are greater than the differences between data sets 1 and 2. However, the locations of the discrepancies are for the most part consistent between the two comparisons and usually occur at the larger events. This could be due to the fact that the largest amount of variation occurs when the occupant mass leaves contact with the seat cushion.

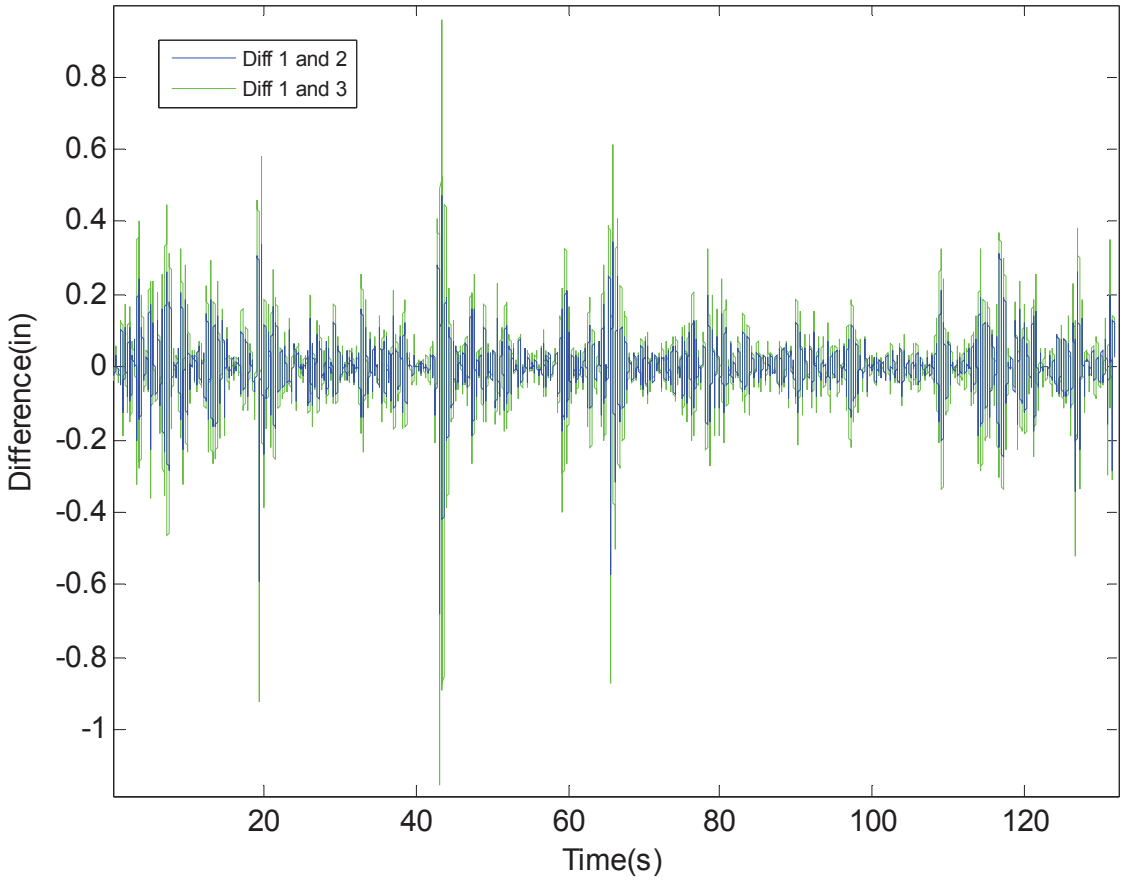

Figure 5-2. Calculated differences between the three runs plotted. The blue trace is the differences between runs 1 and 2. The green trace is the differences between runs 1 and 3

The data sets are further examined by calculating the probability density function of the two comparisons. The probability density function calculates the percentage of data points of the total test that fall into set difference intervals. This portion of the analysis was done using MATLAB's histogram function which takes a data set and interval vector, and then calculates the amount of data points within each set interval. By dividing the histogram data by the total amount of data points a percentage of the overall data set is calculated. Using this process a probability density function of the difference between data sets 1 and 2, then data sets 1 and 3 was calculated. Figure 5-3 shows the probability density function of the difference between data sets 1 and 2. From the probability density function shown in Figure 5-3 it can be seen that 41.9 percent of the data points have a

difference of less than ±0.025 inches between the two runs and 79.2 percent of the data have a difference of less than ±0.075 inches between the two runs.

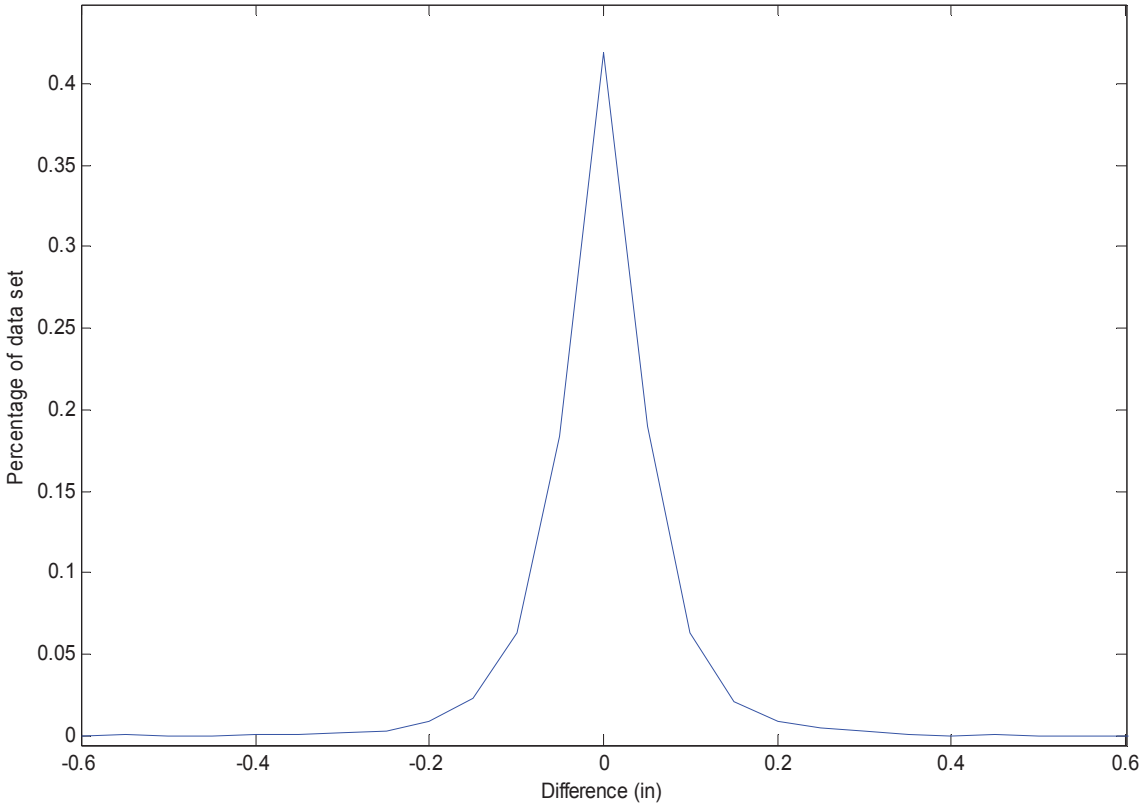

Figure 5-3. Probability density function of the difference between data sets 1 and 2

The probability density function of the difference between data sets 1 and 3 is shown in Figure 5-4. From probability density function 29.3 percent of the data had differences of less than ±0.025 inches between runs and 65.7 percent of the data had a difference of less than ±0.075 inches between the runs. When examining the differences and percentages between the three runs it is important to take into consideration that the overall stroke of the actuator is ± 2 inches and a difference of even 0.075 inches is only 3.75 percent of the stroke. Averaging the results from analyzing the three runs 35.6 percent of the data have differences less than ±0.025 inches and 72.5 percent of the data points have a difference of ±0.075 inches or less. When reviewing all the facts previously stated, the largest source of variability between tests only has a difference of ±0.075 inches about 72.5 percent of the time during tests.

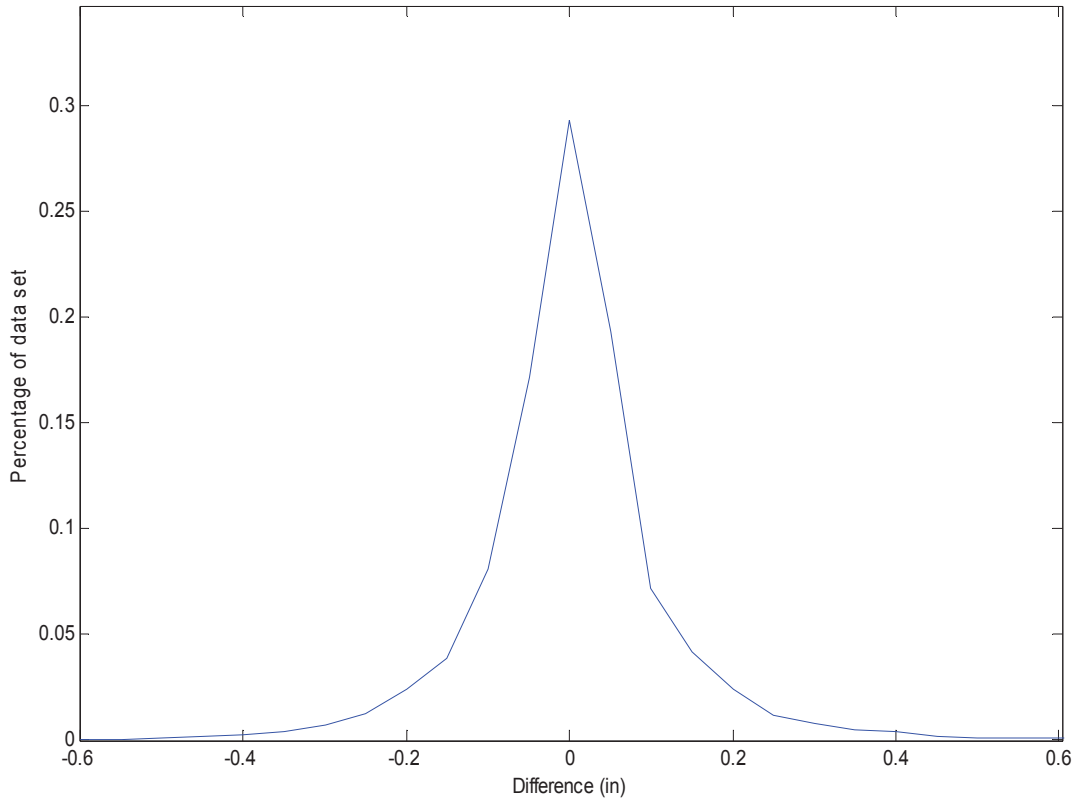

Figure 5-4. Probability density function of the difference between data sets 1 and 3

To further support the high repeatability of the seat testing rig the statistical probability density function was calculated. The probability density function of a continuous random variable is a function that describes the relative likelihood for this random variable to occur at a given point. The variable of concern is the difference between two data sets using the same input excitation. The difference between data sets 1 and 3 was used since it had the largest differences. The calculated mean of the data set is -1.4903×10^{-5} inches and the standard deviation is 0.0769 inches. Using MATLAB the probability density function is calculated and shown below in Figure 5-5. The x axis represents the difference between data sets 1 and 3. When examining the data set, 1 standard deviation from the mean represents a 68.3% confidence level and 2 standard deviations from the mean represents a 95% confidence level. For purposes of this study this translates to having a 95% confidence level that the difference between two data sets being within ±0.15 inches and also having a 68.3% confidence level that the difference will be within ±0.0769 inches of each other.

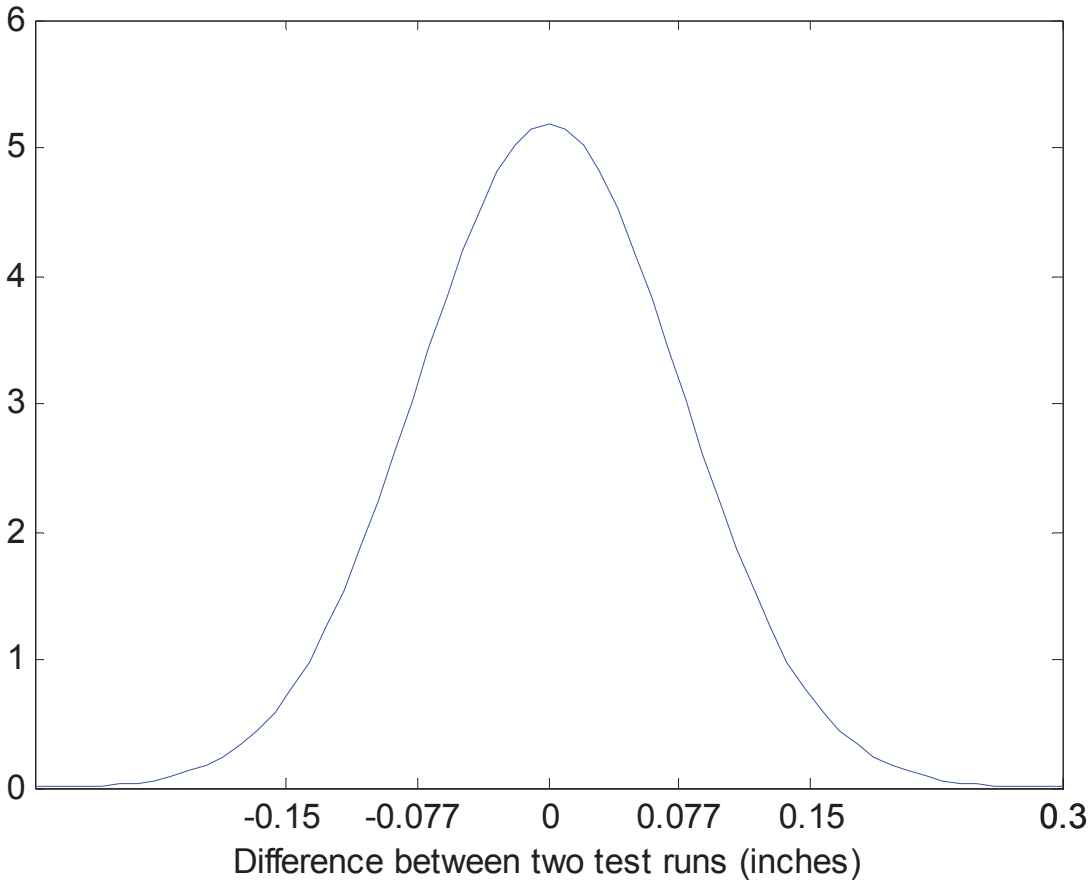

Figure 5-5. Statistical probability density function of data sets 1 and 3

Chapter 6. Effectiveness of Shock Mitigation

The following chapter includes a detailed description of the comparison between the response of the seat with and without a shock mitigation system. The comparison was conducted by replacing the shock mitigation system with a solid aluminum bar. The chosen conditions for the shock mitigation system were a suspension preload of zero and an occupant mass weight of 200 pounds. The effectiveness of the shock mitigating system was calculated two ways. The first is by comparing the Dynamic Response index (DRI) between the shock mitigating seat with that of the non-shock mitigating seat from the same input excitation. The other method used to analyze the effectiveness of the system is to determine the magnitude of the 90th percentile of the acceleration values from each data set.

6.1 Examination of the DRI

The main objective when placing shock mitigating seats on high speed craft is to reduce the effect of extreme shock events on the craft occupants. Most injuries from at-sea voyages are a result of a few extremely large impacts. To gauge the effectiveness of the shock mitigating seat at reducing the shock and acceleration experienced by the occupant the Dynamic Response Index (DRI) was calculated since it is based on the largest singular event in a data set. DRI was created in the 1970's by Payne to assess the effect of isolated shock events on the sitting human, mainly for jet ejection seats [34]. DRI is calculated using equation 6-1.

$$DRI = \frac{\delta * \omega_n^2}{g} \tag{6-1}$$

Where δ is the maximum displacement of the spine, ω_n^2 is the square of the natural frequency of the human modeled as a spring mass damper system and g is the acceleration of gravity. Essentially the numerator of the equation represents the peak acceleration that the human spine observes. This simplifies the equation to that shown in equation 6-2.

$$DRI = \frac{peak\ acceleration\ on\ spine}{g} \tag{6-2}$$

Using equation 6-2 and the peak acceleration of the occupant mass from each test the DRI values are calculated. The percentage reduction of the DRI due to implementing a shock mitigation system is shown in Table 6-1. The amount of reduction in DRI ranges from 39.4 to 64.2 percent. This range of reduction is fairly significant and can noticeably reduce the likelihood of injury. The Air Force has established that a DRI value of 5 translates to a high likelihood of spinal damage and permanent injury [8]. By implementing a shock mitigating system the DRI value for the square wave input is reduced from an injuring value of 5.03 to a value of 1.80, greatly reducing the likelihood of personal injury.

Table 6-1. DRI values calculated using the peak acceleration from each test

Test Input	Shock Mitigating	Non-Shock Mitigating	Percentage Reduction
USN Head	2.21	4.33	48.8
USN Stern	1.34	2.22	39.4
MLB	1.69	3.17	46.7
89 ft	1.63	3.19	49.0
Impulse	1.55	3.55	56.3
Square	1.80	5.03	64.2

6.2 Examination of the Acceleration Values Observed

The examination of the DRI value is the main focus of the analysis since most injuries are due to a singular high impact event, represented well by the DRI value. To examine the effectiveness of the shock mitigation system when compared with a rigid mounted seat the acceleration data points are categorized into percentile groups based on the absolute value of their magnitudes. The experimental data that was chosen for this example was the 36 ft USN. The percentile groups that exhibited a difference are shown in Table 6-2. The percentile groups below 70 are not shown because the differences between the two groups were minimal, mostly around 1%. What was noticed was that the main differences

between the two tests were truly at the 99 percentile or higher range. The 100 percentile group, representing the largest shock event, had a reduction of 48.8% in acceleration and the 99 percentile group had a 46.2% reduction in acceleration when the shock mitigation system was implemented. The reductions in acceleration became smaller for the lower percentile groups. For example, the 70^{th} percentile group had a reduction of 14% while the 90 percentile group had a 29% reduction. The main purpose of shock mitigation seats is to reduce the harshness of the most extreme impacts. With that in mind the shock mitigation system provides significant shock reduction.

Table 6-2. Percentile groups of the occupant acceleration.

	Percentile						
	70	**80**	**90**	**95**	**98**	**99**	**100**
Rigid	0.163	0.231	0.414	0.685	1.09	1.46	4.33
Shock	0.140	0.189	0.296	0.417	0.622	0.784	2.22

Chapter 7. Seat Response to Sea Input

This section presents the analysis of the response of the seat to at-sea excitation inputs. The at-sea excitation inputs are divided into three different categories based on ship size. These sizes are small for the 36 foot USN planing craft, medium for the 47 foot Motor Life Boat (MLB) and large for the 89 foot high speed planing craft. All three ships were tested in similar high sea state conditions. The first of the three to be presented here is the USN. Then the data from the MLB is presented. This is then followed by the data collected running the 89 foot high speed planing craft. Each test is examined to determine the effect of varying weight and suspension preload had on the response of the seat to each excitation. The spring preload was set at values of 0, 1 and 2 inches and the occupant mass was changed to weights of 150, 200 and 250 pounds for every test, thus creating nine separate tests for each excitation file. The main comparison is based on the response of the occupant mass accelerometer data since the main concern of shock mitigating seats is to isolate the occupant from shock and vibration.

7.1 Seat response to the 36 foot USN excitation

The USN input excitation consists of a four minute duration test file that was partitioned into two smaller two minute files to be able to be run on the seat testing rig due to limitations of the computer hardware. Both two minute excitations were run on the seat testing rig to record the response of the seat to the entire excitation file. Each test was examined for any unique events such as a multiple wave impact or extremely high amplitude impacts. It was determined that the second two minutes of the total four minutes of excitation is representative of the entire data set and was used to characterize the response of the seat.

Examination of the effects of suspension preload

The criterion examined was the effect of suspension preload on the response of the seat. For each occupant weight the effect of different suspension preloads was examined. The DRI value for each test was determined based on the maximum acceleration value. This

also allows a quick examination of the changes in severity between tests. The calculated DRI value for all nine tests is plotted on Figure 7-1. At weights of 150 and 250 pounds the DRI value increases significantly when the preload is increased from 0 to 1 inch and then drops slightly when the preload is increased to 2 inches. At a weight of 200 pounds the DRI value increases with a near linear trend when the preload is increased. Based on the results from analyzing DRI values an increase in suspension preload can either initially increase and then decrease the severity of the ride, or it can increase the severity of the ride with a direct relationship.

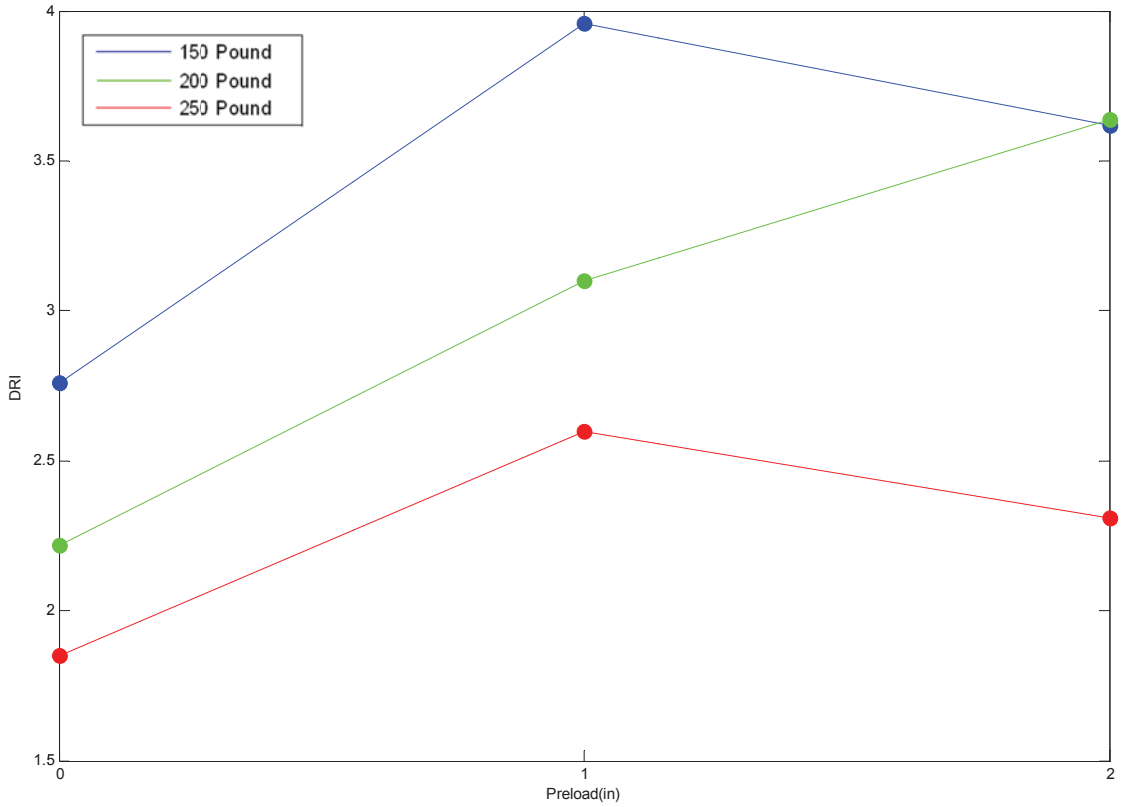

Figure 7-1. Analysis of DRI values provided inconclusive trends when the effects of preload were examined

To determine the true nature of the response a manual examination of the acceleration data was conducted. The entire two minute data set was reviewed for trends that are not represented by the changes in DRI values. The response of the seat with an occupant mass of 200 pounds is examined since it was the data set that did not share a similar pattern with the other two weight conditions. Since the main discrepancy in question is

the variation in trends of the DRI value, the event within which the DRI value is based on is shown in Figure 7-2 beginning at a time value of 57.3 seconds. The acceleration increased for this event as the preload is increased. The behavior of the response is fairly consistent at preload settings of 0 and 1 inch, with exception to the magnitude of the large impacts. However, at a preload setting of 2 inches the response is noticeably different than the other two settings. First, the acceleration during rebound did not increase substantially for most impacts when compared to that of the 1 inch preload. However, the acceleration during jounce did increase for most events and even more after larger rebound events. A prime example of this is shown in the event beginning at 56 seconds, the first minimum is increased in magnitude then the following local maximum is increased slightly in magnitude then the following minimum is greatly increased in severity when compared to the response of 0 and 1 inch preloads. Second important difference is that there is more oscillation in acceleration, meaning that the motion of the seat and the response is not as damped or smooth. These are very important changes that are not well represented by the changes in DRI values.

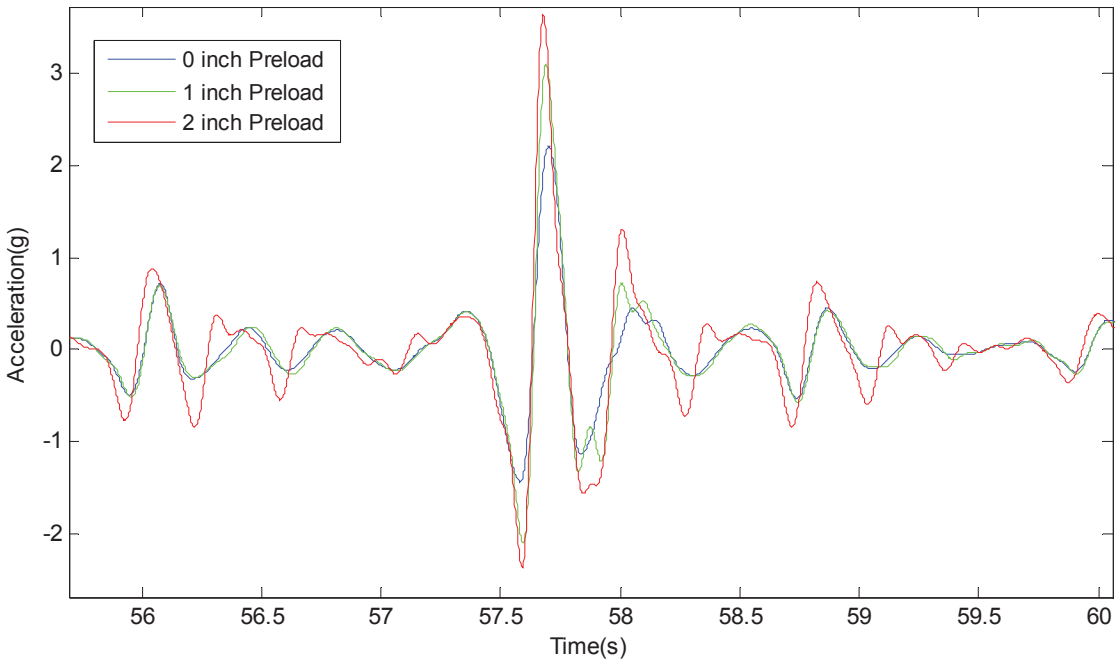

Figure 7-2. Analysis of the acceleration resulted in the conclusion that ride severity increases with preload

By picking multiple events throughout the entire time span of the test and recording the peak acceleration in the positive and negative direction the average percentage change is found. The acceleration during rebound increases by 37% when the preload is changed from 0 to 1 inch, then further increases by 18.7% when the preload is changed from 1 to 2 inches. However, the acceleration increases by 25.8% during jounce when the preload is changed from 0 to 1 inch and then increases by 63.8% when the preload is changed from 1 to 2 inches. The acceleration during jounce increases by about 100% its value at 1 inch of preload compared to that of the preload at 2 inches.

Examination of the effects of occupant mass

The effect of varying the occupant weight was examined next to determine how the dynamics of the system are affected when a different occupant uses the seat. The first criterion examined was the DRI value of each test that was used previously in the examination of the effects of preload. The DRI values are plotted at three different weights to determine the trends; the plot is shown in Figure 7-3. Just as before, the DRI trends for the preload settings of 0 and 1 inch are fairly consistent in that the DRI value decreases for increasing weight. However, for a preload setting of 2 inches the trends are somewhat different. When the weight is increased from 150 to 200 pounds the DRI value is unchanged but when the weight is increased to 250 pounds the DRI value drops significantly.

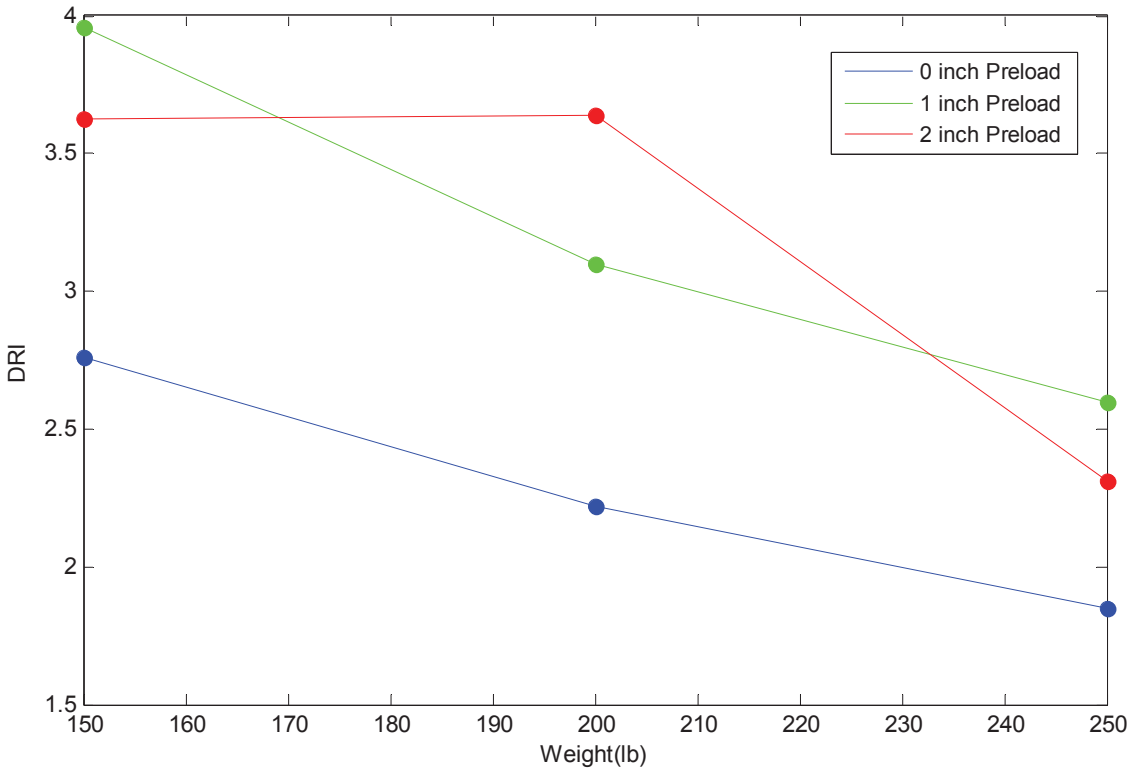

Figure 7-3. The DRI values from different occupant mass weights indicates that the ride severity decreases with weight

By the examination of the DRI values at a preload of 2 inches it would seem like the dynamics of the system are unchanged for weights of 150 and 200 pounds while the ride harshness is decreased as weight is increased for preloads of 0 and 1 inch. The acceleration data from the occupant mass accelerometer was examined for changes in the response between the different weights. The plot of the impact event in which the DRI value is based on is shown in Figure 7-4. A detailed examination of the data revealed that there is a decrease in severity of most events when the occupant weight increases. At a 2 inch preload there is a average decrease of 15.2% in severity when the occupant weight is increased to 200 pounds. The average decrease in severity of impacts, when the occupant weight increases from 200 to 250 pounds, is 21.5%. These percentages were calculated by examining the impacts which were affected by the change in weight during both rebound and jounce. The decrease in acceleration translates to less motion of the occupant mass and an increase in suspension travel. This can be seen in the increased

damped nature of the red trace when compared to those of the green and blue in Figure 7-4. The motion of the seat is more damped, with a lower frequency of motion. The responses of the 0 and 1 inch preload case show similar trends which is representative of the decrease in DRI.

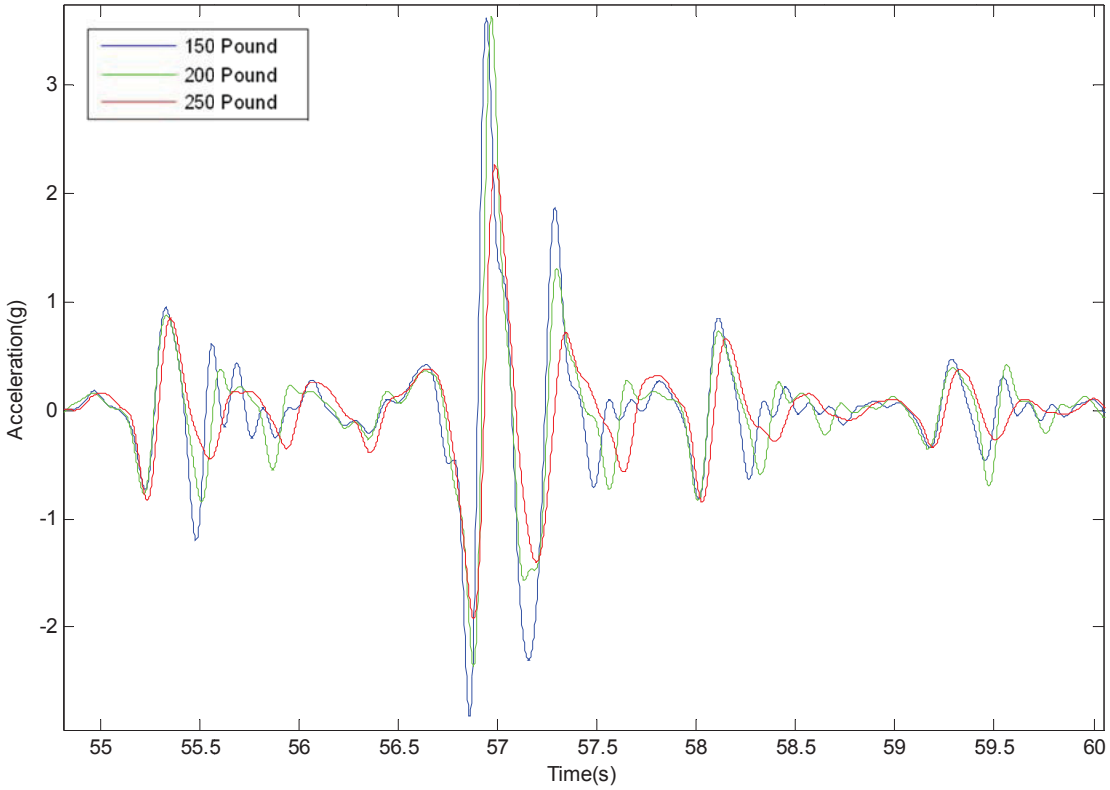

Figure 7-4. Analysis of the acceleration revealed that there was a decrease in acceleration when the occupant weight increases

7.2 Seat Response to the 47 foot Motor Lifeboat(MLB) Excitation

The MLB test input file is a 14 minute test that was broken into 7 smaller two minute tests. When examining the entire data set it was found that four minutes of tests in the middle of the test was a good representation of the entire file since most of the high acceleration events and some of the smaller distinct motions are within this four minute time span.

Examination of the effects of suspension preload

As with the case of the analysis of the seat to the 36 foot USN craft input excitation, the response of the seat to the MLB input excitation was examined for changes in seat dynamics at different preload settings. The DRI value for each test was calculated and then examined to determine any trends, the values are plotted in Figure 7-5. Testing at all weight settings revealed a common trend, when the preload is increased from 0 to 1 inch the DRI value also increases. However, when the preload is increased from 1 to 2 inches the DRI value drops for the cases when the occupant mass is 200 and 250 pounds. However, the DRI value does increase for the case when the occupant mass is 150 pounds. This does seem like a similar occurrence to the response of the tests to the RHIB input excitation.

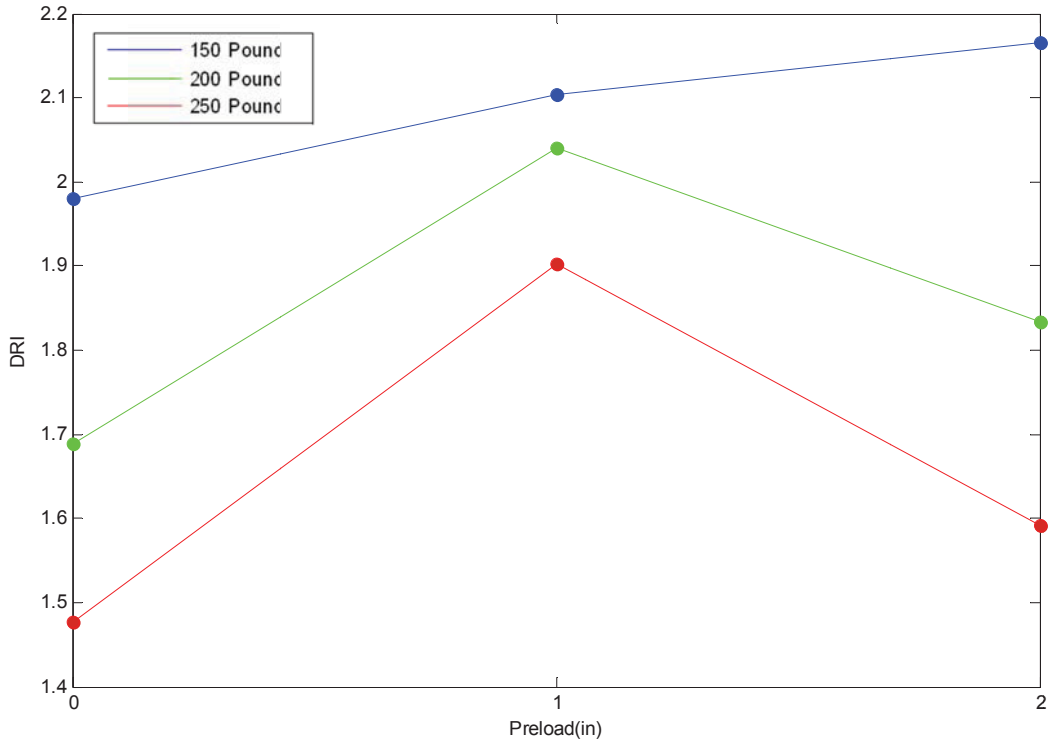

Figure 7-5. Examination of the DRI values provided limited conclusions

The data was then reviewed manually by examining the entire time response to determine if the DRI value was a good representation of the response. The tests with a 150 pound occupant were the first to be examined. The shock event in which the DRI value is based on is shown in Figure 7-6 below. Agreeing with the results from the USN tests and the DRI value trend, the ride harshness does increase with preload. As with the USN test results there are slight increases in acceleration magnitude when the preload is changed from 0 to 1 inch for large impacts, more so during jounce. Multiple peaks were analyzed in the data set and it was found that during jounce there was an average increase of 31.6% while there was a smaller increase of 12.0% during rebound. When the preload is increased from 1 to 2 inches the average increase in acceleration during rebound is 4.99% while the increase in acceleration during jounce is much larger at an average of 65.6%. Besides an increase in peak accelerations there is a significant increase in oscillatory motion after large disturbances, such as those pictured in Figure 7-6 after 71.5 seconds. The other responses from occupant mass weights of 200 and 250 pounds revealed similar responses as the 150 pound response previously described.

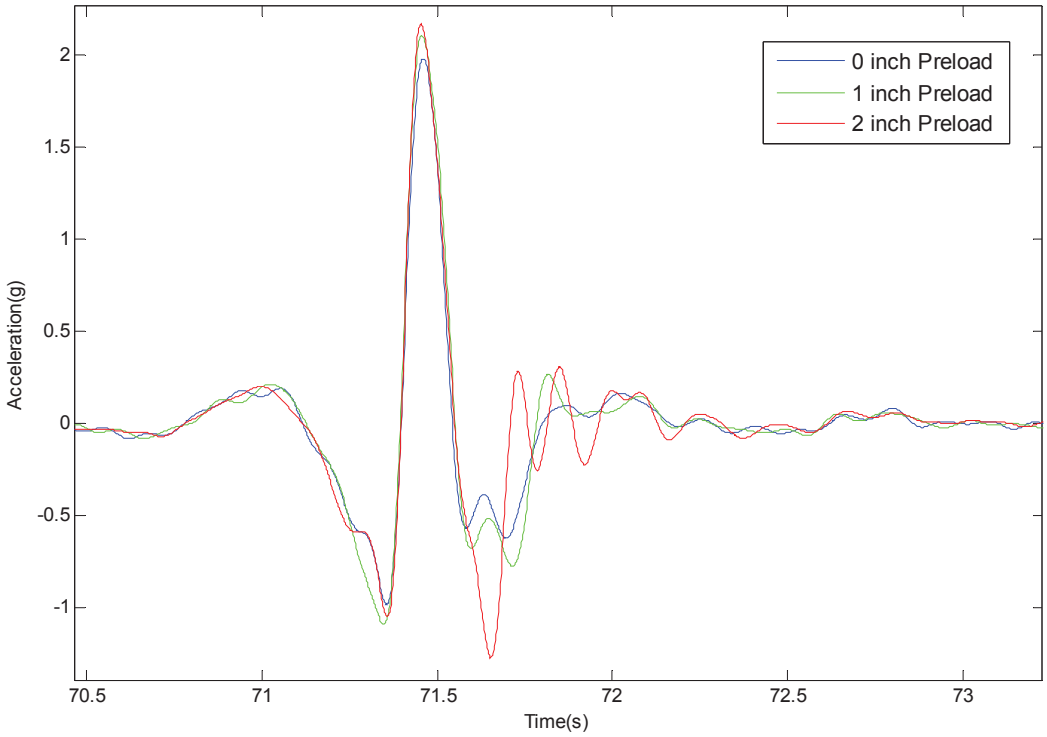

Figure 7-6. When examining the acceleration data is was found that an increase in acceleration is observed when the preload is increased

Examination of the effects of occupant mass on the response

The effect of different occupant weights on the response of the system was then examined. The DRI values were first compared to determine the effects of varying occupant mass. The DRI values at different weights at a constant preload are plotted in Figure 7-7. All three preload settings observed a decrease in DRI value when occupant weight increased. This result would define a conclusive trend in decreasing DRI with increasing occupant weight. To verify that this trend a manual examination of the time series was executed.

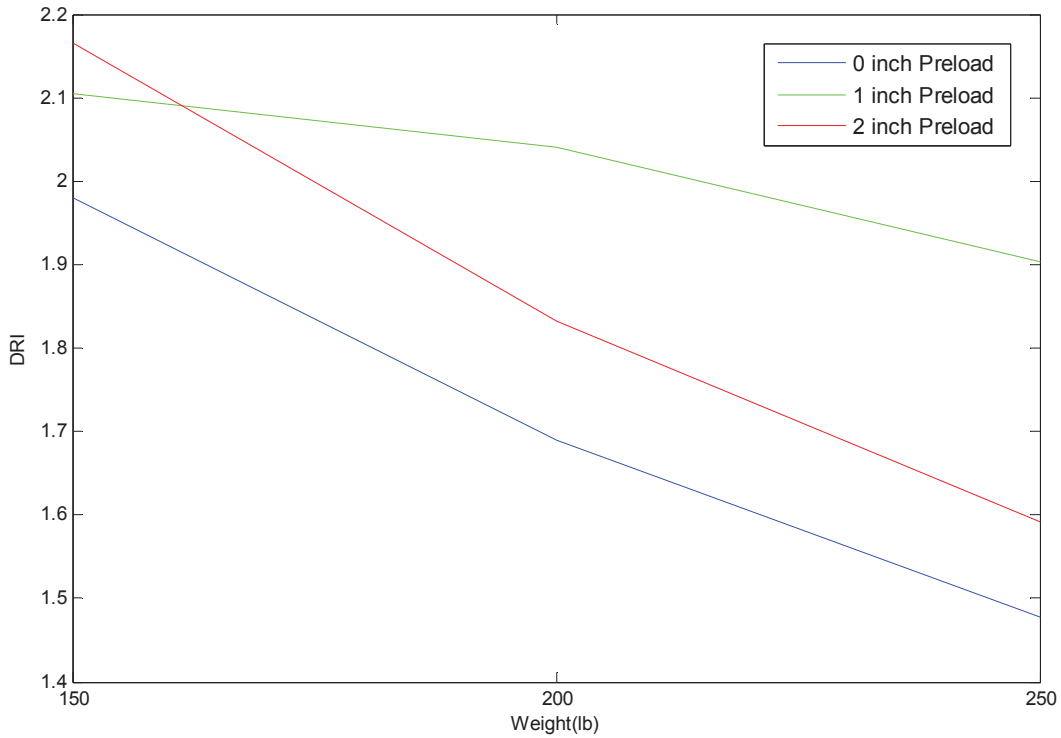

Figure 7-7. Analysis of the DRI values shows that there is a decrease in severity when occupant weight increases

When examining the entire time series for inherent trends and confirming the conclusive trend from the analysis of the DRI the least conclusive data set of a 1 inch preload was examined. The plot of the responses with a preload of 1 inch is shown in Figure 7-8 during the event in which the DRI value is based on. The event in which the DRI value is based on is fairly representative of the trends which occurred throughout the test. When the occupant weight increases from 150 to 200 pounds the acceleration during rebound dropped an average of 10.1% while the acceleration during jounce decreased in magnitude by an average of 24.6%. The trend at the first large local minimum shown in Figure 6.8 is not truly representative of the overall time span, the accelerations during jounce do decrease in magnitude when the occupant weight is increased. When the occupant weight is increased from 200 to 250 pounds the acceleration during rebound decreases by 20.9% and the acceleration during jounce decreases in magnitude by 14.6%. The response of the seat is also more damped in nature when weight is increased which can be seen by the rather damped nature of the motions of the occupant mass, this

characteristic is much more noticeable with the smaller low frequency motions. Thus, the DRI value trends are a good representation of the changes in response when the occupant weight is increased.

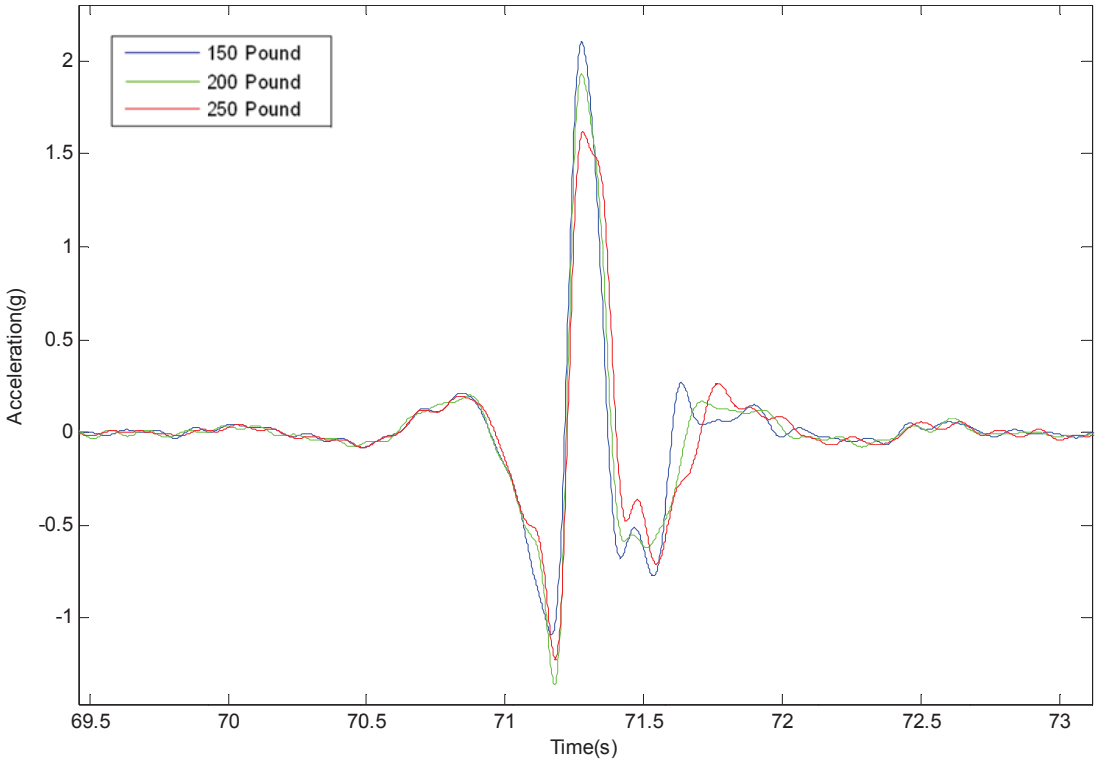

Figure 7-8. Analysis of the acceleration data confirms that the acceleration magnitude increases with increased occupant weight

7.3 Seat Response to the 89 foot High-Speed Planing Craft Excitation

The input file used to simulate the motion of an 89 foot high speed craft is an 8 minute test that was partitioned to 4 separate files that are 2 minutes in duration. When all four tests were examined it was found that a majority of the events characteristic to the ship are evident in the second two minutes of testing. The results from this two minute segment were chosen to represent the response of the seat to an 89 foot high speed planning craft.

Examination of the effects of preload

The seat response to changes in suspension preload were examined to determine any changes in dynamics when only the suspension preload is changed while the occupant weight remains constant. The DRI value was calculated to determine the change in ride harshness at different preloads. The plot of the DRI values at preloads of 0,1 and 2 inches is shown in Figure 7-9, where the test with 150, 200 and 250 pounds is represented by colors of blue, green and red respectively. From analyzing the DRI values calculated both the tests with 200 and 250 pound occupants revealed trends which have been observed in the USN and MLB testing described previously. Based on previous observations the ride harshness increases when the preload is increased. However, when the occupant weight was set at 150 pounds the DRI value decreased slightly and remains fairly consistent with the largest fluctuation being 0.04 as the preload is increased. This would normally be indicative of decreased or similar response severity.

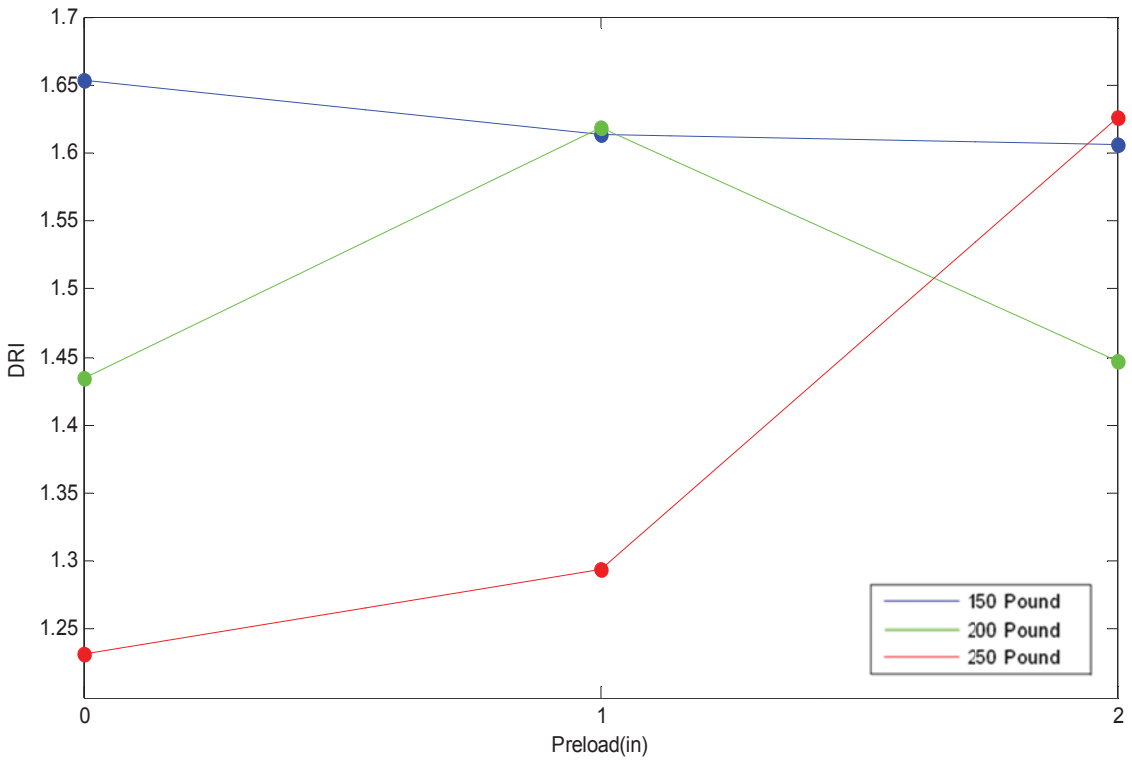

Figure 7-9. Trends from DRI analysis are completely inconclusive for this data set

To fully determine the response characteristics the time series data for the case of a 150 pound occupant was examined to further investigate this new trend. The event in which the DRI value is based on is examined first, this event is shown in Figure 7-10 at various preload settings of 0(blue), 1(green) and 2(red) inches. There is a significant amount of over shoot after the large impact event at 107 seconds. This trend occurs multiple times over the duration of the test. When the preload is increased from 0 to 1 inch the increase in the acceleration during rebound was an average of 12.9%, while the increase in the acceleration during jounce was much larger at 42.6%. This trend can be seen by comparing the response of the green and blue lines in Figure 7-10 where there is a large increase in the minimums from the 0 inches preload to that of 1 preload. But when the preload is increased from 1 to 2 inches this trend does not carry over directly. Smaller motions do experience an increase in acceleration magnitude of an average of 20.7% during both rebound and jounce. Larger impacts actually had a shift in acceleration in the negative direction of about 0.1 g. This would appear as a decrease in severity when analyzing DRI. However, these large impact events had a large overshoot after the first

disturbance when the system attempts to return to its steady state position. When multiple overshoot events are examined it is found that the overshoot increases by an average of 63.5%.

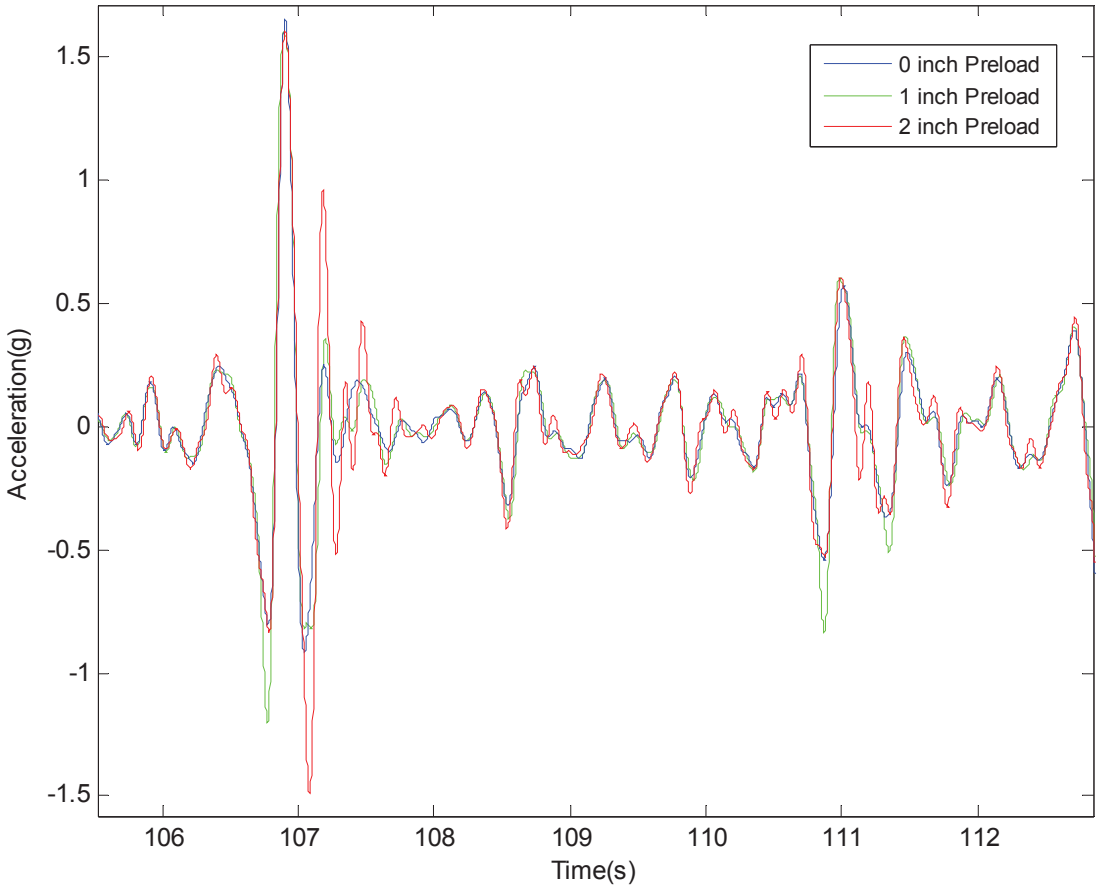

Figure 7-10. There is an increase in acceleration when preload is increased and the results from a 1 inch preload can severe at parts, indicated by the green spikes in the data

Examination of the effects of occupant weight

The effects of different occupant weights on the dynamics of the seat were then investigated. The DRI values from the tests were plotted to reveal any trends, the plot is shown in Figure 7-11. The results of the 0 inch preload case are as expected based on previous analysis of the USN and MLB tests in that the DRI and ride harshness decreased when the weight is increased. The trend when the preload is set to 1 inch is also similar to a previous test and is indicative of a decrease in ride harshness when occupant weight increases. The response to increased occupant weight for a 2 inch preload setting is unexpected, the DRI value drops when the weight is increased from 150 to 200 pounds, and then increases when the weight is increased to 250 pounds.

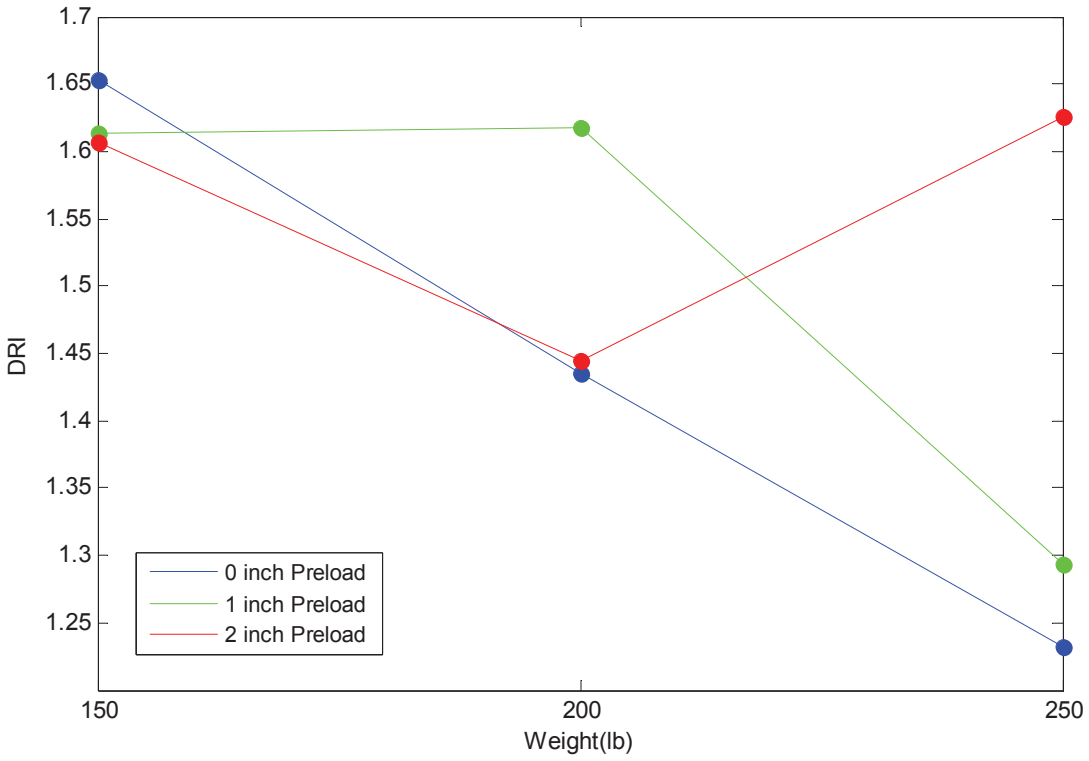

Figure 7-11. Examination of the DRI values for changes due to occupant weight increases revealed a very random nature in the trends

Since the DRI values revealed no conclusive trends the acceleration data was then reviewed for any new characteristics distinct to this test. The series of data that was reviewed was that of the 2 inch preload because it produced an uncharacteristic trend. The overlaid plot of varying weights at a 2 inch preload is shown in Figure 7-12 with weights of 150(blue), 200(green) and 250(red) pounds. The event in which the DRI value is based on is shown in Figure 7-12. As the weight increases from 150 to 200 pounds the response showed a reaction that was similar to that of increasing preload, the acceleration during jounce increased by an average of 42.4% while the acceleration during rebound remained fairly constant. When the weight is increased from 200 to 250 pounds the magnitude of the acceleration events are unexpectedly increased, contrary to previous analysis. The acceleration during jounce increased an average of 36.4% while the acceleration during rebound remains constant. Smaller motions, those with accelerations below the magnitude of 0.5 g, are well attenuated as can be seen in Figure 7-12 from 33.4 to 34 seconds where the occupant almost experiences slight motion.

The results from analyzing the 2 inch preload data were not representative of all of the tests. The trends from the other data sets with a preload of 0 and 1 inch show a decrease in acceleration and motion when the weight is increased by an average amount of 13.9% when the weight is increased from 150 to 200 pounds and 19.6% when the weight is increased from 200 to 250 pounds. These trends agree with all of the previous results presented.

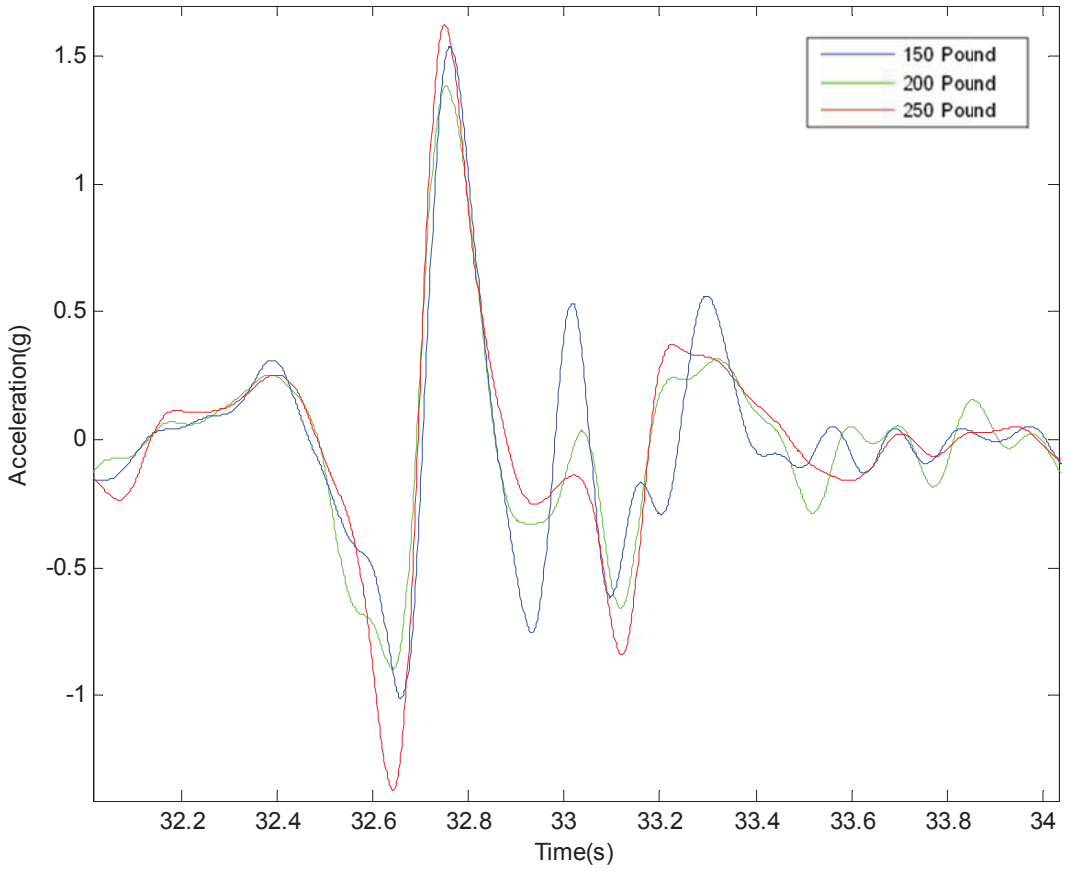

Figure 7-12. Acceleration increased when the occupant weight is increased to 250 pounds, which is an unusual trend

7.4 Summary

After analyzing the trends from each test separately all the results are combined to gain a better perspective on the response of the seat. Since the DRI value was calculated first when examining data because it is representative of the worst singular impact event that is usually the cause for serious injury. Although it is a quick and effective way of determining the greatest amount of shock that the human body will be subject to it is not effective at characterizing the response of the seat. The DRI value is based on the largest acceleration value experienced during a test, when comparing multiple tests the DRI value is sometimes based on a different acceleration event between tests. DRI is not the best gauge of severity when comparing multiple impact tests.

Effects of occupant weight considerations

An increase of occupant weight resulted in a decrease in the acceleration observed by the occupant mass. Only one test (89 ft. high speed planning craft input with a 2 inch preload) did not agree with the majority of the trends, this being when the occupant weight is increased the amount of acceleration and motion of the seat decreases. But it is important to note that a decrease in occupant motion equates to an increase in suspension movement if the input is constant. The amount of suspension activity for an increase in occupant mass for the 89 foot high speed planning craft is shown in Figure 7-13 for the whole time span and a small time span in Figure 7-14, with the spring displacement at occupant weights of 150(blue), 200(green) and 250(red) pounds. The increase in occupant weight causes an increase in suspension travel throughout the entire test, as can be seen in Figure 7-13. By examining the extremes, like those in Figure 7-14, there is a percentage increase of 56.3% in motion when the occupant weight is increased from 150 to 200 pounds. An increase in occupant mass from 200 to 250 pounds resulted in an increase of 46.6% in motion. With the percent increase in motion being somewhat close to each other there is a near linear relationship between occupant weight and suspension motion.

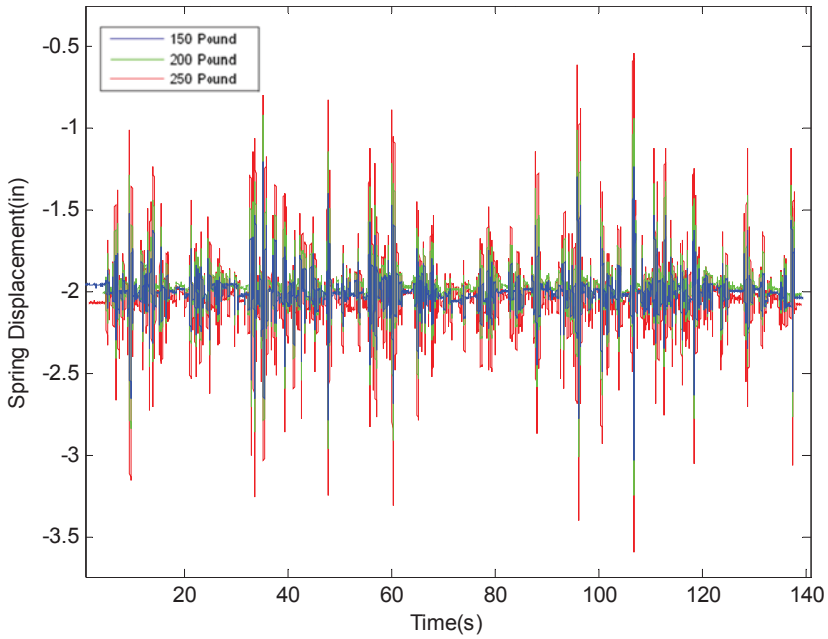

Figure 7-13. Spring displacement increases with increasing occupant weights

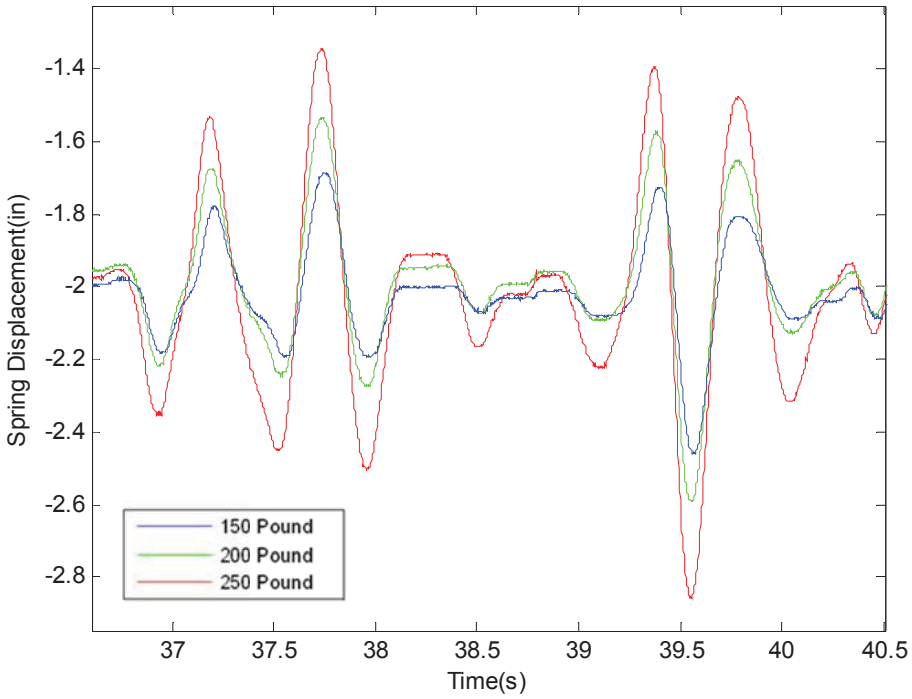

Figure 7-14. Spring displacement increases during both rebound and jounce

Effects of different suspension preloads

When examining the preload results it is important to note that the seat operates optimally with no preload. Knowing this it can be predicted that adding preload would have negative effects on the system. Overall the trends conclude that an addition of suspension preload creates an adverse effect on the suspension dynamics. All the tests but one revealed an increase in acceleration which translates to an increase in forces and motion observed by the occupant. A summary of the changes in acceleration is expressed in Table 7-1. There was a much more significant increase in acceleration during jounce throughout the tests at all levels. In most tests the increase in jounce acceleration is much greater than that during rebound. This is due to the increased initial force which is placed on the coil over spring from the preload. The preload causes the suspension to behave as a rigid system until the initial force is overcome by much larger impacts.

Table 7-1. Changes in acceleration magnitudes for various preloads.

Preload Change	Direction	USN (%)	MLB (%)	89ft HSC (%)
0 to 1 in	Rebound	37.0	12.0	12.9
0 to 1 in	Jounce	25.8	31.6	42.6
1 to 2 in	Rebound	18.7	4.99	20.7
1 to 2 in	Jounce	63.8	65.6	20.7

Since there are significant effects to the dynamics of the system due to an addition of a suspension preload the movement of the suspension is further investigated. The plot of the suspension displacement during the 36 foot USN input excitation with a 150 pound occupant and 2 inch preload is shown in Figure 7-15. When the preload is at 2 inches the suspension is only active for the large impact events and reacts much like a rigid system for most of the test with a majority of the compressions being less than half an inch. The nature of the motions is also really severe, the largest displacement event having a duration of 2 tenths of a second. This high frequency nature is the cause of the high oscillations in the occupant acceleration data observed earlier.

The additional preload affects at 2 inches creates a non-linear nature within the spring. There is a greater amount of force that must be exerted on the spring during compression and then the spring exerts a larger force during rebound for movements near the top of the suspension stroke. The spring behaves more like a linear spring at greater compression displacements where the effects of preload are less apparent. The overall response of the spring is similar to that of a non-linear spring. This could be a contribution to the differences in the trends when compared to preloads of 0 and 1 inch.

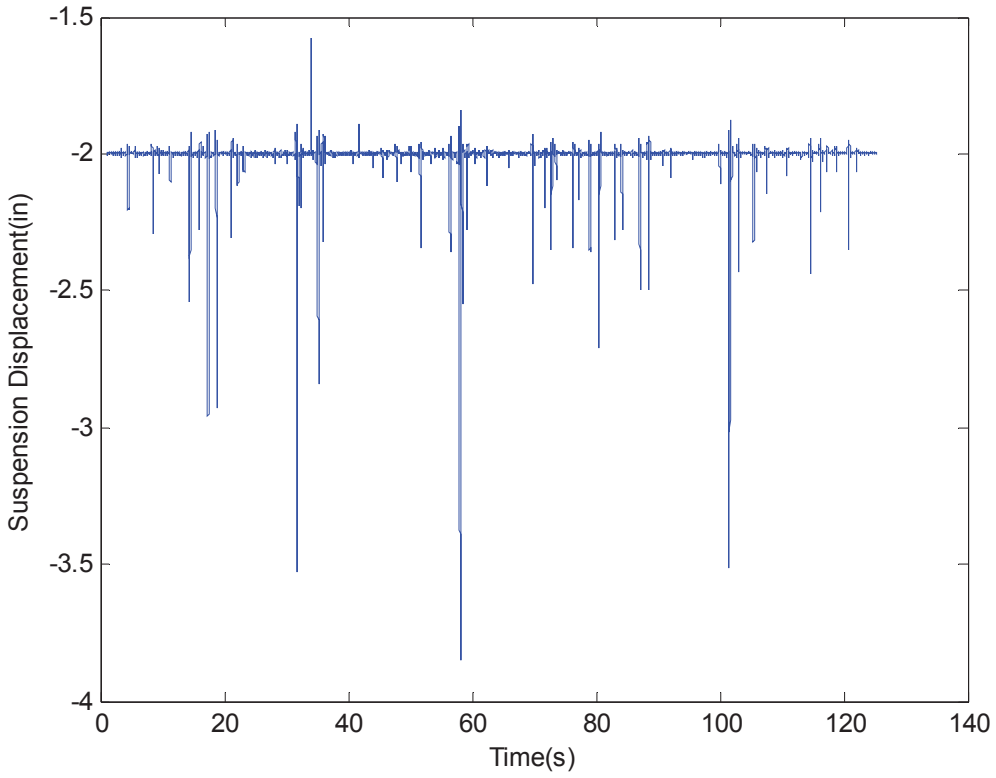

Figure 7-15. Suspension motion with a 150 pound occupant and 2 inch preload to a RHIB excitation

Chapter 8. Seat Response to Created Inputs

This section presents the analysis of the response of the seat to created input excitations. Three inputs were created to further characterize the seat dynamics. The first is a square wave with amplitude of 2 inches and frequency of 0.1 Hz. The goal of the square wave was to create the greatest amount of displacement at the fastest rate possible from the hydraulic system. The second is a half sine wave with amplitude of 4 inches and a frequency of 1.5 Hz. This is the fastest possible up and down motion utilizing the full dynamic stroke of the actuator. The third and last input was a chirp input with an amplitude beginning at 0.9 inches and frequency of 0.5 Hz, then ending with amplitude of 0.05 inches and a frequency of 15 Hz. This allows the analysis of the frequency response of the seat throughout the simulated frequency band. All three inputs are created in mind to obtain a unique response from the system.

8.1 Response to a Square Wave

This section presents the analysis of the response of the seat to the square wave input. The square wave input was first used to calculate the damping ratio of the coil over suspension. Then the response data was used to calculate the settling time of the system.

Calculation of Damping Ratio

The square wave produced the free response of the system from a step excitation. Since the frequency of the square wave was 0.1 Hz there was a 10 second pause between consecutive up and down motions of the seat. The first analysis was accomplished by using logarithmic decrement to determine the damping ratio of the suspension system. The damping ratio is calculated using the equations below and the response of the system to the square wave input. The logarithmic decrement δ is first calculated using equation 8-1.

$$\delta = \frac{1}{n}\ln\left(\frac{x_o}{x_n}\right) \tag{8-1}$$

Where n is the peak number after the initial peak, x_o is the magnitude of the initial peak of the series and x_n is the magnitude of the nth peak in the series. The peaks used for the values of x_o and x_n were the two positive peaks in the displacement of the seat after the hydraulic actuator has come to rest. An example of the two peaks that would be used for the calculation is shown in Figure 8-1. An example of two peaks that would be used, with the first one being x_o and the second being x_n are circled in red in Figure 8-1.

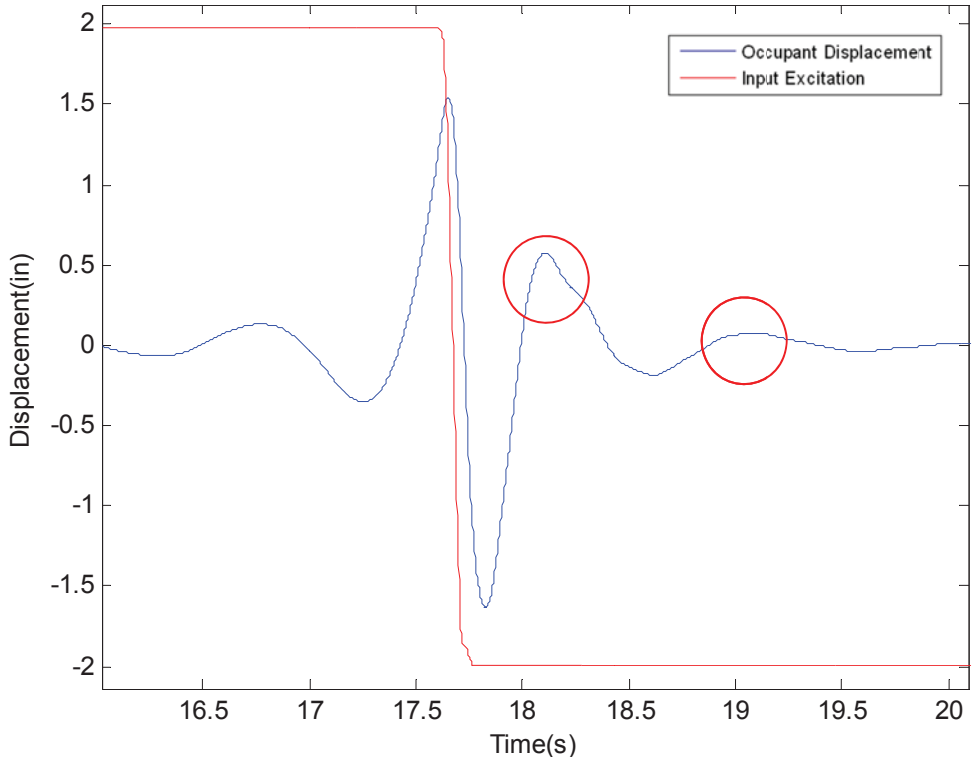

Figure 8-1. The damping ratio is calculated by choosing 2 peaks after actuation has ceased

The two peaks from the response are then plugged into equation 8-1 to gain the logarithmic decrement. The logarithmic decrement is then substituted into equation 8-2 to get the critical damping ratio ζ.

$$\zeta = \frac{1}{\sqrt{1+\left(\frac{2\Pi}{\delta}\right)^2}} \tag{8-2}$$

The damping ratio is calculated at all the different occupant weights and preload settings. The calculated damping ratios are shown in Table 8-1 with the corresponding test conditions. The damping ratio is consistent between the various test conditions and is not effected significantly by the changes in occupant weight and suspension preload. The average damping ratio of all of the tests was 0.261. Indicating that the system is under damped, shown by a damping ratio which is significantly less than a value of 1.

Table 8-1. The calculated damping ratios for the square wave input.

Weight	Preload	Damping Ratio
150	0	0.255
150	1	0.255
150	2	0.252
200	0	0.285
200	1	0.300
200	2	0.250
250	0	0.254
250	1	0.280
250	2	0.224

Calculation of Settling Time

The square wave input excitation was also used to calculate the settling time of the shock mitigating seat to a step input. Before determining the settling time from the square wave test data it is important to note the equation for the theoretical settling time to estimate what variables effect the resulting time. The equation for settling time is expressed as equation 8-3.

$$t_s = \frac{\ln(F_{\%})}{\zeta \omega_n} \tag{8-3}$$

Where $F_{\%}$ is the percent of the final steady state value, ζ is the critical damping ratio and ω_n is the natural frequency. Of the two parameters being varied occupant weight should

cause an increase in settling as the occupant weight increases. An increase in occupant weight should decrease the natural frequency and thus cause the settling time to increase. The preload should not have an effect on the settling time since the damping ratio, spring rate and mass are the only variables that affect the settling time.

The settling time for the experimental data was calculated by plotting the actuator motion and the displacement of the occupant mass on the same plot to compare the time values when the actuator motion ceased and when the seat motion settled to within 5% of its final value. The settling times calculated are shown in Table 8-2 at various test conditions. Most of the settling times were fairly consistent with a average time of 1.41 seconds required for the system to settle within 5% of the steady state value. The three instances where the settling time varied significantly were when the occupant weight was at 200 pounds with a preload of 2 inches, when the occupant weight was 250 pounds with preload settings of both 1 and 2 inches. When the preload increases from 1 to 2 inches for the case of 200 and 250 pound occupant weights the settling time increased substantially, for a 200 pound occupant the settling time more than doubles. The settling time for the case of a 250 pound occupant and a 2 inch preload is indicated by a "~10?" in Table 8-2 because the system did not fully settle within 5% of the final value within the 10 second interval between steps. When comparing the cases of 0 preload at various weights the settling time is fairly unaffected by the change in weight, the difference between the values is in the order of hundredths of a second. However, for the cases of 1 and 2 inch preloads the settling time fluctuates at higher occupant weights. With a 1 inch preload the settling time stays fairly constant when the weight is increased from 150 to 200 pounds but when the weight is increased to 250 pounds the settling time increases from 1.386 to 1.549 seconds. With a preload of 2 inches the settling time increases when the weight changes from 150 to 200 pounds and then again when the weight is increased to 250 pounds, to the point where the system does not settle within the 10 seconds between step actuations.

Table 8-2. The calculated settling time for the square wave input.

Weight	Preload	Settling Time(s)
150	0	1.408
150	1	1.427
150	2	1.402
200	0	1.422
200	1	1.386
200	2	3.016
250	0	1.414
250	1	1.549
250	2	~10?

Based on the theoretical equation 8-3 used to calculate settling time previously mentioned, it would be expected that the occupant mass would affect the settling time. The occupant weight did not affect the settling time significantly when the preload was set at 0 or 1 inches. At a preload setting of 2 inches an increase in occupant weight also increases the settling time, as expected.

8.2 Response to a Half Sine Impulse

A half sine wave with amplitude of 4 inches and a frequency of 1.5 Hz was created to simulate the largest veritcal motion possible from the seat shake rig. This half sine wave is a close representation of a single wave impact event. The changes in the response of the seat from varying the preload and occupant weight can be measured without the effects of another subsequent wave, such as the situation when running a HSC simulation.

Effects of Varying Suspension Preload

The first criterion that was examined was the effect of suspension preload on the response of the seat. For occupant weights of 150, 200 and 250 pounds the suspension preload was varied at settings of 0, 1 and 2 inch preload. The DRI value for these tests were calculated, the DRI value is a good method for characterizing the response of the half sine wave because it is a signal event. The DRI values at various preloads are overlaid in Figure 8-2 at weights of 150, 200 and 250 pounds. The plots of all three occupant weights indicate that when the preload is increased the DRI value also increases. The increase in DRI for a 200 pound occupant is almost linear in nature with respect to the DRI. After calculating the change in DRI over the change in preload it is found that the rate of change increases with the weight. For the 150 pound case the DRI increases by 0.4623, for the 200 pound case the increase is 0.5523 and for 250 pounds the increase is 0.6761. There are more significant changes in DRI when the preload is increased from 1 to 2 inches between the different weights. At 150 pounds the amount of increase was by 0.1222, at 200 pounds the increase was at 0.4052 and at 250 pounds the change was 1.007. Overall, the data indicates clearly that additional preload does increase the DRI and thus the severity of the ride harshness.

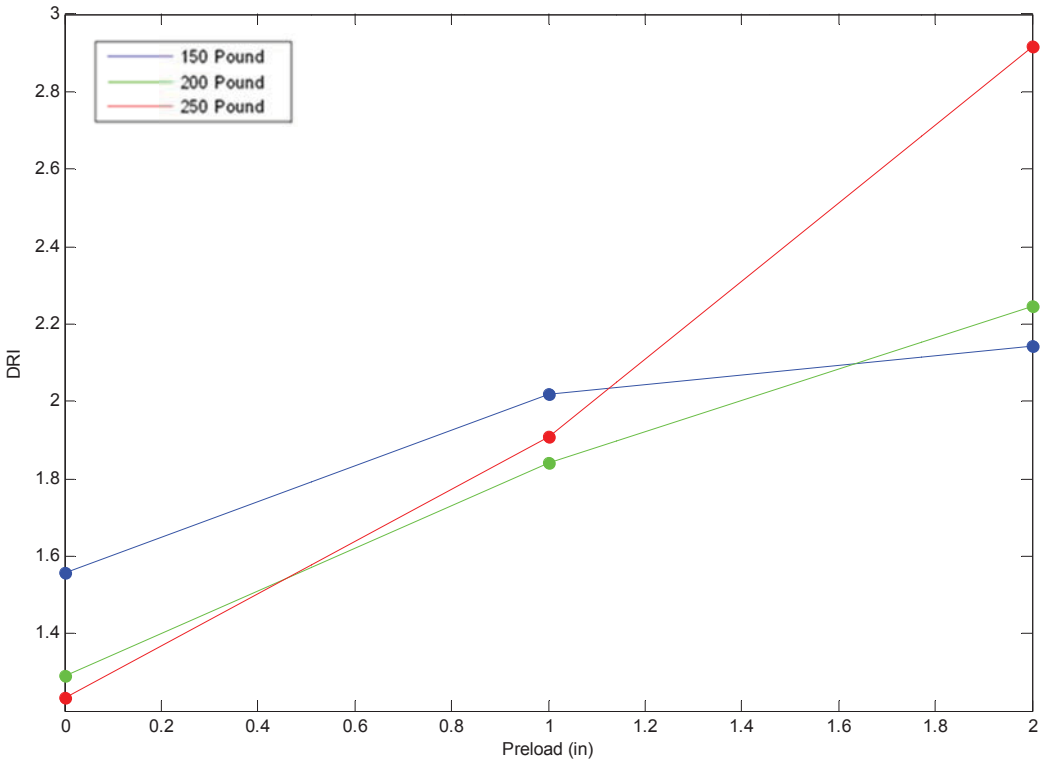

Figure 8-2. DRI is well suited to reveal the trend of increasing severity with preload when analyzing a singular impact event

To further investigate the effects of preload and to verify the conclusions from the DRI analysis the acceleration data was examined. An overlaid plot of an impulse response for a 200 pound occupant is shown in Figure 8-3. For the initial start of motion there are minor differences. The acceleration during jounce increases in magnitude by 29.3 percent when the preload is increased from 0 to 1 and then again by 13.0 percent when the preload is increased from 1 to 2 inches. The acceleration during rebound increases by 43.5 percent when the preload increases from 0 to 1 inch and then increases again by 20.1 percent when the preload increases from 1 to 2 inches. The overall nature of the response is similar between the different preload settings with only magnitudes increasing.

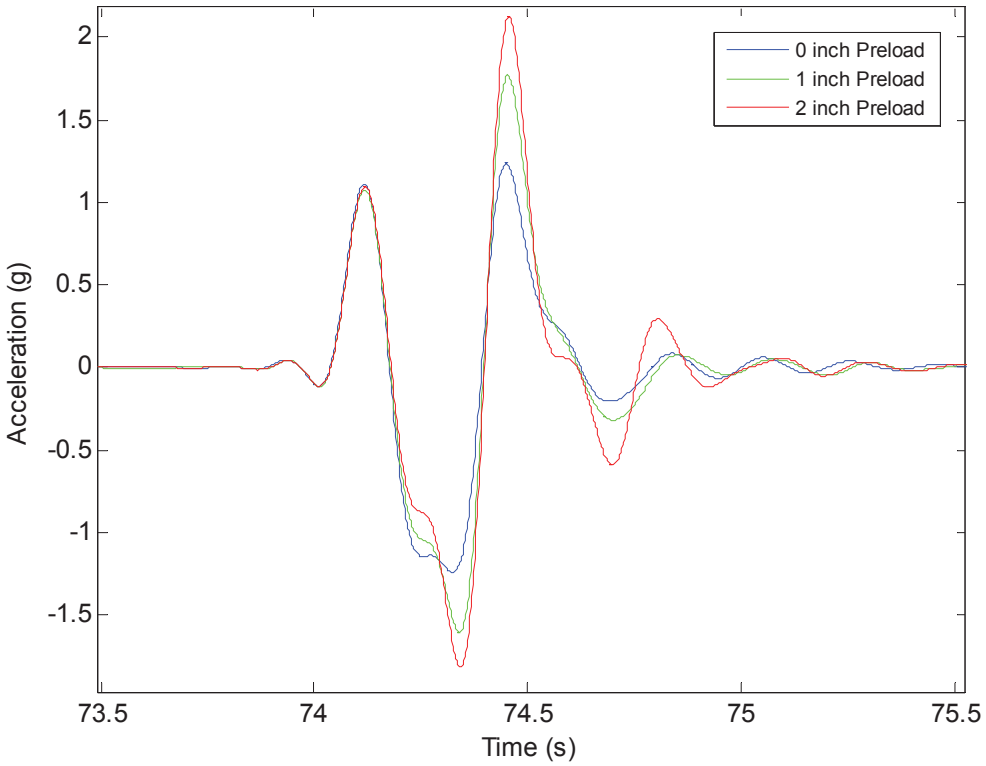

Figure 8-3. Analysis of acceleration data revealed that there is an increasing trend when preload is increased

Effects of Varying Occupant Weight

Just as in the analysis of the effect of varying suspension preload the DRI was used for comparing the response between the occupant weights of 150, 200 and 250 pounds. The DRI at various preloads over weights of 150, 200 and 250 pounds are overlaid in Figure 7-4. There are similar trends between preloads of 0 and 1 inch, the DRI decreases when the occupant weight increases from 150 to 200 pounds and then stays fairly constant with only a slight increase when the occupant weight increases to 250 pounds. The response with a 2 inch preload is completely different and almost opposite. The DRI increases when the occupant weight increases from 150 to 200 pounds and then decreases when the occupant weight increases to 250 pounds.

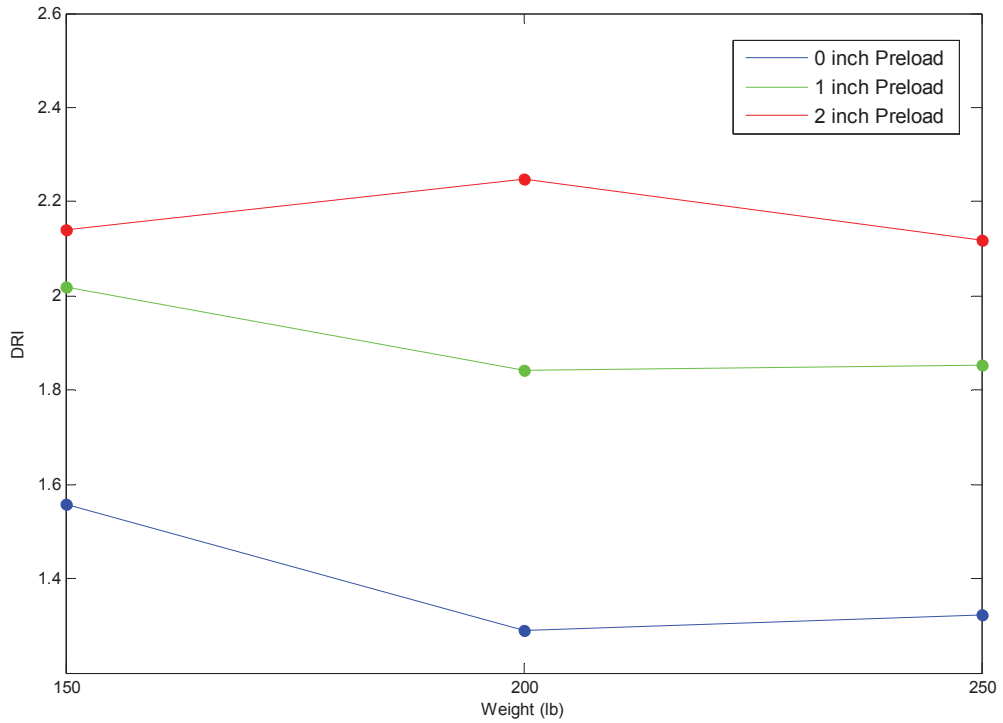

Figure 8-4. Examination of the 2 inch preload data proved results opposite of others

Since analysis of the DRI values provided minimal gains the acceleration data was examined similarly to the at-sea data. The acceleration response from the cases with 0 preload is plotted at weights of 150, 200 and 250 pounds in Figure 8-5. The maximum peak acceleration decreases by 13.5 percent when the occupant weight increases from 150 to 200 pounds and then decreases again by 30.2 percent when the occupant weight increases from 200 to 250 pounds. The minimum acceleration peak also decreased by 7.07 percent when occupant weight increased from 150 to 200 pounds and decreased again by 6.49 percent when the occupant mass increases from 200 to 250 pounds. The overall curve does not change, only the magnitudes differ. The DRI values might not indicate a decrease in severity but on examination of the acceleration data does. This is the predicted outcome of this comparison based on the examination of the sea data excitation. When examining the suspension displacement when the occupant weight was increased there was an increase of 31.3 percent in jounce and an increase of 15.5 percent in compression when the occupant weight increases from 150 to 200 pounds. When the occupant weight increases from 200 to 250 pounds there is a increase of 32.2 percent in

jounce and a increase of 18.7 percent in the compression during peak events. These are significant increases in suspension motion.

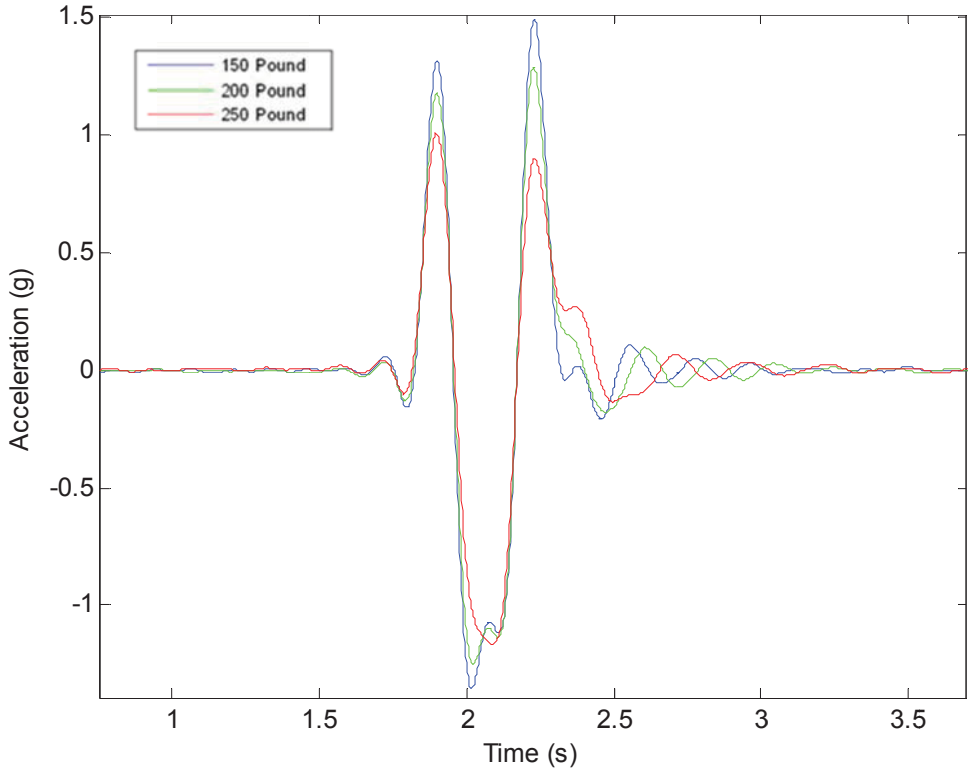

Figure 8-5. Acceleration values decreased when the occupant weight increases

8.3 Response to a Chirp Input

A chirp signal was run through the seat shake rig to test the frequency response of the Stidd 800v5 shock mitigating seat. The initial frequency at the beginning of the test was 0.5 Hz and the ending frequency was 15 Hz. With a test duration of 120 seconds the frequency is swept to the ending frequency in intervals of 0.1208 Hz per second. Before examining the data the theoretical natural frequency of the coil over suspension system is calculated. Equation 8-4 was used to calculate the natural frequency of the suspension.

$$\omega_n = \sqrt{\frac{k}{m}} \tag{8-4}$$

where k is the stiffness of the spring and m is the mass of the system, or occupant and seat pan combined in the case of the seat. With a combined mass of 117.5 kg (258.8 lbf) and a spring stiffness of 1.92x104 N/m(109.4 lbf/in) the natural frequency of the system is 2.03 Hz. In theory the transmissibility plot of the system should have a peak around 2.03 Hz and then decrease towards zero afterwards. The theoretical force transmissibility of the system can be calculated using equation 8-5.

$$\frac{Xk}{F_0} = \frac{1}{\sqrt{(1-r^2)^2+(2\zeta r)^2}} \tag{8-5}$$

where r is the frequency ratio and ζ is the damping ratio. Using the damping ratio calculated with the square wave and the theoretical natural frequency of the system the transmissibility plot is created and shown in Figure 8-6.

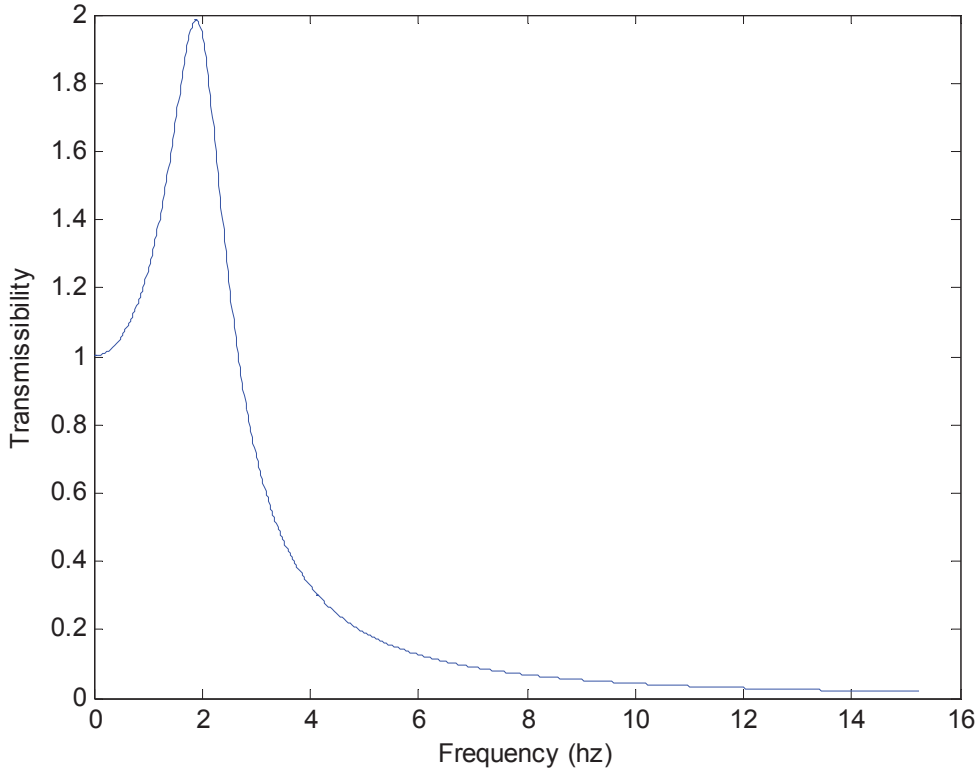

Figure 8-6. Theoretical transmissibility plot created using the experimental damping ratio and the theoretical natural frequency

To calculate force transmissibility the accelerometer data from the chirp test was analyzed. The two exact signals that were used were the acceleration at the base or

carriage of the seat shake rig, and the seat. The accelerometer data was then filtered to isolate the frequencies between 0.5 and 15 Hz, which are the frequencies in which the chirp signal swept through. A Fast Fourier Transform (FFT) was conducted on the filtered accelerometer data to convert the data into the frequency domain. The transmissibility was then calculated from the two FFT signals calculated. The experimental transmissibility is shown in Figure 8-7. The trend is similar to that of the theoretical transmissibility shown in Figure 8-6. The peak value occurs at a frequency of 2.136 Hz, which is only 5.1% different from the theoretical value of 2.0325 Hz. The results of the experimental test validates the experimental calculation of the damping ratio by use of the free response of the system.

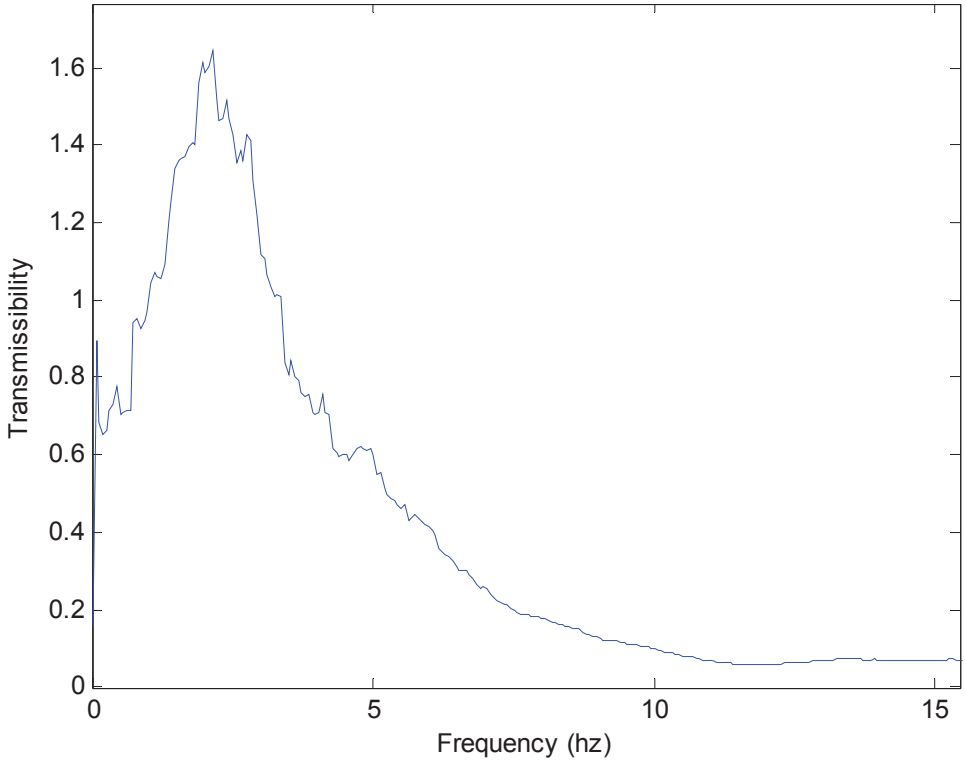

Figure 8-7. Transmissibility plot of the response of the seat to a chirp input

Chapter 9. Seat Simulation Model

The following chapter includes a detailed description of the simulation analysis that was performed by using a Simulink model of the analytical model. This chapter starts with the required assumptions that were made to simplify the model. Then the analytical model is presented along with the free body diagram of the seat and the appropriate equations of motion. Following, the Simulink model is presented with an explanation of how the equations of motion and seat characteristics are implemented. The inputs used in the Simulink model are presented followed by an analysis of the results from simulation.

9.1 Analytical Model

To develop an analytical model of the Stidd 800v5 shock mitigating seat the entire seat assembly is represented by a spring-mass-damper system. Two sets of spring-mass-damper systems are implemented to represent the entire 2-degree-of-freedom system. A visual representation of the entire system is shown below in Figure 9-1. X_1 represents the base excitation or ship motion being input into the system. The spring and damper labeled as K_s and C_s respectively represents the shock mitigating coil over system of the seat. X_2 represents the displacement of the seat pan assembly, while m represents the mass of the seat pan assembly. X_3 represents the displacement of the occupant mass while M represents the mass of the occupant. The spring and damper labeled as K_2 and C_2 respectively represent the characteristics of the seat cushion in which the occupant mass lies on.

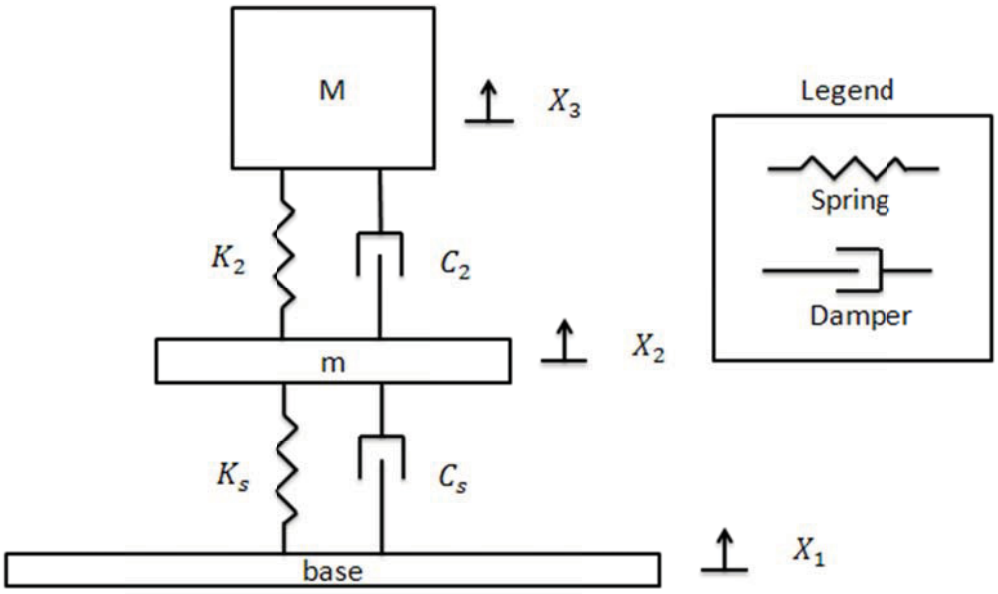

Figure 9-1. Spring-mass-damper representation of the seat

Modeling Assumptions

In order to simplify the model a few assumptions were required to avoid additional complexities in the system. The first assumption is that there is not any significant friction introduced into the system from the vertical guides that the seat pan assembly rides on, shown below in Figure 9-2. These guides limit motion to the vertical direction only. No friction can be assumed due to the fact that any friction forces observed are minute relative to the forces from the spring and damper of the shock mitigating system. This eliminates the need to determine the friction coefficient of the steel guides.

Figure 9-2. Vertical guide assumed to have negligible friction forces present

Another assumption made to simplify the model is that the occupant mass is physically attached to the seat cushion. The occupant mass is strapped on the seat cushion using elastic bands which simulate a real life occupant resisting motion. The mass is additionally strapped down with ratchet straps to restrict motion. When observing tests the occupant mass only leaves contact from the seat cushion briefly during extremely large motions. Making this assumption permits the simplification of the occupant mass and seat cushion interaction to a spring-mass-damper system.

The last assumption taken into account is that the movement of the seat pad assembly is negligible. The seat pad is designed to be changed into a seat bolster position easily and quickly. The seat pad is held in place vertically by gravity and horizontally by pins circled in Figure 9-3 below. However, due to this fact the seat pad is not hard mounted to the suspension carriage allowing the seat pad to move independent of the carriage during high acceleration events. Once again, since this event only surfaces at very few instances

while testing and does not appear to affect the system dynamics greatly it is assumed to be negligible.

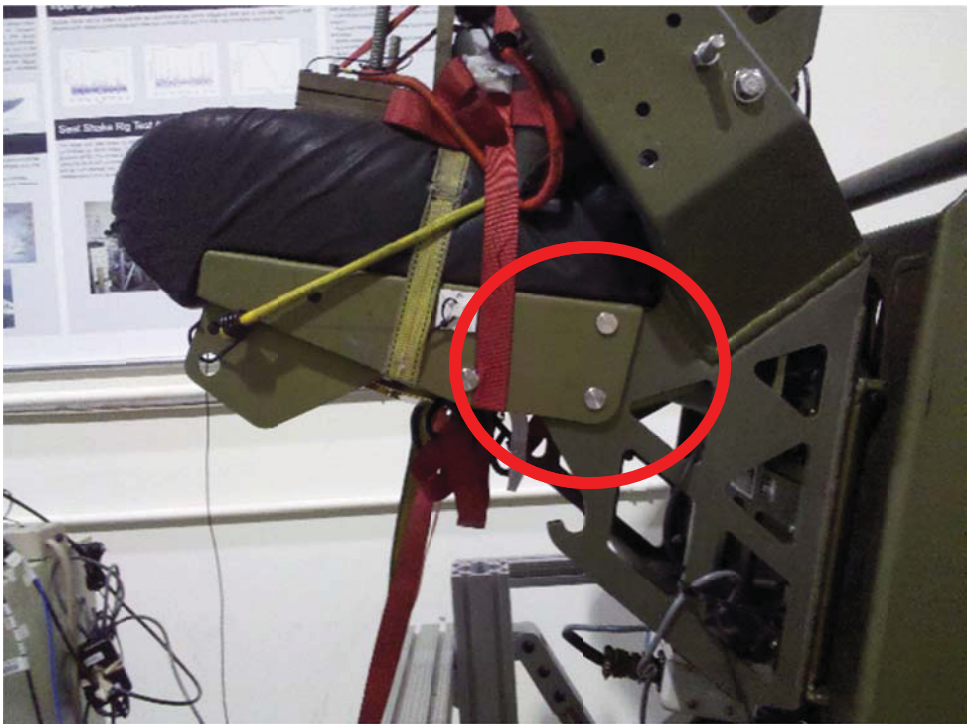

Figure 9-3. The pins that hold the seat pad onto the carriage assembly

Free Body Diagrams and Equations of Motion

The next step towards creating a complete model of the system is to create free body diagrams of each mass so that equations of motion can be derived. The first free body diagram created was of the seat pan assembly. The free body diagram of the seat pan assembly is shown below in Figure 9-4. The forces placed on the seat pan are from both the shock mitigation system and the seat cushion. Using the free body diagram the forces placed on the seat pan are summed in the vertical or X_2 direction to form the equation of motion. The final equation of motion for the seat pan is represented by equation 9-1.

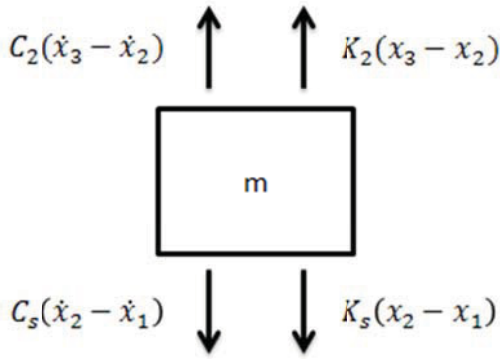

Figure 9-4. Free body diagram of the seat pan showing the forces placed on the system and their directions

$$\sum F = ma$$

$$m\ddot{x}_2 = C_2(\dot{x}_3 - \dot{x}_2) + K_2(x_3 - x_2) - C_1(\dot{x}_2 - \dot{x}_1) - K_1(x_2 - x_1) \quad (9\text{-}1)$$

The second free body diagram derived was of the occupant mass. The free body diagram of the occupant mass is shown in Figure 9-5. The only force observed by the occupant mass is from the seat cushion. This can be noticed in the free body diagram as well as the equation of motion. The equation of motion for the occupant mass was determined by summing the forces in the vertical or X_3 direction. The final equation of motion is expressed in equation 9-2 below.

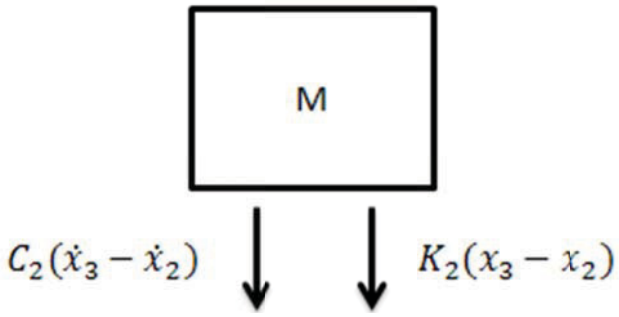

Figure 9-5. Free body diagram of the occupant mass showing the forces placed on the system and their directions

$$\sum F = ma$$

$$M\ddot{x}_3 = -C_2(\dot{x}_3 - \dot{x}_2) - K_2(x_3 - x_2) \tag{9-2}$$

9.2 Numerical Model

The equations of motion derived from the free body diagrams described earlier are then modeled in MATLAB/Simulink for simulation. The Simulink model is separated into three major portions which represent the variables X_1, X_2 and X_3 for better organization. The first portion of the model represents X_1 which is simply the motion of the base plate. The Simulink blocks that represent X_1 are shown in Figure 8-6 below. The input signal is converted to meters and then is differentiated to calculate the input velocity; both signals are then sent to the rest of the model.

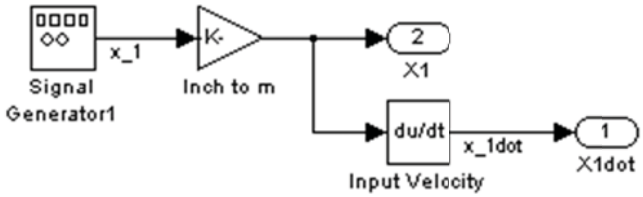

Figure 9-6. Simulink blocks that represent the base excitation

The next portion of the Simulink model represents the motion of the seat pan assembly or X_2. The equation of motion used to describe the dynamics of the seat pan is rearranged in a form that is easily modeled in Simulink, shown in equation 9-3. The Simulink blocks used to calculate the response the equation represented by equation 9-3 is shown in Figure 9-7.

$$\ddot{x}_2 = (\frac{1}{m})(C_2(\dot{x}_3 - \dot{x}_2) + K_2(x_3 - x_2) - C_1(\dot{x}_2 - \dot{x}_1) - K_1(x_2 - x_1)) \tag{9-3}$$

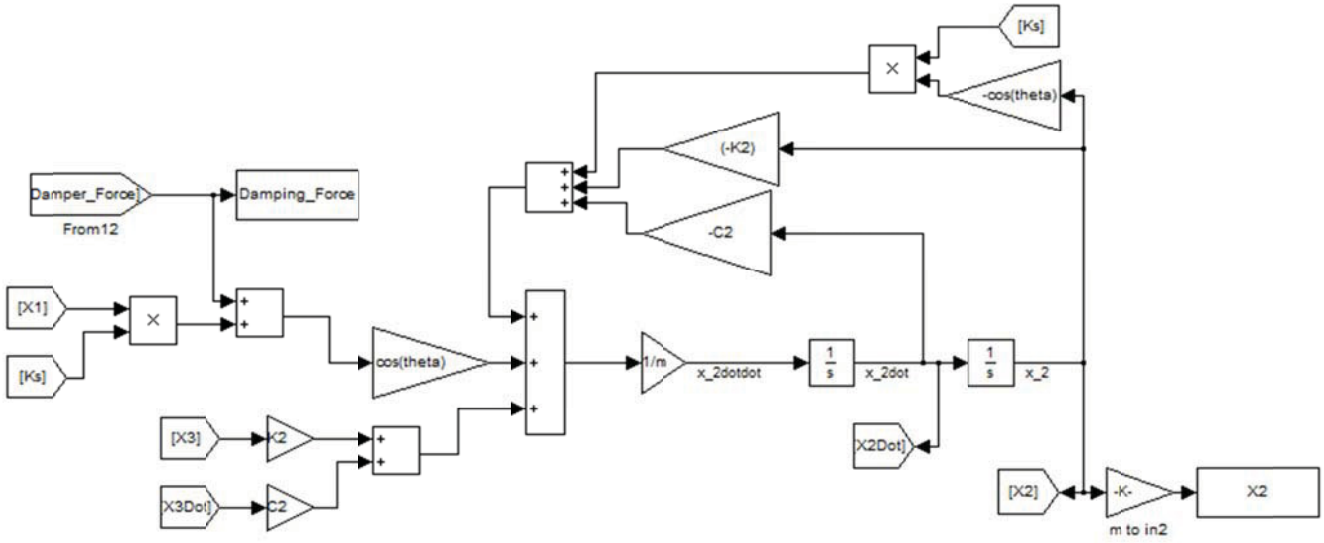

Figure 9-7. The Simulink blocks used to calculate the response of the seat pan (X_2)

The last large group of blocks in Simulink represents the equation of motion used to calculate the response of the occupant mass or X_3. The equation of motion used to describe the response of the occupant mass on top of the seat cushion was rearranged to the form represented in equation 9-4 to be modeled using Simulink. The Simulink blocks used to simulate the response of the seat pan that is represented by equation 9-4 is shown in Figure 9-8.

$$\ddot{x}_3 = \left(\frac{1}{M}\right)\left(-C_2(\dot{x}_3 - \dot{x}_2) - K_2(x_3 - x_2)\right) \tag{9-4}$$

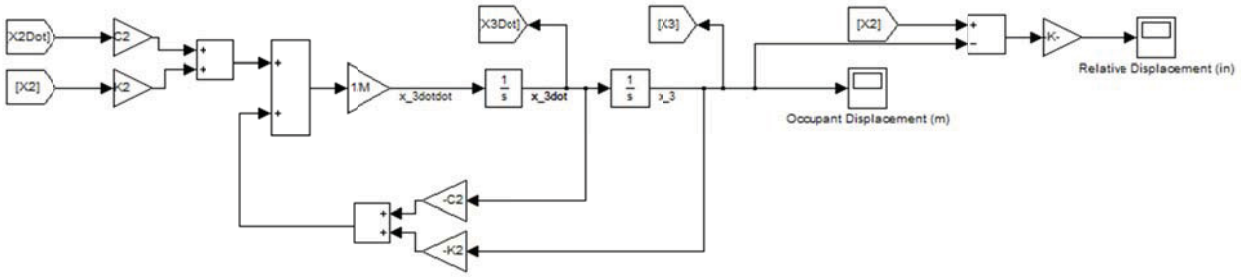

Figure 9-8. The Simulink blocks used to calculate the response of the occupant mass (X_3)

In addition to modeling the three equations of motion used to calculate the response of the entire seat and occupant there were a few additional specifics that required special

attention. The first is to incorporate the mechanical bump stops that limit the motion of the shock mitigating system. Without incorporating the bump stops into the model the system would be assumed to have an infinite amount of suspension travel, which is not be truly representative of the shock mitigating system. The mechanical bump stops were simulated in Simulink through the use of a varying spring rate as a function of displacement. By using a look up table the spring rate would be the normal 109 pounds per inch during the 6 inch suspension stroke but increase greatly to a value of 100,000 pounds per inch at the ends of the 6 inch stroke. The group of Simulink blocks used to calculate the proper spring rate for a given displacement is shown in Figure 9-9. The relative displacement of X_1 and X_2 are calculated to obtain the total compression or extension of the spring. The relative displacement is then sent to the look up table where the correct spring rate is output and then sent to the rest of the model.

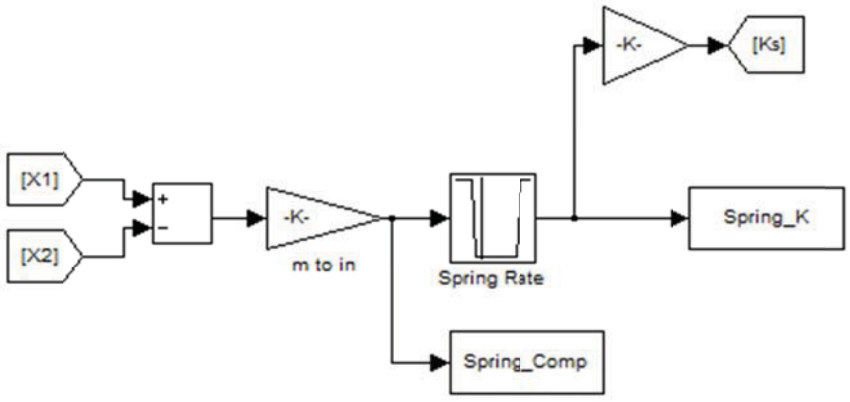

Figure 9-9. The look up table system used to implement a bump stop system into the model

The other addition to the model is the need to determine the appropriate damping coefficient needed for a specific velocity. This is also accomplished by use of a look up table with the appropriate damping coefficients for various velocities. The Simulink blocks used to create this look up system is shown in Figure 9-10. The relative velocity of the base and seat pan is calculated to gain the compression or rebound velocity of the damper. The relative velocity is then sent to a look up table to determine the correct damping coefficient for that specific velocity. The damping coefficient is then sent to the model.

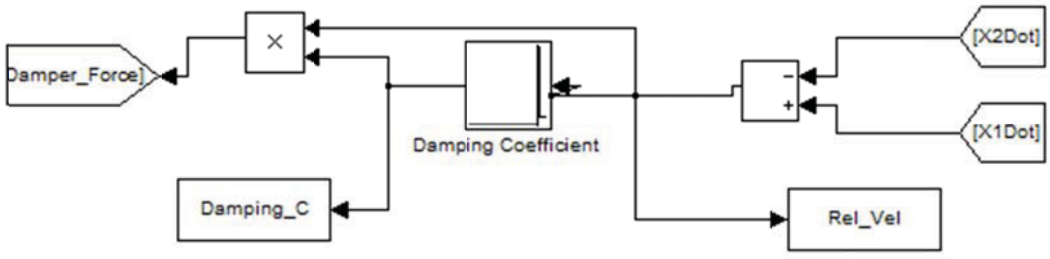

Figure 9-10. The Simulink blocks used to create the damping coefficient look up system

9.3 Model Validation

This section details the comparison of the seat rig data with the results from the Simulink model previously described in section 9.2. A 200 pound occupant and a suspension preload of 0 inches were simulated. The input or excitation file chosen for this comparison was the 89 foot high speed planing craft. The suspension displacement or relative displacement of the seat and the floor was used for comparison. By using the relative displacement measured by the string potentiometer on the seat shake rig any sensor offsets are eliminated, making for an easy comparison. The overlaid plot of the experimental data and the model data is shown in Figure 8-11. This portion of the entire dataset was chosen for Figure 9-11 since it displays different types of motion within a short time span. The model is able to follow the response of the experimental data very well. The largest differences between the two data sets happen at the largest impact and when the seat comes to a point of rest temporarily during the testing. The largest suspension movement has an amplitude of 1.4 inches in compression and jounce. During jounce the model and experimental data differ by 0.234 inches and during compression the difference is 0.168 inches. These differences are less than 10% of the total motion of this single event.

The second source of most of the differences is due to the friction within the damper which is noticeable when initiating motion from steady state that was not modeled. This causes the damper to come to rest at different locations, being extremely difficult to model. These differences in initial motion are very slight with a magnitude typically less than a tenth of an inch. Being that a majority of the differences are a result of these

frictions, which are very small differences, the model is a more than adequate representation of the seat dynamics.

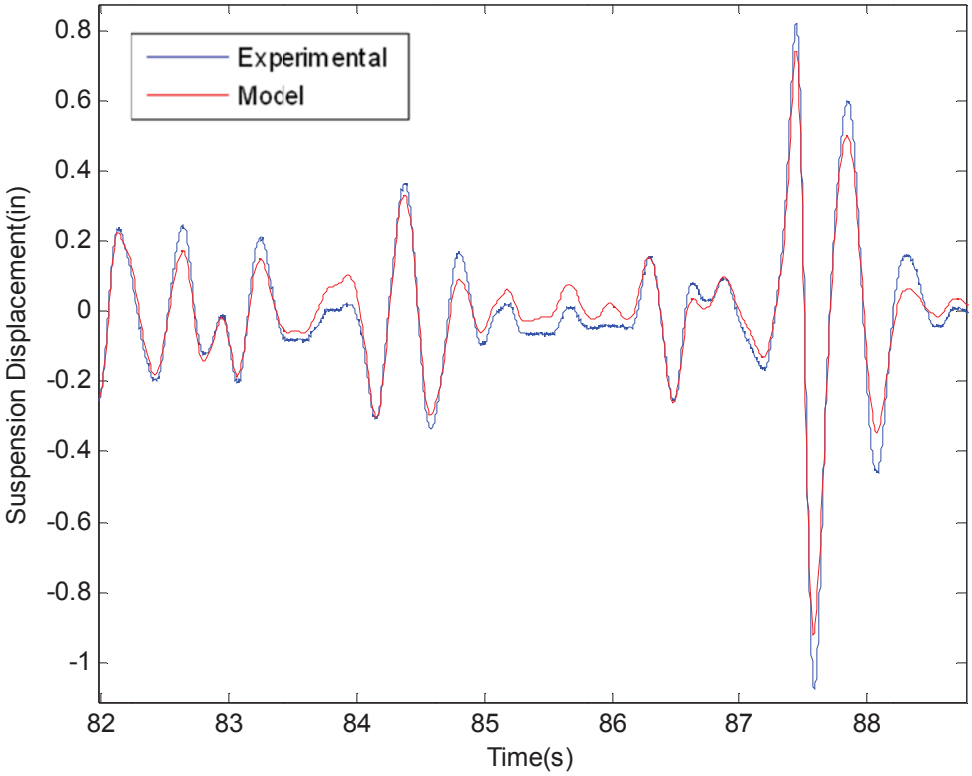

Figure 9-11. There is a close match between the experimental data and Simulink model data

Since the two data sets have different sampling rates, probability density function could not be calculated. Another method that was used to compare the response of the seat to that of the model was by comparing the percentile values from each data set. The peak values are grouped into percentile groups based on absolute values. The percentile values are shown in Table 9-1 for the occupant mass accelerometer. The largest difference is at the 100 percentile or largest impact. There is a difference of 0.316 g between the model and the experimental data. Most of the differences are on the order of a hundredth of a g. This indicates that the model accurately represents seat since 95% of the time the differences are slight.

Table 9-1. Acceleration percentile values of the occupant mass for the model and experimental data.

	Percentile Value										
	10	**20**	**30**	**40**	**50**	**60**	**70**	**80**	**90**	**95**	**100**
Exp.	0.012	0.030	0.045	0.063	0.081	0.101	0.127	0.167	0.239	0.307	1.390
Model	0.008	0.021	0.035	0.049	0.063	0.081	0.104	0.144	0.226	0.303	1.074

9.4 Model Testing

This section details the use of the model to further analyze the dynamics of the Stidd 800v5 shock mitigating seat. The model is used to vary parameters that are not easily adjustable on seat during lab testing. The two parameters that were chosen to be examined with the model are the spring rate and damping coefficient. The simulation was run using the 89 foot high speed planing craft excitation while the spring rate and damping coefficient within the model was varied at values of 50%, 100% and 150% of their original values.

Effects of different damping rates

To examine the effects of different damping rates on the dynamics of the seat suspension the damping rate was changed to 50%, 100% and 150% of the original rate at constant spring rates of 50%, 100% and 150% also. The DRI value for the tests are shown in Figure 9-12. When the damping rate is increased from 50% to 100% the DRI value drops significantly by as much as 70.2% at a spring rate of 100%. This extreme drop is due to the damping force provided from the damper is extremely inadequate for the spring force placed on the system. With a damping ratio of 0.261 determined experimentally the model of the system would have a damping ratio of about 0.131, which is very low. When the damping is increased to 150% of the original value the results for the DRI change are different between the various spring rates. For the spring rate of 50% the DRI rose by 13.6% while for a spring rate of 100% the DRI rose by 7.94%. This is due to the damping rate being larger than optimal for the spring rates associated with them. For a spring rate of 150% of the original value the DRI actually decreased slightly by 1.61%.

The increase in damping rate matched the 50% greater spring rate that was chosen for this test.

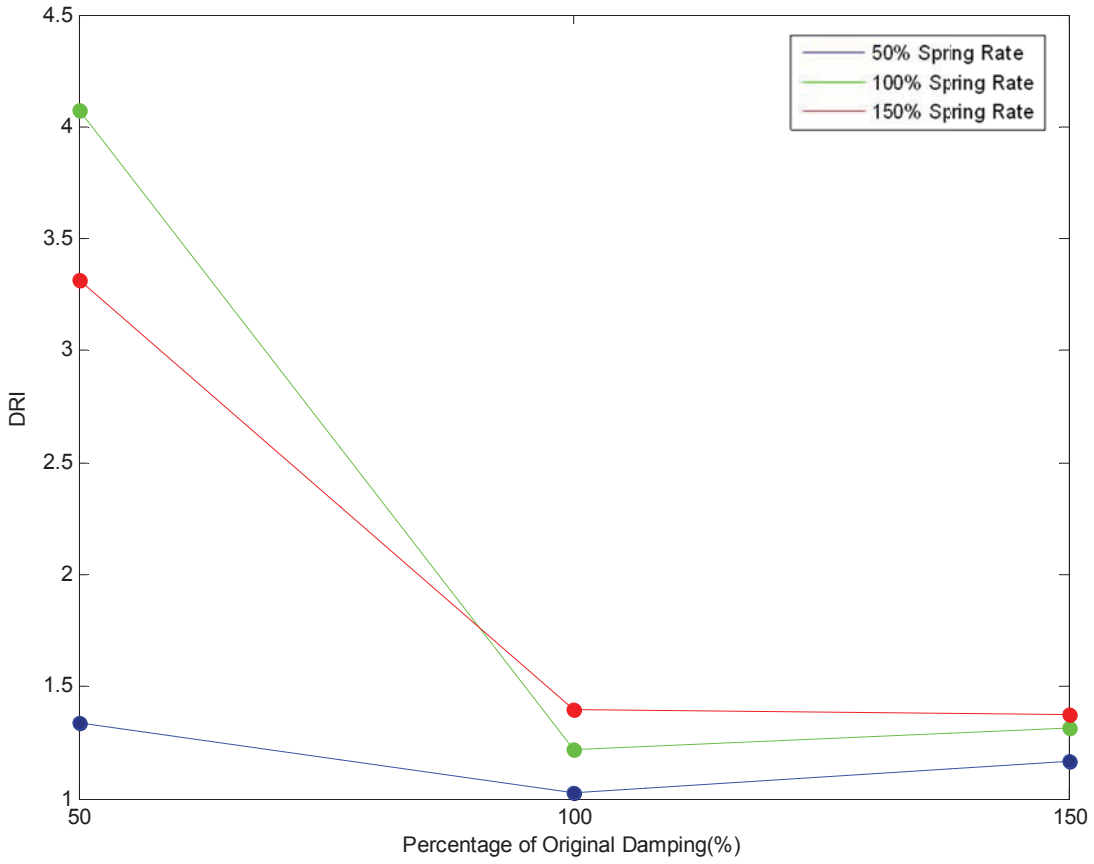

Figure 9-12. At all spring rates there is a sharp decrease in severity when damping is increased to 100%

Another examination of the percentile values of the acceleration peaks was done. The changes in the acceleration response of the seat are shown within the percentile groups shown in Table 9-2. The percentile range of 80 to 100 percent were shown since a majority of the data was below this value had a very low magnitude of acceleration which is not the focus of this research. The 100% percentile group represents the impacts used to calculate the DRI value mentioned and discussed previously. The 95 to 99 percentile groups represent the medium impacts and confirm the trends found earlier that when the damping is increased from 50% to 100% the acceleration magnitudes observed are decreased and when the damping is increased from 100 to 150% the acceleration typically increases. For the medium and smaller impacts with the system using a 50%

spring rate the medium acceleration events experienced an increase of as much as 11% in amplitude when the damping rate is increased. When the damping rate is increased to 150% the acceleration magnitudes of the medium and small impacts increases by as much as 21%. When examining the percentiles for a 100% spring rate the acceleration drops by as much as 16% when the damping rate is increased from 50% to 100% for small to medium impacts and then increase by as much as 11% when the damping is raised to 150%. The case of 150% spring rate is when the harshness decreases when the damping rate is increased to 150%, which does not follow the trend at the other spring rates. The small to medium impacts

Table 9-2. Percentile groups for the acceleration experienced

		Percentile					
Damper	Spring	80	90	95	98	99	100
50	50	0.1274	0.1872	0.2593	0.3732	0.4515	1.3418
100	50	0.1383	0.2159	0.2877	0.3892	0.465	1.0246
150	50	0.1465	0.2259	0.3272	0.4592	0.5625	1.1639
50	100	0.1678	0.2541	0.3369	0.477	0.6206	4.0734
100	100	0.1447	0.2326	0.3106	0.4307	0.5235	1.2157
150	100	0.1485	0.2262	0.325	0.4644	0.5835	1.3122
50	150	0.1959	0.2958	0.3849	0.556	0.687	3.3137
100	150	0.153	0.2512	0.3423	0.4788	0.584	1.4001
150	150	0.1512	0.2296	0.3273	0.472	0.6056	1.377

To verify the results taken from the DRI and percentile examination the time series data of the occupant displacement was examined. This will also show how the trends in acceleration relate to those of the displacement. The time series displacement data with a spring rate of 50% at various damping rates are shown in Figure 9-13. The impact event at 112 seconds experienced the most change at the different damping rates. The amount of negative displacement decreased by 28.5% when the damping is increased from 50% to 100% of the original damping coefficient. The response of the system at small displacement motions, those with an amplitude smaller than 0.5 inches, experienced less

displacement with a 50% damping rate. When the damping rate is 150% of the original value the seat experiences a degradation in performance, as indicated by an increase of 15.4% in negative displacement at the largest impact event. The displacement experienced at smaller motions are relatively consistent with those of the 100% damping rate.

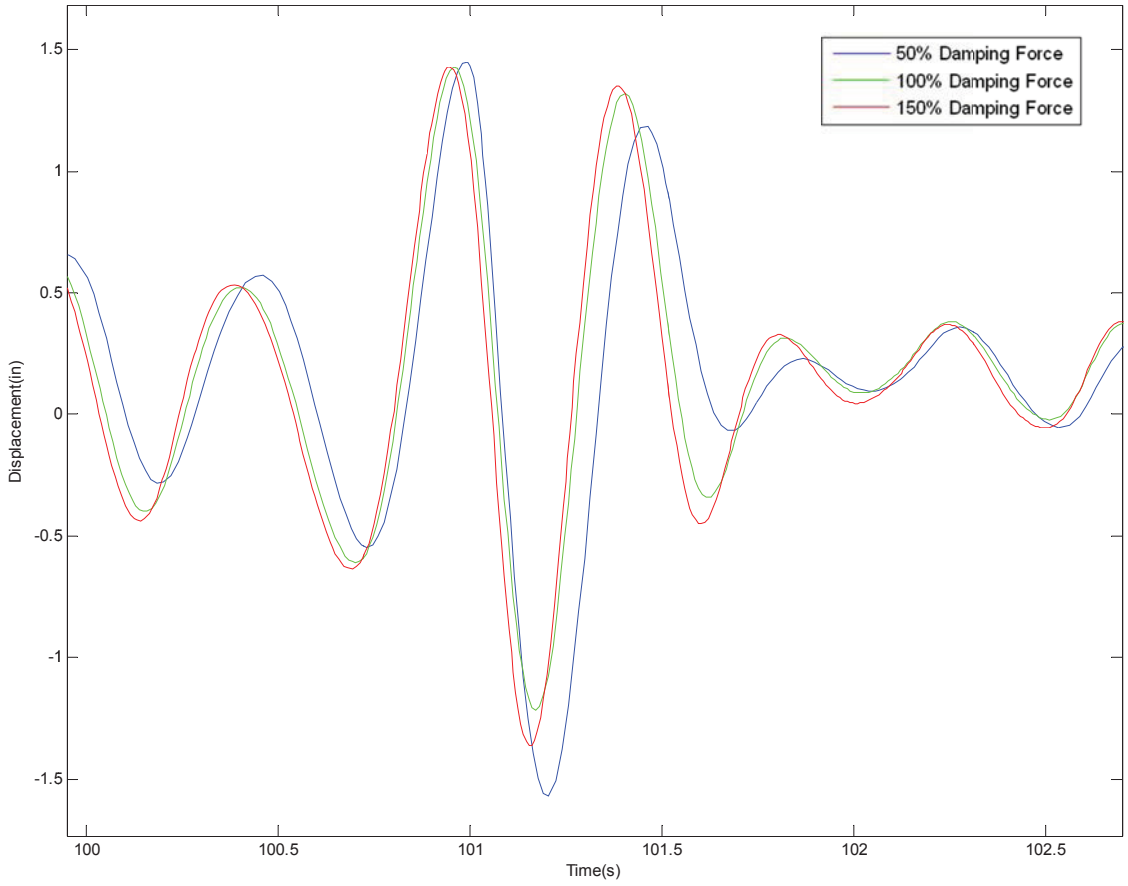

Figure 9-13. The response of the system to motion less than 0.5 g experienced little change from various damping rates

When the spring rate is at 100% of the original value the changes in the dynamics of the seat from the different damping rates slightly differ to those of the 50% spring rate case. The plot of the displacement when the spring rate is at 100% of the original value is shown in Figure 9-14. There remains to be a significant reduction in displacement observed when the damping rate is changed from 50% to 100%, like mentioned previously for the 50% spring rate. However, when the damping is increased to 150% the

amplitude of the largest impact event does increase slightly as predicted by the increase in DRI. But when examining the entire time series many impact events are mitigated more by the increase in damping, although slightly with a reduction of about 5% in either direction for the largest peaks with magnitudes of greater than 1 inch. The motion a majority of the test was unaffected when comparing the cases of 100% and 150% damping rates.

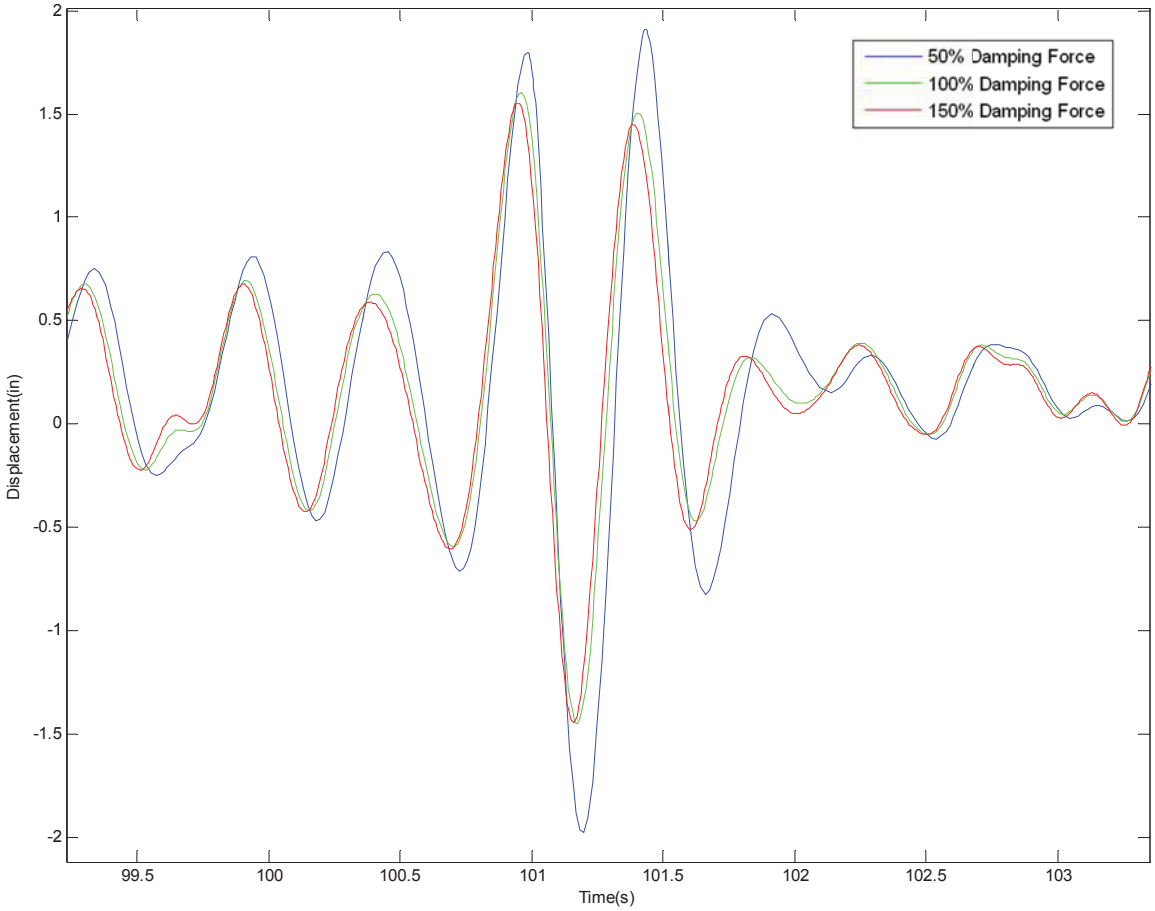

Figure 9-14. There are minimal changes in dynamics between a 100% and 150% damping force

When the spring rate is 150% of the original value the system reacts differently to the changes in damping rate. The plot of the displacement when the spring rate is at 150% of the original value is shown in Figure 9-15. When the damping rate is increased to 100% from 50% the amount of acceleration drops greatly by as much as 24.6%. This trend matches with those of the previous results from the 50% and 100% spring rates. When

the damping rate is increased to 150% of the original value the severity of a majority of all the impact events decreases by about 7% of the values experienced at 100% damping. This is probably a result of the increased spring rate which also requires an increase in damping to complement the higher spring rate.

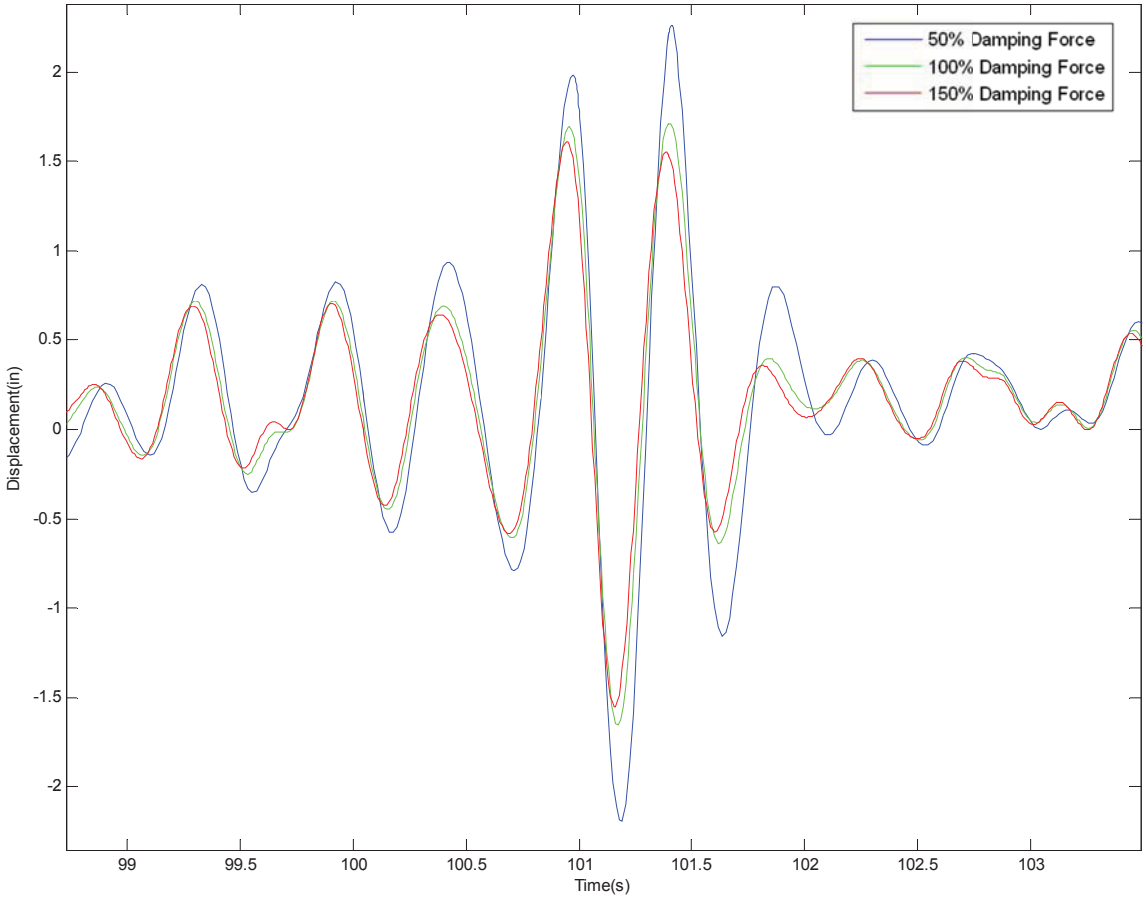

Figure 9-15. With a spring rate of 150% an increased damping rate(150%) produced better results

Effects of different spring rates

The same data that was taken for the analysis of the damping rate is now used to examine the effects of different spring rates. The DRI values that were previously calculated are then used to gauge the effect of different spring rates. The DRI value at different damping rates over the span of spring rates of 50%, 100% and 150% are shown in Figure 9-16. The majority trend at the damping rates of 100% and 150% is that the DRI value

increases with an increase in spring rate. When the damping rate is at 50% the DRI value increases greatly when the spring rate is increased from 50% to 100% and then decreases when the spring rate is increased to 150%. When the damping rate is much lower, at a value of 50% in this case, the spring rate dominates the response. The spring force is much greater relative to the damping force at the 50% rate when compared to the 100% and 150% rates.

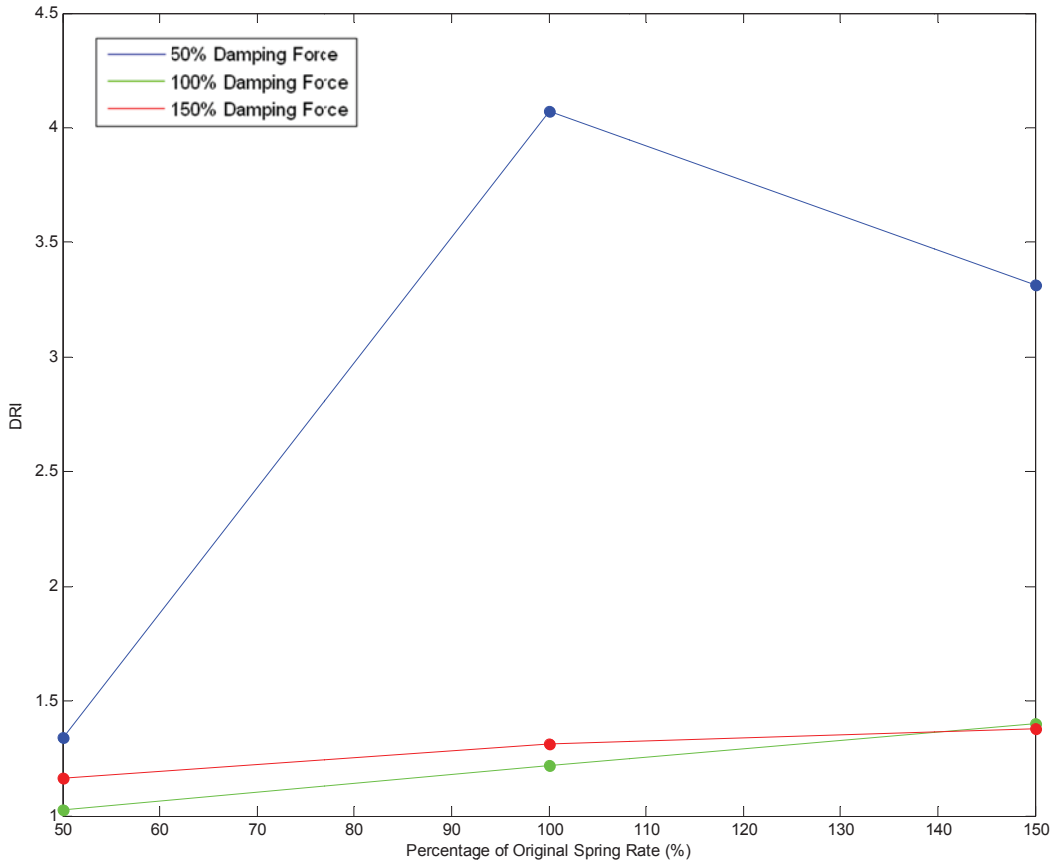

Figure 9-16. At a damping force of 50% the spring rate dominates the response

To further understand the trends gained from plotting the DRI value at various spring rates the acceleration data was grouped into percentile groups to examine the changes in the small and medium events. The percentile groups of the acceleration data is shown in Table 9-3. The 100 percentile represents the largest events, percentiles of 95 to 99 represent the medium events and percentiles of 90 and lower represent the small events. For all but one cases the acceleration experienced by the occupant increases with an

increase in spring rate. When the damping rate is at 50% and the spring rate is increased from 100% to 150%, there is a reduction of 18.7% in acceleration in the 100 percentile group. When the damping rate is held constant at 50% the acceleration levels increase by about 30% for all sized motions when the spring rate increases from 50% to 100% and then increases by 15% when the spring rate increases from 100% to 150%. The increase for the 100 percentile group was an outlier with an increase of 204% when the spring rate went from 50% to 100%. When the damping rate is held constant at 100% the acceleration increases by 18.7% for the 100 percentile group and 10% for the medium events and 6% for the small events when the spring rate is increased from 50% to 100%. When the spring rate is further increased to 150% the acceleration for the 100 percentile events increase by 15%, the medium events increase by 11% and the small events increase by 7%. When the damper is set to 150% the changes in acceleration when the spring rate is increased are much smaller. The 100 percentile group does experience a 12.7% increase in acceleration when the spring rate is increased from 50% to 100%, while the medium and small events experience little to no change with the average increase being 1.1% throughout. When the spring rate increases to 150% the 100 percentile group increases by 5%, the medium and small events increase by 2%.

Table 9-3. Occupant acceleration data grouped into percentiles

		Percentile					
Damper	**Spring**	**80**	**90**	**95**	**98**	**99**	**100**
50	**50**	0.1274	0.1872	0.2593	0.3732	0.4515	1.3418
50	**100**	0.1678	0.2541	0.3369	0.477	0.6206	4.0734
50	**150**	0.1959	0.2958	0.3849	0.556	0.687	3.3137
100	**50**	0.1383	0.2159	0.2877	0.3892	0.465	1.0246
100	**100**	0.1447	0.2326	0.3106	0.4307	0.5235	1.2157
100	**150**	0.153	0.2512	0.3423	0.4788	0.584	1.4001
150	**50**	0.1465	0.2259	0.3272	0.4592	0.5625	1.1639
150	**100**	0.1485	0.2262	0.325	0.4644	0.5835	1.3122
150	**150**	0.1512	0.2296	0.3273	0.472	0.6056	1.377

From the analysis of the displacement data when studying the effects of different damping rates on the dynamics of the seat it was confirmed that the acceleration curve is representative of the displacement. The displacement data was reviewed for any under lying trends when the spring rate was changed. No under lying trends were found that would refute the trends found when examining the acceleration data using the DRI value and the percentile tables. The acceleration trends are representative of the dynamics of the seat.

9.5 Model Testing Summary

The analysis of the test data received from the Simulink model has proved beneficial. The Simulink model of the seat assembly created by implementation of the equations of motion replicated the response of the seat well. When compared to the experimental results the model results differed by only a few hundredths 95% of the time when examining the acceleration observed by the occupant mass. Once the model results were verified against the experimental data different spring rates and damping coefficients were tested. The spring rate and damping coefficient were varied at values of 50, 100 and 150 percent of the original values to determine their effects on the system.

When the damping coefficient is varied while the spring rate is held constant it was found that the acceleration magnitudes observed by the occupant decrease when the damping rate is increased from 50% to 100%. The maximum acceleration values do increase slightly, for most of the spring rates, when the damping is increased to 150% as the damping force becomes larger than the spring rate. When the spring rate was set to 150% and the damping was increased from 100% to 150% the acceleration of a majority of the test was decreased slightly. The displacement data was examined and it was found that the reduction in accelerations found from analysis of the DRI value and percentile values translated to a reduction in motion for all the spring rates.

When the spring rate was varied while the damping coefficients were held at a constant value it was found that the accelerations observed by the occupant increase when the spring rate is increased. The only case where the acceleration decreased was with the 100% spring rate 100 percentile group when the spring rate increased from 100% to

150%. The increase of 204% in acceleration when the spring rate was increased from 50% to 100% should be considered an outlier because most of the increases in acceleration are typically consistent between all the data points.

Chapter 10. Conclusion

This chapter summarizes the work previously presented in this thesis. First a summary of the results obtained from testing by use of the seat shake rig and Simulink model are reviewed. Then suggestions for future work that should be performed in the field of shock mitigating seats to better the seat performance conclude the chapter.

10.1 Summary

A comprehensive analysis on the dynamics of a Stidd 800v5 shock mitigating seat was performed to determine the response of the seat to changes in occupant weights and adjustable preload, as well as changes to the spring rate and damping coefficient. A single axis seat shake rig designed specifically to simulate the extreme environment of high speed craft was built for testing. Accelerometer data from at sea testing of a 36 foot USN, 47 foot MLB and 89 foot high speed planing craft were integrated and filtered to be used as input excitations to simulate a sea environment. A square wave, impulse half sine wave and chirp signal were also created and used to analyze specific dynamics of the seat. The system was then modeled as a two degree of freedom system with base excitation for modeling purposes. Equations of motion were derived and converted into a Simulink block diagram. The Simulink model was compared and validated to the experimental data obtained from the seat shake rig. The model was used to vary the non-adjustable suspension parameters of spring rate and damping coefficient to analyze the response of the system if different suspension settings were used.

The initial test results indicated that the seat shake rig provided accurate and repeatable tests. When multiple runs of the same input excitation with similar test conditions were taken the difference in the response of the seat was insignificant. When examining the differences between three consecutive test runs 35.6 percent of the data had zero differences and 72.5 percent of the data differed by 0.075 inches or less, proving a large level of repeatability was present.

Once the repeatability was established the seat was run on the testing rig with different weights and different suspension preloads, these being the only adjustable parameters of the system. The accelerometer data was analyzed to gauge the response of the system throughout the various changes; acceleration is directly related to force and also gives a good representation on the nature of the motion of the seat. Overall it was found that as the occupant weight increases the acceleration levels decreased. This is indicated by a decrease in DRI, which is based on the largest singular impact event, as well as a decrease in overall peak magnitude levels of acceleration. The average reduction in magnitude was about 20 percent when an additional 50 pounds was added. The added mass did increase suspension displacement by about 50 percent per 50 pounds added.

When analyzing the effects of suspension preload it was found that the DRI value was not a good representation of the changes in seat dynamics. In general, an increase in preload resulted in an increase in acceleration observed by the occupant. Increases in acceleration levels were observed when the spring preload was increased from 0, which is the suggested operating condition, to 1 or 2 inches were between 5 and 66 percent. The increased preload made the system respond similar to a rigid mounted seat. It was also found that an increase in acceleration resulted in a decrease in suspension displacement.

The created input was used to analyze specific responses from the system. The square wave was used to calculate the damping ratio of the coil over system by implementing logarithmic decrement and analyzing the free response of the system. The damping ratio was fairly unaffected by changes in preload and occupant weight with an average value of 0.261. The 5 percent settling time of the system was found to be about 1.41 seconds. The impulse half sine wave was used to analyze the seat's response to a singular impact event at different occupant weights and preload levels. The results were similar to that of the sea data analysis, as the preload increases the acceleration observed by the occupant increases and when the occupant weight increases the acceleration levels decrease. The response to a chirp input with frequencies ranging from 0.5 hz to 15 hz resulted in a transmissibility plot similar to a theoretical plot with a natural frequency of 2.03 hz.

The Simulink model was created and verified to with that of the experimental data obtained from the seat shake rig. The spring rates and damping coefficient within the seat

model were then varied from the original value to measure the effects. It was found that as the spring rate increases the acceleration levels increase. When the damping coefficient was set below its original value the DRI level increased, representing an increase in severity. However, the DRI increased when the damping coefficient was increased above its original value. A percentile data analysis proved that most of the changes were within the 90 percentile groups and higher.

10.2 Recommendation for Future Research

While the results presented in this study are significant towards understanding shock mitigating seats and seat testing there are still opportunities for further improvement. One area for further research would be to test the same seat and instrumentation in an at sea test on one of the ships which the input acceleration data was provided. By using the same instrumentation variation in the response are reduced greatly so the laboratory and at sea data can be directly compared. This will confirm that the seat shake rig can be used to properly test a shock mitigating seat.

Areas of improvement are revealed after an extensive data analysis was conducted. The first proposed change is to use an occupant mass that is more representative of a human occupant. This would provide a better representation of how the seat will be operated in a real at sea environment. A better representation of a human occupant would allow a more in-depth analysis of the effects of the seat cushion.

The data analysis was mainly conducted in the time domain due to the simplicity of the analysis. The focus of this study was the evaluation of the seat shake rig and its ability to analyze the dynamics of a shock mitigating seat. Since the abilities to test in the time domain is now verified future research could be done in the frequency domain. Much research in vehicle dynamics is done in the frequency domain. This will also provide another tool to evaluate shock mitigating seat dynamics.

The seat shake rig did not occur any failures during the duration of all tests conducted in this study. The system is extremely durable and reliable. With that mentioned, human

testing would provide a vast array of insight towards improving shock mitigating seats. By using a human for an occupant mass and having the test subject answer a simple survey it would be possible to correlate experimental test data to human subjective results. This could lead to improvements in testing procedures by further reducing the need for human testing if direct correlations are found.

References

1. Mark V Special Operations Craft. *Federation of American Scientists.* [Online] 2010.

2. **Babb, Colin.** Office of Naval Research Spearheads Development of New All-Composite Mark V.1 Patrol Boat. *Office of Naval Research.* [Online] 2008.

3. **Buxbaum, Peter.** Averting Personnel Injuries. *SOTECH.* 2010, Vol. 8, 9.

4. Pierson - Moskowitz Sea Spectrum. *Army.mil.* [Online] http://www.eustis.army.mil/WEATHER/Weather_Products/seastate.htm.

5. **Dobbins, Trevor.** *High Speed Craft Human Factors Engineering Design Guide.* West Sussex : ABCD, 2008.

6. **Gollwitzer, Richard M.** *Repeated Water Entry Shocks on High-Speed Planing Boats.* Panama City : Naval Surface Warfare Center, 1995.

7. *Longitudinal Motion of Super High-Speed Planing Craft in Regular Head Waves.* **Katayama, Toru.** Sakai : Osaka Prefecture University, 2000.

8. **Kearns, Sean D.** *Analysis and Mitigation of Mechanical Shock Effects on High Speed Planing Boats.* Naval Architecture, Massachusetts Institute of Technology. 1994. Thesis.

9. **Peterson, Ronald.** *Drop Tests to Support Water-Impact and Planing Boat Dynamics Theory .* 1997. CSS/TR-97/25.

10. **Haupt, Kelly.** *High-Speed Craft Motions: a Case Study.*

11. *Slamming Response of a Large High-Speed Wave-Piercer Catamaran.* **Thomas, G. A.** 2, s.l. : Marine Technology, 2003, Vol. 20.

12. *Transient Dynamic Slam Response of Large High Speed Catamarans.* **Giles, Thomas.** Tasmania : s.n.

13. *The Whipping Vibratory Response of a Hydroelastic Segmented Catamaran Model .* **Lavroff, Jason.** Shanghai : s.n., 2007.

14. *Characterization of Sea Fighter, FSF-1, Wave Slam Events.* **Fu, T. C.** Ann Arbor : s.n., 2007.

15. **Rosén, Anders.** *Loads and Responses of Planing Crafts in Waves.* Aeronautical and Vehicle Engineering, KTH. Stockholm : s.n., 2004. Thesis. 1651-7660.

16. *Assessment of Human Performance during High-Speed Marine Craft Transit.* **Nikolic, Dragana.** Southampton : IFMBE, 2010. Vol. 29.

17. **Klembczyk, Alan R.** *Analysis, Optimization, and Development of a Specialized Passive Shock Isolation System for High Speed Planing Boat Seats.* North Tonawanda : s.n.

18. **Shen, Wenqi and Vertiz, Alicia.** *Redefining Seat Comfort.* s.l. : SAE 970597, 1997.

19. *Commercial Motor Vehicle Driver Fatigue and Alertness Study.* s.l. : U.S. Department of Transportation, 1996.

20. *An Investigation of Driver Discomfort and Related Seat Design Factors in Extended Duration Driving.* **Reed, M. P., et al.** SAE Technical Paper 910117.

21. *Heavy Truck Ride.* **Gillespie, T.** 1985. SAE Technical Paper 850001.

22. **Chaffin, D. and Anderson, G.** *Occupational Biomechanics.* s.l. : John Wiley & Sons Inc, 1991.

23. **Peterson, Dr. Ron.** *Shock Mitigation for the Human on High Speed Craft:.* 2004. RTO-MP-AVT-110.

24. *Evaluating Short and Long Term Seating Comfort.* **Thakurta, Kuntal.** 1995. SAE Paper 950144.

25. **Goonetilleke, Ravindra S.** *Designing to Minimize Discomfort. Ergonimics in Design.* 1998.

26. **USAF.** Seat System, Upward Ejection, Aircraft General Specification. [Online] 1999. http://www.everyspec.com. MIL-DTL-9479E.

27. **Griffin, M. J.** *Handbook of Human Vibration.* s.l. : Elsevier Science and Technology Books, 1996. 0123030412.

28. **Kirstein, J. C.** *Suspension System Optimisation to Reduce Whole Body Vibration Exposure on an Articulated Dump Truck.* Mechanical Engineering, Stellenbosch University. Matieland : s.n., 2005. Thesis.

29. *Fast Vessels in Heavy Seas - a "Shocking" Experience!* **Burgess, Marion.** Canberra : s.n., 2009.

30. [Online] www.sportcarbuzz.com.

31. **Peterson, R.** At-Sea Evaluation of Ullman Cockpit. [Presentation]. 2001.

32. **Swinbanks, Malcolm A.** *Active & Passive Shock Attenuation for Repeated and Single Shock Inputs to Boats & Vehicles.* MAS Research Ltd. 2008.

33. **Stidd.** Shock Mitigation Seats. *Stidd Systems Inc.* [Online] http://www.stidd.com/products/cat_pages/CAT15/CAT15_P17.pdf.

34. **Gollwitzer, Richard M.** *Repeated Water Entry Shocks on High Speed Planing Boats.* 1995. CSS/TR-96/27.

35. **Inman, Daniel J.** *Engineering Vibration.* Upper Saddle River : Pearson Prentice Hall, 2008. 0-12-228173-2.

Appendix A: MATLAB Code

A.1 FFT Code

```
function [frequencies,final] = MyFFT(FileName,option)
%Assign and open data file
open(FileName);
opened=ans;
displacement=opened.(option)'; %Add the filename after the "opened."
for the data if structured

%Setting FFT window(bin) size
nfft=2^11; %Resolution is nsample/nfft

% Sample frequency
nsample=500;

% Create and adjust frequency axis
frequencies=0:nfft-1;
frequencies=frequencies*(nsample/nfft);

% Setting initial window
initial=fft(displacement(1:nfft));
previous=initial;

% Averages 2 windows at a time
N=floor((length(displacement)/nfft))-1;
for i = 2:N
    newData=fft(displacement(i*nfft+1:(i+1)*nfft));

    sum=previous+newData;
    average=sum/2;
    previous=average;
end
final=abs(average);

% Plot final results
figure('Name','Frequency Spectrum','NumberTitle','on')
plot(frequencies,final)
ylabel('Magnitude of X(omega)')
xlabel('Frequency (Hz)')
end
```

A.2 Filtering and Plotting

```
function [time,
acceleration,velocity,displacement]=MyFilt(fname,option)
%% User interface
c=1;
test_num=1;

prompt = {'Enter High Pass Filter Frequency:','Enter low Pass Filter
Frequency:'};
dlg_title = 'Data Selection';
num_lines = 1;
def = {'.5','7'}; % enter estimated values
answer = inputdlg(prompt,dlg_title,num_lines,def);

highpass = str2double(answer(1));
lowpass = str2double(answer(2));

path = 'C:\Documents and Settings\Christopher
Liam\Desktop\Accelerometer
calibration\SensorCalibration\7in5freqtest1\';
logger_tstart = '1732';
data_tstart = '0';
data_tend = '8';
offset = 0.3;
nn = 60;

%% sample time
n = str2double(data_tend) - str2double(data_tstart) + 1;
n_start = str2double(data_tstart);
sampling_frequency = 500; % sampling frequency in Hz
Starttime= 0; %seconds
Endtime = n* 60; %seconds of simulation to run
n_channel = 3;
data_length = sampling_frequency*nn; %data per minute
sample = 0:(data_length - 1);
time_array = [0:( 1 / sampling_frequency ):Endtime];
tsize = length(time_array);

%% Loading and decimating data
    %Decimator = zeros(
for b = 1:n_channel
    Decimator{b} = sample*n_channel + b;
end

TimeOut = [];
DataOut = [];

%Data input
open(fname);
opened=ans;
DataOut = opened.(option)';%acceleration data. MAKE SURE DATA is in
units of G
DataOut=double(DataOut);
Time = opened.Time';%time;
```

```
%% Detrending and applying sensitivity for units

% 10 G Accel's
LF.Acc.Data.Raw = DataOut(:,1);

% Conversion to m/s^2 per accel sensitivity
LF.Acc.Data.Scale = LF.Acc.Data.Raw*9.81; %EDITTED for 32.3 ft/sec^2

% Detrending accel data for gravity DC offset
LF.Acc.Data.ZM = detrend(LF.Acc.Data.Scale);

%% Low Pass Filter (5th order butterworth @ 2.5 Hz)

Fs = sampling_frequency;  % 512 Hz sampling freq
Fn = Fs/2; % Nyquist Frequency

[b,a] = butter(5,lowpass/Fn,'low');

LF.Acc.Data.Filt = filtfilt(b,a,LF.Acc.Data.ZM);

%% Velocity Integration and Detrending

LF.Vel.Data.Scale = cumtrapz(LF.Acc.Data.Filt)/Fs;

[b,a] = butter(5,(highpass-0.0)/Fn,'high');
[bb,aa] = butter(5,(highpass+0.0)/Fn,'high');
[bbb,aaa] = butter(5,(highpass-0.0)/Fn,'high');

% Zero Phase Shift filtering scheme
LF.Vel.Data.ZM = filtfilt(bb,aa,LF.Vel.Data.Scale);

%% Displacement Integration and Detrending

LF.Disp.Data.Scale = cumtrapz(LF.Vel.Data.ZM)/Fs;

LF.Disp.Data.ZM = filtfilt(bbb,aaa,LF.Disp.Data.Scale);

%% Outputs for model
LF_Disp = LF.Disp.Data.ZM; %Raw displacement
LF_Vel = LF.Vel.Data.ZM; %Raw Velocity
LF_Acc = LF.Acc.Data.Filt; %Raw Acceleration

%% time
Time_Sim =
linspace(0,1,length(LF_Disp))*length(LF_Disp)/sampling_frequency;

%% convert names
data_string = DataOut;
data_size = 13*length(data_string);

%% preallocate matrices
time_input = zeros(tsize,1);
```

```
lp_lf_input = zeros(tsize,1);
n = zeros((data_size/13),1);
t = zeros((data_size/13),1);
time_input(1) = 0;
lp_lf_input(1) = 0;

%%
%don't need this loop (using code above to populate matrix)
for i = 1:(data_size/13)
n(i) = ((i-1) * 13)+1;
t(i) = i;
end
datamatrix = DataOut;

%% name data
%timeout = t / 512;
time=Time;
displacement=LF_Disp/0.0254;
velocity=LF_Vel/0.0254;
acceleration=LF_Acc/(0.0254*386.4);

%% Displacement Plot
figure('Name','input position vs time','NumberTitle','off')
plottools on
%plot(Time_Sim,StringDisp,'b')
hold on
plot(time,displacement,'r')
grid on
xlabel('Time (s)')
ylabel('Amplitude (inches)')
Title( 'Displacement')

%% Velocity Plot
figure('Name','input velocity vs time','NumberTitle','off')
plottools on
%plot(Time_Sim,StringVel,'b')
hold on
plot(time,velocity,'r')
grid on
xlabel('time(s)')
ylabel('amplitude inches or inches/sec')
Title( 'Velocity')

%% Acceleration Plot
figure('Name','input acceleration vs time','NumberTitle','off')
plottools on
%plot(Time_Sim,StringVel,'b')
hold on
plot(time,acceleration,'r')
grid on
xlabel('time(s)')
ylabel('acceleration(g)')
Title( 'Acceleration')

end
```